40490

National Library of Canada | Bibliothèque nationale du Canada

CANADIAN THESES ON MICROFICHE | THÈSES CANADIENNES SUR MICROFICHE

NAME OF AUTHOR/*NOM DE L'AUTEUR* WILLIAM JAMES ROWLEY

TITLE OF THESIS/*TITRE DE LA THÈSE* MASS TRANSFER AND TREATABILITY STUDIES OF CYANIDE OZONATION

UNIVERSITY/*UNIVERSITÉ* UNIVERSITY OF ALBERTA

DEGREE FOR WHICH THESIS WAS PRESENTED/
*GRADE POUR LEQUEL CETTE THÈSE FUT PRÉSENTÉE* MASTER OF SCIENCE IN CHEMICAL ENGINEERING

YEAR THIS DEGREE CONFERRED/*ANNÉE D'OBTENTION DE CE GRADE* 1979

NAME OF SUPERVISOR/*NOM DU DIRECTEUR DE THÈSE* DR. F.D. OTTO

Permission is hereby granted to the NATIONAL LIBRARY OF CANADA to microfilm this thesis and to lend or sell copies of the film.

The author reserves other publication rights, and neither the thesis nor extensive extracts from it may be printed or otherwise reproduced without the author's written permission.

*L'autorisation est, par la présente, accordée à la BIBLIOTHÈQUE NATIONALE DU CANADA de microfilmer cette thèse et de prêter ou de vendre des exemplaires du film.*

*L'auteur se réserve les autres droits de publication; ni la thèse ni de longs extraits de celle-ci ne doivent être imprimés ou autrement reproduits sans l'autorisation écrite de l'auteur.*

DATED/*DATÉ* 79/04/11 SIGNED/*SIGNÉ* W J Rowley

PERMANENT ADDRESS/*RÉSIDENCE FIXE* 340 OAKWOOD PLACE S.W.
CALGARY ALBERTA
T2V 3Y7

NL-91 (3-74)

National Library of Canada

Cataloguing Branch
Canadian Theses Division

Ottawa, Canada
K1A 0N4

Bibliothèque nationale du Canada

Direction du catalogage
Division des thèses canadiennes

## NOTICE

The quality of this microfiche is heavily dependent upon the quality of the original thesis submitted for microfilming. Every effort has been made to ensure the highest quality of reproduction possible.

If pages are missing, contact the university which granted the degree.

Some pages may have indistinct print especially if the original pages were typed with a poor typewriter ribbon or if the university sent us a poor photocopy.

Previously copyrighted materials (journal articles, published tests, etc.) are not filmed.

Reproduction in full or in part of this film is governed by the Canadian Copyright Act, R.S.C. 1970, c. C-30. Please read the authorization forms which accompany this thesis.

THIS DISSERTATION
HAS BEEN MICROFILMED
EXACTLY AS RECEIVED

## AVIS

La qualité de cette microfiche dépend grandement de la qualité de la thèse soumise au microfilmage. Nous avons tout fait pour assurer une qualité supérieure de reproduction.

S'il manque des pages, veuillez communiquer avec l'université qui a conféré le grade.

La qualité d'impression de certaines pages peut laisser à désirer, surtout si les pages originales ont été dactylographiées à l'aide d'un ruban usé ou si l'université nous a fait parvenir une photocopie de mauvaise qualité.

Les documents qui font déjà l'objet d'un droit d'auteur (articles de revue, examens publiés, etc.) ne sont pas microfilmés.

La reproduction, même partielle, de ce microfilm est soumise à la Loi canadienne sur le droit d'auteur, SRC 1970, c. C-30. Veuillez prendre connaissance des formules d'autorisation qui accompagnent cette thèse.

LA THÈSE A ÉTÉ
MICROFILMÉE TELLE QUE
NOUS L'AVONS REÇUE

NL-339 (3/77)

THE UNIVERSITY OF ALBERTA

# MASS TRANSFER & TREATABILITY STUDIES OF CYANIDE OZONATION

by

W. J. ROWLEY

(C)

A THESIS

SUBMITTED TO THE FACULTY OF GRADUATE STUDIES AND RESEARCH

IN PARTIAL FULFILMENT OF THE REQUIREMENTS FOR THE DEGREE

OF MASTER OF SCIENCE IN

CHEMICAL ENGINEERING

DEPARTMENT OF CHEMICAL ENGINEERING

EDMONTON, ALBERTA

SPRING, 1979

THE UNIVERSITY OF ALBERTA

FACULTY OF GRADUATE STUDIES AND RESEARCH

The undersigned certify that they have read, and recommend to the Faculty of Graduate Studies and Resarch, for acceptance, a thesis entitled Mass Transfer & Treatability Studies of Cyanide Ozonation submitted by W. J. Rowley in partial fulfilment of the requirements for the degree of Master of Science in Chemical Engineering.

.....
Supervisor

.....

.....

Date March 27/79...

ABSTRACT

The cyanide leach process for the extraction of gold results in toxic gold mill wastewaters containing cyanide compounds and heavy metals. This reasearch project was undertaken to evaluate aspects of mass transfer and effectiveness of using ozone to oxidize cyanide species to less toxic products. The mass transfer studies were based on enhancement of ozone physical mass transfer by a liquid phase reaction(s) for (1) simple cyanide, NaCN, and (2) complex cyanides found in the barren bleed of Giant Yellowknife Mines Ltd.

A quiescent surface reaction (Danckwerts cell) was chosen for the mass transfer studies so as to establish the interfacial area for mass transfer. Hydrodynamic conditions were varied by stirring at the interface. A theoretical analysis of the simultaneous absorption and reaction of ozone in a cyanide solution was used along with an assumed reaction mechanism to calculate rate constants for the ozone reaction. The model found to most successfully describe the experimental results was the transition from fast to instantaneous reaction regime (transition regime) coupled with an ozone to cyanide/cyanate stoichoimetric ratio of 1.2:1. This figure was found experimentally and implies a equimolar stoichoimetry for the ozone-cyanide reaction plus an appreciable ozone-cyanate reaction influence. The enhancement faction ($I = k_L/k_L^o$) was found to range between 2.5 and 9.1 corresponding to a range of bulk liquid cyanide concentrations of 7.3 to 98.3 mg/L, respectively. The resultant second order kinetic

constant was found to have an order of magnitude value of $10^4$ to $10^5$ L/gmole s at room temperature upon reaction model evaluation.

The value of I for the barren bleed ozonation was found to be an order of magnitude higher than for equivalent simple cyanide concentrations. This was possibly due in part to the multiplicity of reactions involved and the catalytic effect of copper. No kinetic data could be gleaned from this series of runs since the instantaneous reaction regime appeared to apply.

Ozone was found to be effective in reducing barren bleed cyanides and thiocyanate to low levels. Total cyanide was reduced to 1-2 mg/L and thiocyanate to below detectable limits. The residual cyanide was likely iron cyanide species which are not amenable to direct ozone destruction. The treated levels obtained are probably environmentally acceptable since other gold mill wastewaters devoid of cyanide would dilute this residual and the high intermediate product concentration (cyanate) below actuely lethal levels. Based on the Giant Yellowknife Mines Ltd. operation a 294 kg/day ozonation plant would be required to treat the cyanide stream at an estimated capital cost of 1.2 million dollars and before tax operating costs near $300,000 per year.

ACKNOWLEDGEMENT

The author wishes to gratefully acknowledge the support provided by Dr. F. D. Otto for the study and the continued interest of Mr. G. A. Webster, Environmental Protection Services, Fisheries and Environment Canada.

The prompt and excellent co-operation of the Department of Chemical Engineering technical staff, particularly Mr. J. Moser, is much appreciated.

The author also wishes to acknowledge with thanks the Department of Fisheries and Environment for the education leave opportunity, Giant Yellowknife Mines Ltd., and CanMet, Department of Energy, Mines and Resources.

TABLE OF CONTENTS


| CHAPTER OR SECTION | | PAGE |
|---|---|---|
| 1 | INTRODUCTION | 1 |
| 2 | LITERATURE REVIEW AND THEORY | 4 |
| 2.1 | The Cause; Cyanide Chemistry | 4 |
| 2.2 | The Effect; Biological Response to Cyanide | 11 |
| 2.3 | Treatment; Ozonation of Cyanide | 13 |
| 2.3.1 | Ozone Characteristics | 13 |
| 2.3.2 | Ozone Generation | 15 |
| 2.3.3 | Ozone Oxidation of Cyanide | 16 |
| 2.3.3.1 | Mass Transfer Studies | 19 |
| 2.4 | Mass Transfer Fundamentals | 22 |
| 2.4.1 | Physical Mass Transfer | 22 |
| 2.4.1.1 | Film Theory | 23 |
| 2.4.1.2 | Penetration Theory | 24 |
| 2.4.1.3 | Surface Renewal Theory | 26 |
| 2.4.2 | Simultaneous Absorption & Chemical Reaction | 27 |
| 2.4.2.1 | Slow Reaction Regime | 28 |
| 2.4.2.1.1 | Diffusional Sub-regime | 29 |
| 2.4.2.1.2 | Kinetic Sub-regime | 29 |
| 2.4.2.2 | Fast Reaction Regime | 30 |
| 2.4.2.3 | Instantaneous Regime | 31 |
| 2.4.2.4 | Transition from Fast to Instantaneous Reaction Regimes | 33 |
| 2.5 | Summary | 34 |

| CHAPTER OR SECTION | | PAGE |
|---|---|---|
| 3 | EXPERIMENTAL | 36 |
| 3.1 | Choice of System | 36 |
| 3.2 | Description of Apparatus | 37 |
| 3.2.1 | Reactor | 37 |
| 3.2.2 | Auxiliary Equipment | 40 |
| 3.2.2.1 | Ozone-Cyanide Studies | 40 |
| 3.2.2.2 | Treatability System | 43 |
| 3.3 | Quantification of Reactor Characteristics | 45 |
| 3.3.1 | Equipment Modifications for Reactor Quantification | 47 |
| 3.3.1.1 | Residence Time Distribution System | 47 |
| 3.3.1.2 | Carbon Dioxide - Water System | 47 |
| 3.3.1.3 | Sulphur Dioxide - Sodium Hydroxide System | 47 |
| 3.4 | Procedure | 49 |
| 3.4.1 | Equipment Operation | 49 |
| 3.4.1.1 | Procedure Common to Residence Time Distribution, $CO_2$ Absorption, Ozone-Cyanide and Sulphur Dioxide Study Phases | 49 |
| 3.4.1.2 | Ozone-Cyanide System Procedure | 50 |
| 3.4.1.3 | Treatability Studies Procedure | 53 |
| 3.4.1.4 | Residence Time Distribution Procedure | 54 |
| 3.4.1.5 | $CO_2$ Absorption into Water Procedure | 55 |
| 3.4.1.6 | $SO_2$ Absorption into NaOH Solution Procedure | 56 |
| 3.4.2 | Analytical Procedures | 56 |

| CHAPTER OR SECTION | | | PAGE |
|---|---|---|---|
| 3.4.2.1 | | Ozone-Cyanide and Treatability Systems | 56 |
| 3.4.2.1.1 | | Cyanide | 56 |
| 3.4.2.1.2 | | Ozone in Air | 60 |
| 3.4.2.2 | | Residence Time Distribution | 60 |
| 3.4.2.3 | | Carbon Dioxide-Water System | 61 |
| 3.4.2.4 | | Sulphur Dioxide Absorption into Sodium Hydroxide System | 61 |
| 3.5 | Treatment of Data | | 62 |
| 3.5.1 | | Residence Time Distribution | 62 |
| 3.5.2 | | Physical Mass Transfer Measurement | 64 |
| 3.5.3 | | Measurement of Gas Phase Resistance | 65 |
| 3.5.4 | | Absorption with Simultaneous Chemical Reaction - Simple Cyanide Reactions | 66 |
| 3.5.4.1 | | Mass Transfer Characteristics | 66 |
| 3.5.4.2 | | Calculation of Kinetic Constants | 68 |
| 3.5.4.2.1 | | Transition Regime | 68 |
| 3.5.4.2.2 | | Fast Reaction Regime | 70 |
| 3.5.5 | | Complex Cyanide Reactions | 72 |
| 3.5.5.1 | | Mass Transfer Studies | 72 |
| 3.5.5.2 | | Treatability Studies | 73 |
| 4 | RESULTS | | 74 |
| 4.1 | Residence Time Distribution | | 74 |
| 4.2 | Carbon Dioxide Absorption | | 77 |
| 4.2.1 | | Ozone-Water Physical Transfer Coefficients | 79 |

| CHAPTER OR SECTION | | PAGE |
|---|---|---|
| 4.3 | Sulphur Dioxide Absorption into Sodium Hydroxide | 79 |
| 4.4 | Ozone Absorption & Simultaneous Reaction with Cyanide | 81 |
| 4.4.1 | Simple Cyanide Reactions | 81 |
| 4.4.1.1 | Mass Transfer Coefficients | 85 |
| 4.4.1.1.1 | Affect of Changing Hydrodynamics | 85 |
| 4.4.1.2 | Kinetic Constants | 87 |
| 4.4.1.2.1 | Transition Regime Model | 87 |
| 4.4.1.2.2 | Fast Reaction Regime Model | 89 |
| 4.4.2 | Ozonation of Giant Yellowknife Mines' Barren Bleed | 93 |
| 4.4.2.1 | Treatability Studies | 93 |
| 4.4.2.1.1 | Ozone Uptake | 97 |
| 4.4.2.1.2 | Observed Solution Change During Ozonation | 97 |
| 4.4.2.2 | Mass Transfer Studies | 100 |
| 4.4.2.2.1 | Ozone Uptake | 100 |
| 4.4.2.2.2 | Mass Transfer Coefficient | 104 |
| 4.4.2.2.3 | Instantaneous Reaction Regime | 104 |
| 5 | DISCUSSION | 106 |
| 5.1 | Treatability | 106 |
| 5.2 | Ozone Use | 107 |
| 5.3 | Enhancement Factors | 108 |
| 5.3.1 | Affect of Physical Mass Transfer Coefficient | 108 |
| 5.3.2 | Affect of Ozone Decomposition | 109 |

| CHAPTER OR SECTION | | | PAGE |
|---|---|---|---|
| 5.3.3 | | Affect of Gas Phase Resistance | 111 |
| 5.4 | Kinetic Data | | 111 |
| 5.4.1 | | Temperature Effects | 112 |
| 5.4.2 | | Verification of Reaction Regime Applicability | 113 |
| 5.4.3 | | Ratio of the Cyanide to Cyanate Rate Constants | 114 |
| 5.4.4 | | Affect of $D_2/D_1$ | 115 |
| 5.5 | Economic Evaluation | | 115 |
| 6 | CONCLUSIONS AND RECOMMENDATIONS | | 122 |
| 6.1 | Conclusions | | 122 |
| 6.2 | Recommendations | | 125 |
| BIBLIOGRAPHY | | | 127 |
| APPENDIX A | Analytical Methods | | 133 |
| | A-1 | Details of Silver Nitrate Titration | 134 |
| | A-2 | Carbon Dioxide Measurement | 135 |
| APPENDIX B | Reactor Conditions and Detailed Results | | 139 |
| APPENDIX C | Calculation Details | | 142 |
| | C-1 | Diffusivities of Ozone and Cyanide in Water | 143 |
| | C-2 | Mass Transfer Coefficient for Carbon Dioxide Water System | 147 |

CHAPTER OR SECTION PAGE

C-3 Gas Phase Resistance from $SO_2$ Absorption Study 149

C-4 Calculation of $k_L$ and I based on Run II Data (Simple Cyanide System) 153

C-5 Calculation of Kinetic Constants 157

C-6 Calculations for Barren Bleed Runs 160

LIST OF TABLES


| | | PAGE |
|---|---|---|
| 1 | Mass Transfer Coefficient for Ozone-Water System @ 25°C | 80 |
| 2 | Gas Phase Mass Transfer Coefficients | 81 |
| 3 | Gas Phase Operating Conditions for $O_3$ Absorption Into NaCN Solutions | 82 |
| 4 | Liquid Phase Reactor Conditions for $O_3$ Absorption Into NaCN Solutions | 83 |
| 5 | Measured Liquid Phase Mass Transfer Coefficients and Associated Enhancement Factors | 84 |
| 6 | Enhancement Factors and Calculated Kinetic Constants Using Transition Regime | 90 |
| 7 | Fast Reaction Regime Calculated Results | 92 |
| 8 | Reactor Conditions for $O_3$ Absorption Into Barren Bleed Solution | 101 |
| 9 | Results of $O_3$ Absorption Into Barren Bleed Solution | 102 |
| 10 | Barren Bleed Characteristics of Giant Yellowknife Mine | 116 |
| 11 | Economic Evaluation | 119 |
| 12 | Cost of Financing and Repayment Schedule for a Loan of $1,200,000 @ 12% Over 10 Years | 120 |
| 13 | Profit/Loss Schedule and Cash Flow Statement | 121 |
| B.1 | Reactor Conditions and Results - $CO_2$ Absorption Into Water | 140 |
| B.2 | Barren Bleed Runs - Contact Conditions and Solution Analyses | 141 |
| C.1 | Run II Data | 152 |

## LIST OF FIGURES


| | | PAGE |
|---|---|---|
| 1A | Boundary Contour Diagram of d Orbital | 6 |
| 1B | Energy Level Diagram for d Orbitals Splitting in an Octahedral Field | 6 |
| 2 | Quiescent Surface Reactor | 38 |
| 3 | Equipment Configuration - Mass Transfer Studies | 41 |
| 4 | Equipment Configuration - Treatability Studies | 44 |
| 5 | Equipment Modifcations - Reactor Quantification Studies | 48 |
| 6 | Response Curves - Residence Time Distribution - Sodium Chloride Tracer | 75 |
| 7 | Residence Time Distribution - Hydrochloric Acid Tracer | 76 |
| 8 | $k_L^o$ for Carbon Dioxide Absorption Into Water versus Stirring Speed | 78 |
| 9 | I verus $k_L^o$ for Runs 1-27 Showing Pairing Based on the Same Value of $b_o$ (approximately) | 86 |
| 10 | I versus Modified Reaction Modulus | 94 |
| 11 | Rate of Ozonation of Cyanides - Giant Yellowknife Mine Barren Solution | 95 |
| 12 | Ozone Uptake During Ozonation of Barren Bleed | 96 |
| A.1 | Typical Potentiometric Titration Curve for Carbon Dioxide Back Titration and NaOH Titration with HCl | 137 |
| C.1 | Equivalent Conductance vs Concentration - KCNS | 145 |
| C.2 | Equivalent Conductance vs Concetration - KCN | 145 |

## NOMENCLATURE

m, mole; M, mass; L, length; t, time

| | |
|---|---|
| $a$ | interfacial area, $L^2$ |
| $a_i$ | interfacial area per unit volume of absorber, $L^{-1}$ |
| $b$ | concentration of cyanide reactant, $mL^{-3}$ or $ML^{-3}$ |
| $b_i$ | initial concentration of cyanide, $mL^{-3}$ or $ML^{-3}$ |
| $b_o$ | bulk liquid value of b, $mL^{-3}$ or $ML^{-3}$ |
| $b_N$ | cyanate concentration, $mL^{-3}$ or $ML^{-3}$ |
| $b_T$ | thiocyanate concentration, $mL^{-3}$ or $ML^{-3}$ |
| B | bubbled system |
| $c$ | concentration of absorbing gas in liquid, $mL^{-3}$ or $ML^{-3}$ |
| $c'$ | equilibrium value of c, $mL^{-3}$ or $ML^{-3}$ |
| $c_o$ | bulk-liquid value of c, $mL^{-3}$ or $ML^{-3}$ |
| $c_o'$ | interface value of c, $mL^{-3}$ or $ML^{-3}$ |
| C | tracer concentration, $mL^{-3}$ or μmho/cm |
| $C_o$ | initial tracer concentration, $mL^{-3}$ or μmho/cm |
| d | d oribital |
| $D_i$ | diffusivity of component i, $L^2t^{-1}$ |
| $D_1$ | diffusivity of absorbing component into a solvent, $L^2t^{-1}$ |
| $D_2$ | diffusivity of cyanide, $L^2t^{-1}$ |
| $D_3$ | diffusivity of cyanate reactant, $L^2t^{-1}$ |
| $D_4$ | diffusivity of thiocyanate, $L^2t^{-1}$ |
| E | energy level |
| e | exponential |

| | |
|---|---|
| $k$ | kinetic constant for cyanide reaction, $L^{3}m^{-1}t^{-1}$ or $t^{-1}$ |
| $k'$ | kinetic constant, $L^{3}m^{-1}t^{-1}$ or $t^{-1}$ |
| $k_1$ | extended kinetic constant, $L^{3}m^{-1}t^{-1}$ or $t^{-1}$ |
| $k_2$ | kinetic constant for cyanate reaction, $L^{3}m^{-1}t^{-1}$ |
| $k_3$ | kinetic constant for thiocyanate reaction, $L^{3}m^{-1}t^{-1}$ |
| $k_L$ | chemical absorption coefficient, $Lt^{-1}$ |
| $k_L^o$ | physical absorption coefficient, $Lt^{-1}$ |
| $K_L$ | overall chemical absorption coefficient, $Lt^{-1}$ |
| $K_L^o$ | overall physical absorption coefficient, $Lt^{-1}$ |
| $k_G$ | gas phase absorption coefficient, $mL^{-2}t^{-1}atm^{-1}$ |
| $k_g$ | gas phase absorption coefficient, $Lt^{-1}$ |
| $K$ | equilibrium constant. Units depend on stoichiometry of reaction. |
| $H$ | Henry's constant, $L^{3}m^{-1}$ or atm $L^{3}m^{-1}$ |
| $I$ | $k_L/k_L^o$, dimensionless |
| $I_\infty$ | asymptotic value of I, dimensionless |
| $n_\pm$ | valence of cation or anion |
| $N$ | normality, $mL^{-3}$ |
| $M$ | $= t_D/t_r$, reaction modulus, dimensionless |
| $P$ | pressure, $ML^{-2}$ (atm.) |
| $p$ | partial pressure, $ML^{-2}$ (atm.) |
| $Q$ | flow rate, $L^{3}t^{-1}$ |
| $q$ | stoichiometric coefficient, dimensionless |
| $r$ | reaction rate, $mL^{-3}t^{-1}$ |
| $s$ | stirring speed, rpm |
| $s'$ | Danckwerts' model parameter, $t^{-1}$ |

| | |
|---|---|
| S | sparged system |
| R | gas constant, $Jm^{-1}\ K^{-1}$ or atm $L^3_m{}^{-1}\ K^{-1}$ |
| $R_T$ | ozone absorption rate, $mL^{-3}t^{-1}$ |
| $R_c$ | cyanide destruction rate, $mL^{-3}t^{-1}$ |
| t | time, t |
| $t^*$ | Higbie model parameter, $t^{-1}$ |
| $t_r$ | reaction time, t |
| $t_D$ | diffusion time, t |
| T | temperature, $^oC$ or K |
| v | volume, $L^3$ |
| V | instantaneous rate of chemical absorption per unit interfacial area, $mL^{-2}t^{-1}$ |
| $V^o$ | instantaneous rate of physical absorption per unit interfacial area, $mL^{-2}t^{-1}$ |
| $\overline{V}$ | average rate of chemical absorption per unit interfacial area, $mL^{-2}t^{-1}$ |
| $\overline{V}^o$ | average rate of physical absorption per unit interfacial area, $mL^{-2}t^{-1}$ |
| $u_\pm$ | ionic mobility |
| x | directional parameter, L |
| y | directional parameter, L |
| z | direction parameter, L |
| erf | error function |
| $\Psi$ | age distribution function, $t^{-1}$ |
| $\tau$ | value of x where c=c', L |
| $\pi$ | pi |
| $\delta$ | film thickness, L |

| | | |
|---|---|---|
| $\Phi$ | | volume of liquid per unit interfacial area, L |
| [ ] | | concentration symbol |
| [[ ]] | | function of |
| $\mu$ | | viscosity of solution, centipoise |
| $\upsilon$ | | solute molal volume at boiling point, $L^3m^{-1}$ |
| $\xi$ | | energy of molecular interaction, ergs. |
| $\bar{\theta}$ | | average residence time, t |
| Jn(t) | | residence time distribution function; t |
| $\Lambda$ | | electrolyte conductance, mhos equivalent$^{-1}$ |
| F | | Faraday = 96500 C/g equivalent |
| $\lambda\pm$ | | limiting ionic conductance, mhos equivalent$^{-1}$ |
| $\alpha$ | | diffusivity for reaction plane, $L^2t^{-1}$ |
| Subscripts | F | simple cyanide |
| | R | total cyanide |
| | N | cyanate |
| | T | thiocyanate |
| | i | initial |
| | o | bulk phase |
| | n | nth order reaction |
| | av | average |
| | $\ell$ | liquid |
| | y | numerical parameter |
| | x | numerical parameter |
| Superscripts | o | physical absorption |

# 1 INTRODUCTION

Currently, the gold mining industry through Canada utilizes the cyanide leach recovery system for extracting gold from the host ore. Variation of the flotation circuits and beneficiation do occur but the final step in the recovery of gold requires the formation of a gold-cyanide complex which allows for replacement of gold by zinc, thus precipitating the gold out of solution.

Almost inevitably the cyanide rich stream becomes contaminated by other metals, primarily copper, present in the ore and recovery efficiency would decrease if precautions were not taken. The precaution is the bleeding of some of the stream with replacement by fresh water.

The waste "barren bleed" usually joins with other wastewater flows, including the tailings solids, and is deposited into the tailings pond. The cyanide, relying on chemical oxidation for destruction, is deposited approximately at the same concentration to the receiving waters. Common discharge rates are 0.75-1.1 cubic meters per day per ton of ore milled containing 30-50 mg/L cyanide.

Cyanide is an extremely toxic agent and the adverse effects of this practice of gold mining wastewater deposition have been documented by *Wallace and Hardin (1974)*. Cyanide toxicity to *Salmo gairdneri* Richardson (Rainbow trout) has been reported by *Herbert and Merkins (1952)* as a mean survival time of 74 hours for 0.07 mg/L KCN and 2.66 min for 2.0 mg/L KCN.

Not withstanding the synergisms caused by complexing with metals and the toxicity exerted by the other pollutants, the need for waste treatment is obvious.

Treatment for gold mining wastes has not been employed in Canada with the exception of a small cyanide recovery unit at Hudson Bay Mining & Smelting Co. Ltd. operation in Flin Flon, Manitoba. At this location cyanide recovery by acidification was performed until 1975 when gold recovery was suspended.

As cyanide is susceptible to oxidation it is possible that ozonation, currently gaining global popularity for wastewater treatment, could be used as a treatment mechanism. In fact, several electroplating operations utilize ozone to treat cyanide bath solutions.

In order to explore the practicality and the possibilities of ozonation of electroplating and gold mining wastes, previous bench studies (*Sondak and Dodge (1961), Khandelwal et al. (1959), Balyanskii et al. (1978)* and others) have been reported in the literature. These studies set out to expand the knowledge of ozone chemistry, kinetics and mass transfer; unfortunately most of the results are specific to the system being used with the kinetic and mass transfer properties interwoven into an overall rate constant. *Heist (1973)* indicated "the determination of basic ozone mass transfer properties from the gas to water have been largely unexplored." Since that time more detailed work has been conducted by *Richards and Fleischman (1976)*; however, this work was primarily related to physical absorp tion of ozone into water. Reacting systems with enhancement of mass transfer by way of a chemical reaction have not been used successfully to determine fundamental kinetic data for ozonation of cyanide.

Thus, in 1974 this study was undertaken to address the following objectives:

(1) Design an experiment to facilitate the comparison of physical transfer of ozone from the gas phase to the liquid phase with that of ozone transfer enhanced by a reaction occurring in the liquid phase.

(2) Obtain the true mass transfer characteristics of ozone in a reacting system with cyanide and utilize this information, if possible, to obtain a reaction rate constant for the ozone cyanide reaction.

(3) Evaluate the treatment of gold milling wastewater using ozone and determine the practicality of such a treatment system with regards to both capital cost and operational costs.

(4) Compare ozone destruction of synthetic cyanide wastewaters and a gold mine barren bleed. For the purposes of the study mill barren solution from Giant Yellowknife Mines Ltd. was used.

## 2 LITERATURE REVIEW AND THEORY

In order to conduct this study it was important to be aware of previous work on ozonation of cyanide wastes, the chemistry of cyanide and ozone, mass transfer principles and techniques and, to a lesser degree, the effects of a chemical such as cyanide on an aquatic ecosystem. The latter point did not influence the experimental design, however, the toxicological effect on aquatic life necessitated the study and dictated the treatment levels required to adequately "safeguard" that resource. To facilitate this understanding this section will be divided into the following categories;

(1) the cause; cyanide chemistry

(2) the effect; biological response to cyanides

(3) the treatment; ozonation of cyanide and ozone chemistry

(4) insights to treatment design; mass transfer with simultaneous chemical reaction and,

(5) a summary relating the above to experimental design.

### 2.1 The Cause; Cyanide Chemistry

Gold mine processing solutions and wastes contain both waste cyanide and trace amounts of metals available in the ores as well as zinc, which is added as a process reagent. The stability of the complex compounds formed by cyanide and metal elements is defined through the ligand field theory.

Cyanide is a ligand having the strongest ligand field of all common ligands. Ligands, which are regions of negative charge,

most strongly affect d orbitals. The transition metals are elements which have d electrons and incompletely filled d orbitals.

If one envisages a cartesian coordinate system with a ligand symmetrically placed on each of the six axes, the d orbitals are traditionally arranged and labelled as per Figure 1A. This results in the $d_{xy}$, $d_{xz}$ and $d_{yz}$ orbitals having the greatest density of electrons between the coordinate axes while the $d_{x^2y^2}$ and the $d_{z^2}$ orbitals have the greatest electron density in the direction of the axes. As the imaginary ligands are brought toward the center, electrostatic repulsive forces are stronger on the $d_{x^2y^2}$ and $d_{z^2}$ than on the other three and hence, the d orbitals "split" into higher and lower energy doubled and tripled orbitals, respectively. The magnitude of this splitting is designated $\Delta E$. Figure 1B visually shows in an energy level diagram the splitting of the orbitals and the $\Delta E$ associated with the split.

Zero energy is arbitrarily taken as the weighted mean of the energies of these two sets of orbitals and hence, the lower three orbitals are stabilized by $-2/5\ \Delta E$ while the higher energy orbitals are destabilized by $3/5\ \Delta E$. The size of $\Delta E$ is obtained by spectroscopically observing the electronic transitions between the two sets of orbitals. By examining a series of complexes using different ligands, the ligand effects can be ordered in increasing ligand field resulting in cyanide being the strongest. The measured transitions occur in the visible or near ultra-violet and is the reason for the strong colours of metal ligand compounds.

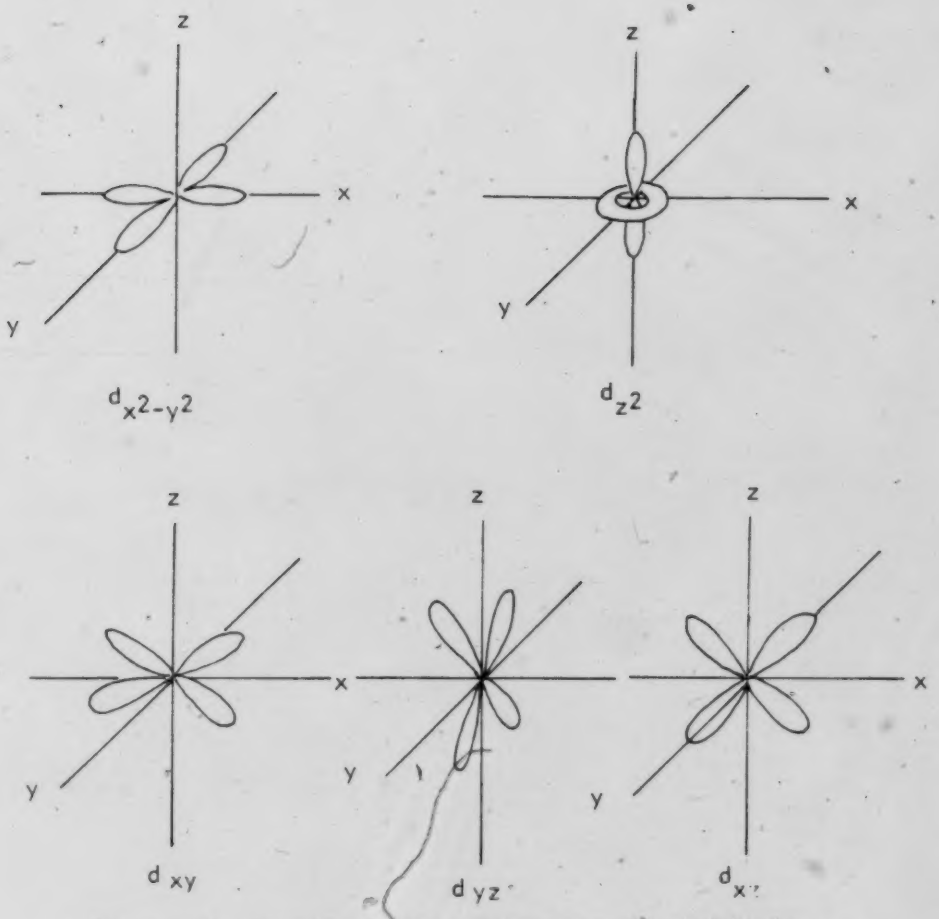


Figure 1A Boundry Contour Diagrams of d Orbitals

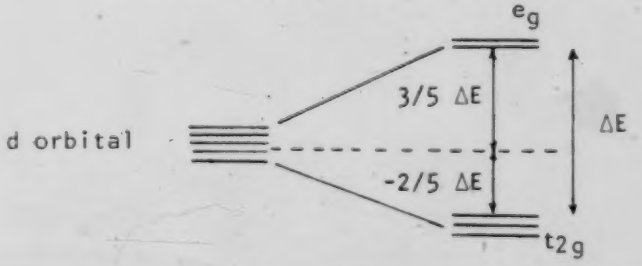


Figure 1B Energy Level Diagram for d Orbitals Splitting in an Octahedral Field

The stability exhibited by the ligand field can be demonstrated by assuming a metal with one d electron (or $d_1$) is complexed. The one electron falls into the orbital of lowest energy, namely one of the lower set orbitals, or $t_{2g}$ orbitals, and the complex is stabilized by -2/5 $\Delta E$.

With cyanide exhibiting the strongest ligand field the stability of the metal complexes is readily understood and in fact ferrocyanide (or the $Fe^{II}$ $(d_6)$) -cyanide complex is stabilized by $-\frac{12}{5}\Delta E$ and is a very stable compound. The significance of this stability will be discussed in section 4.4.2.1.

A wide variety of cyanide metal complexes form and these include such combinations as ferrous ferrocyanide and cuprous ferrocyanide. The presence of the latter was suspected in the barren solution from Giant Yellowknife Mines.

There are several general categories of cyanides. They are free cyanide, simple cyanides and complex cyanides. Free cyanide is simply a triple bonded carbon-nitrogen ion. The localization of electrons suggests it would be susceptible to electrophillic attack, or oxidation. Simple cyanides, such as NaCN or KCN, in water generate HCN. The HCN dissociates into hydrogen and cyanide ions according to;

$$HCN \rightleftharpoons H^+ + CN^- \qquad \ldots\ldots (2.1)$$

until the equilibrium equation

$$\frac{[H^+]\,[CN^-]}{[HCN]} = 7.2 \times 10^{-10} \text{ @ } 25^{\circ}C \qquad \ldots\ldots (2.2)$$

is satisfied. The pH dependence of this relationship is obvious and in fact at pH values below 7 less than 1% of the cyanide molecules are in ion form; at pH 9, only 42%; and at pH 10, 87%. Complex

cyanides, are defined by the chemical formula $A_yM(CN)_x$, where A is an alkali and M is a heavy metal. A complete compilation of cyanide chemistry was written by *Ford-Smith (1964)*. The expression "total cyanide" is sometimes found in the literature. This is the total amount of CN ligand present in any form. This excludes cyanate, $CNO^-$, and thiocyanate, CNS, which are considered separate ligands.

Many terms are given in the literature to describe forms of cyanide in solution. Adjectives such as free, simple, available, chlorine amenable or oxidizable, complex and total lead to considerable confusion when attempting to determine the actual amount and type of cyanide present in treated solutions. In most cases, the appropriate adjective is a function of the analytical method used to determine cyanide in solution.

The following definitions will be used when necessary in this work:

Free cyanide - Determined by selective ion electrode or silver nitrate titration the cyanide measured is in the ionic form as $CN^-$.

Simple cyanide - The alkali or metal compound giving a salt formula $A(CN)_x$, where A is the alkali or metal and x is the valence of A. In solution the CN group is present as free cyanide, $CN^-$.

Complex cyanide - There are many forms of complex cyanides. The most common are the alkali metallic cyanide complexes represented by $A_yM(CN)_x$, where A is the alkali present y times, M is a heavy metal and x is the number of CN groups.

Some complex cyanides are metallic-metallic cyanides where the alkali, A, is replaced by a metal. The soluble product of these complexes is not $CN^-$ but a radical $M(CN)_x$. Complex cyanides are measured by the more labour intensive and difficult techniques. Distillation with acid-reflux, ultra-violet irradiation with acid distillation and other methods promoting vapour HCN with colorimetric determination are used to varying degrees of success. The difficulty of obtaining the true value rests with the stability of the complex cyanide species. The more stable the complex the more elaborate the analytical method required to break the complex converting it to a free cyanide form in acid solution. Generally, the cobalt and iron complexes are extremely difficult to destroy.

The above three definitions are based on chemical form and cover all the forms of cyanide present in solution save for the cyanate, $CNO^-$, and thiocyanate, $CNS^-$, forms. Most papers do not include these in any definition of cyanide choosing to identify them as separate ligands distinct from the CN group. This is generally acceptable however some analytical methods for cyanide determination, namely the ultra-violet stimulation techniques, result in $CNS^-$ breakdown to $CN^-$. Caution is thus required in interpretation of the results based on these analytical methods.

Apart from the definitions based on chemical form there are a set of adjectives used which attempt to provide an indication of the stablity of the complex and simple cyanides. Definitions of these are:

Total cyanide - in most cases, this is meant to include all cyanides present except for cyanate and thiocyanate. Unfortunately, it is likely that most studies did not utilize analytical methods commensurate with the definition. Only the ultra-violet light methods subtracting the thiocyanate component would give a total cyanide value. Some recent papers are beginning to use the term total cyanides inclusive of cyanate and thiocyanate. This is incorrect if the ligand $CN^-$ is meant as cyanide.

Available cyanide, chlorine amenable/oxidizable - in many cases in waste treatment the desire is to reduce deleterious substances to below harmful levels. It has been reported by *Doudoroff (1956)* that the toxicity of complex cyanides is due to molecular hydrogen cyanide formation caused by metal cyanide dissociation. Thus, assuming the very stable components do not result in toxicity, a classification can be made for those substances that are likely to be toxic. This category of simple and complex cyanides measures only those substances that are in solution that can be destroyed by an oxidant; usually chlorine. Analytically this category is determined by performing an acid distillation and color development (classical method) on both raw and chlorine treated samples. The difference is the cyanides amenable to chlorine. The error inherent in subtractive methods must be considered when assessing results. A short cut method exists where cyanide (complexed and free) is converted to the maximum degree possible to cyanogen chloride through addition of chlorine under slightly acidic conditions. (NOTE: Under alkaline conditions cyanogen chloride hydrolyses to

cyanate. This is the alkaline chlorination treatment technique.) Cyanogen chloride is determined colorimetrically and related to cyanide in solution. This category does not include iron or cobalt cyanides.

## 2.2 The Effect; Biological Response to Cyanides

Although it is imperative that all levels of an aquatic ecosystem be maintained, the principle control mechanism to assess the acceptability of an effluent is the toxic response of fish subjected to that solution. The results of this form of bioassay has been reported widely in the literature for cyanide toxicity to various fishes. Cyanide toxicity is dependent primarily on dissolved oxygen content, temperature, pH and mineral concentration and type. The latter two are of main concern to this study.

*Wuhrmann and Woker (1948)* demonstrated that molecular HCN rather than the $CN^-$ ion seemed to be the major toxic constituent. Hence, in accordance with equation 2.2, the lower the pH the greater the cyanide induced toxicity. *Herbert and Merkins (1952)* demonstrated that in a pH range of 7.4 to 8.0, Rainbow trout *(Salmo gairdneri* Richarson) died in continually replenished solutions of as little as 0.07 mg/L cyanide (as $CN^-$). The *Ohio River Valley Sanitation Commission (1960)* recommended establishment of a free cyanide permissible concentration of 0.025 mg/L in receiving waters based largely on this fact.

Cyanide exerts its toxic effect in a number of ways. *Holden and Marsden (1966)* found cyanide concentrations in the gills of fish proportional to cyanide concentrations in the test solutions. High

concentrations were also found in the brain and liver. *McKee and Wolfe (1963)* report the gills become brighter in color to those of normal fish. They suggest this is due to cyanide inhibiting the oxidase responsible for transferring oxygen from the blood to the tissues. The ability of cyanide to strongly complex iron in the hemoglobin eliminates the possibility of oxygen transfer and is one mechanism of cyanide toxicity.

The presence of metals affects the toxic influence of cyanide. In comparative tests to sodium cyanide, zinc and cadmium sulphate added to a sodium cyanide solution proved considerably more toxic than an equivalent cyanide concentration solution. Conversely, nickel cyanide proved to be less toxic than free cyanide at higher pH values. However, when the pH was reduced the toxicity increased up to that exhibited by free cyanide of the same concentration. The dissociation of nickel cyanide and the synergistic effects of zinc and cadmium accounts for this behavior.

Copper and iron appear to detoxify cyanide. Up to 1.0 mg/L $CN^-$ in the presence of 1.0 mg/L Cu did not prove toxic *(Doudoroff (1956))* to fish over a 96 hour test. The complexed copper cyanide proved less toxic than either of its parent species as copper is lethal to fish at approximately 0.1 mg/L. The very stable ferro-cyanide and ferricyanide complexes were used for bioassay testing by *Burdick and Lipschuetz (1948)*. They determined that these compounds were not toxic *per se*, however, they deteriorated with sunlight and increased temperature such that the cyanide ($CN^-$) generated proved toxic at levels of iron cyanides down to about 1-2 mg/L.

It is desirable to establish treatment limits to produce a non-acutely toxic effluent. From the foregoing discussion these limits should require that free cyanide, zinc cyanide and cadmium cyanide be virtually absent while ferrocyanide, cuprous and nickelocyanide may be tolerated at cumulative levels of around 1-2 mg/L. The initial goal of this program was set at a total cyanide concentration in treated solution of 0.1 mg/L.

## 2.3 Treatment; Ozonation of Cyanide

### 2.3.1 Ozone Characteristics

Ozone is an unstable blue gas. Its density is approximately 1.5 times that of oxygen and its solubility in distilled water is approximately 10 times that of oxygen. It has an approximate half-life in water of 15 minutes, which is dependent upon pH. It is toxic and has an odor similar to that of chlorine. It is the fourth most powerful oxidizing agent known following $F_2$, $F_2O$ and the oxygen radical.

Ozone decomposition in aqueous solutions has been investigated by *Alder and Hill (1950)*. They reported the following mechanism:

$$O_3 + H_2O \overset{k1}{\rightarrow} HO_3^+ + OH^- \quad \ldots\ldots (2.3)$$

$$HO_3^+ + OH^- \underset{k2'}{\overset{k2}{\rightleftarrows}} 2HO_2 \quad \ldots\ldots (2.4)$$

$$O_3 + HO_2 \overset{k3}{\rightarrow} HO + 2O_2 \quad \ldots\ldots (2.5)$$

$$HO + HO_2 \overset{k4}{\rightarrow} H_2O + O_2 \quad \ldots\ldots (2.6)$$

The kinetics of ozone decomposition was found to be first order with respect to ozone concentration over a pH range of 1-2.8.

*Hewes and Davison (1971)* reviewed available ozone decomposition studies and found deviations from the *Alder and Hill (1950)* results. They found the rate of ozone decomposition to be second order

with respect to ozone over a pH range of 2-4, three halves to second order at pH 6 and first order at pH 8. This supported *Stumm (1954)*. Stumm found a first order ozone decomposition rate expression, namely;

rate of ozone decomposition = $-k[OH]^{0.75}[O_3]$ gmole/L s ..... (2.7)

over a pH range of 7.6 to 10.4. The experimental value for k was found to be 242 $s^{-1}(L/gmole)^{0.75}$ @ 18°C.

*Hewes and Davison (1971)* correlated the rate of ozone reaction with organics in flocculated secondary sewage effluents to be dependent upon ozone composition and independent of subsequent organic reactions. They postulated that free radicals formed by ozone decomposition were the principal reacting species, not ozone.

Recent articles by *Melnyk and Netzer (1977)*, *Shambaugh and Melnyk (1976)* and *Shambaugh and Melnyk (1977)* have discussed ozone decomposition in the liquid phase. These papers utilize the correlation generated by *Stumm (1954)* and assume ozone decomposes to a product which plays no further part in oxidation reactions. All three of the former papers assume saturated ozone conditions in the bulk liquid phase. *Lee et al. (1977)* proposes a decomposition mechanism with free radical products including nascent oxygen which is a more powerful oxidizing agent than ozone *(Evans (1972))*. All investigators agree that pH influences decomposition and at pH conditions similar to those used for this work, pseudo first order decomposition kinetic constants in the range of 15-25 $s^{-1}$ could be expected. Most ozone decomposition theories are based on *Stumm (1954)* and *Hewes and Davison (1971)*.

2.3.2 Ozone Generation

In a recent paper *(Hardisty and Rosen (1977))*, aspects of ozone generation were reviewed. Ozone is generated by imposing high AC voltage across a discharge gap in the presence of a gas containing oxygen. The process is inefficient as only approximately 10% of the energy supplied results in ozone production while the remainder primarily produces heat. Some factors in optimizing ozone yield are;

(1) type of dielectric material
(2) high frequency AC versus low frequency
(3) efficient heat removal
(4) reduced moisture content of gas
(5) pressure/gap combination constructed to maintain low voltage.

Recent advances in ozone technology, employing high frequencies have resulted in ozone production per square foot of electrode area 10 times that obtained by the 60Hz units of equal size *(Mathieu (1977))*. Mathieu reports that ozone concentrations of 3% by weight can be obtained economically when using an air feed. This increased gas concentration would result in increased solubilities and hence, enhanced oxidation *(Garrison et al. (1974))*.

Heat removal, necessary to prevent rapid ozone decomposition in the gas phase, has traditionally been through cooling water exchangers. A new generation of air-cooled ozone generators have recently been marketed which provide economy of plant size and operting cost *(Klein et al. (1975))*. These air cooled units require a $-40^{o}C$ dew point feed rather than the $-50^{o}C$ requirement for the water

cooled ozonators and power requirements are 18.7 kwh/kg and 6.6 kwh/kg to produce 1% ozone from air or oxygen feed, respectively *(Hardisty and Rosen (1977))*.

2.3.3 Ozone Oxidation of Cyanide

The multiple electron rich carbon-nitrogen bond of cyanide is a likely subject for the oxidation process. The reaction of ozone with cyanide has been reported by *Selm (1959)* to be very rapid. Whereas cyanide could ideally be oxidized to form carbon dioxide and nitrogen, he reports the relative stability of the intermediate product (Eqn. 2.8), cyanate, probably allows for the hydrolysis to ammonium carbonate (Eqn. 2.9) or the rearrangement to urea (Eqn. 2.10).

$$CN^- + O_3 \rightarrow CNO^- + O_2 \quad \ldots\ldots (2.8)$$

$$CNO^- + 2H^+ + H_2O \rightleftarrows CO_2 + NH_4^+ \quad \ldots\ldots (2.9)$$

$$CNO^- + NH_4^+ \rightleftarrows NH_2CONH_2 \quad \ldots\ldots (2.10)$$

The use of redox potential to trace cyanide destruction did not provide *Selm (1959)* with sufficient information required to determine a satisfactory overall reaction. *Tyler et al. (1951)* provided the unbalanced cyanate oxidation scheme of;

$$2CNO^- + H_2O + 3O_2 \rightarrow 2HCO_3^- + 3O_2 + N_2 \quad \ldots\ldots (2.11)$$

while more likely the mechanism postulated by *Walker and Zabban (1952)* occurs, namely;

$$2CNO^- + H_2O + 3O_3 \rightarrow 2HCO_3^- + N_2 + 3O_2 \quad \ldots\ldots (2.12)$$

*Balyanskii et al. (1972)* reported a nitrate product from the cyanate ozonation according to the unbalanced operation;

$$CNO^- + 4.5\ O_3 \xrightarrow{OH^-} 0.7\ NO_3 + 0.15\ N_2 + HCO_3^- \quad \ldots\ldots (2.13)$$

In accordance with equation 2.8 one mole of cyanide ions requires one mole of ozone. However, ozone demands of as low as 0.6-0.87 mole $O_3$/mole of $CN^-$ reported by *Walker and Zabban (1952)* gave rise to the suggestion that all oxygen atoms react simultaneously by the equation;

$$3CN^- + O_3 \rightarrow 3CNO^- \quad \ldots\ldots (2.14)$$

Contradictory more recent results support the mechanism of equation 2.8.

*Sondak and Dodge (1961)* and *Balyanskii et al. (1972)* have determined that the cyanate ozonation rate is approximately one-fifth that of the cyanide ozonation rate under the same experimental conditions.

The ability and likelihood of cyanide complexation with metals was reviewed in Section 2.1. Ozonation of cyanides has been generally accepted to be catalyzed by the presence of some metals, especially copper. Contrary to this tendency, *Sondak and Dodge (1961)* provided data suggesting the rate of ozone absorption with instantaneous cyanide destruction was controlled by gas phase resistance except at very low $CN^-$ concentrations; hence, catalysts in the liquid phase would not have appreciable effects on the rate. Unpublished test work performed by the Environmental Protection Service at the Canada Center for Inland Waters *(Leclair (1977))* supports the copper catalytic affect.

Mechanisms for metal cyanide ozonation were suggested by *Eiring (1969)*. In summary the following reactions were reported for zinc cyanide (under alkaline conditions).

$$Zn(CN)_4^{2-} \rightleftarrows Zn^{++} + 4CN^- \quad \ldots\ldots (2.15)$$

$$4CN^- + 2O_3 \rightarrow 4CNO^- + O_2 \quad \ldots\ldots (2.16)$$

$$Zn^{++} + 2OH^- \rightarrow Zn(OH)_2 \quad \ldots\ldots (2.17)$$

Zinc precipitates out of solution completely until the pH dependent equilibrium of zincates in water is satisfied. The dissociation constant of zinc cyanide has an order of $10^{-16}$.

The iron cyanide ozone reaction is given in Equation 2.18.

$$Fe(CN)_6^{4-} + O_3 + 2OH^- \rightarrow Fe(CN)_6^{3-} + 2O_2 + H_2O \quad \ldots\ldots (2.18)$$

No reduction in iron cyanide occurs, however the oxidation from ferro to the ferri form allows for ferricyanide photodecomposition to a mixture of ferric hydroxide, simple cyanide and hydrocyanic acid.

$$4Fe(CN)_6^{3-} + 12H_2O \overset{uv}{\rightleftarrows} 4Fe(OH)_3 + 12CN^- + 12HCN \quad \ldots\ldots (2.19)$$

Ferrocyanide is extremely stable in alkali or acid media and has a dissociation constant order of $10^{-37}$.

Nickelocyanide, with a dissociation constant of $1.0 \times 10^{-22}$, completely oxidizes under ozonation so that both simple and complex cyanides are destroyed and nickel hydroxide precipitates out of solution. The copper cyanide complex, $Cu(CN)_3^{2-}$, ($K=1 \times 10^{-24}$) is also readily oxidized under ozonation with hydroxide removal of the metal.

Thiocyanate, $CNS^-$, is usually found in the barren bleed waste stream in concentrations varying from 47-1000 mg/L *(Ritcey (1977))*. The stoichiometry of the thiocyanate ozonation, like cyanide and cyanate, is not clearly understood. *Kelada et al. (1977)* suggests

$$CNS^- + 3O_3 + 2OH^- \rightarrow CN^- + SO_4^{2-} + 3O_2 + H_2O \quad \ldots\ldots (2.20)$$

while *Nebel et al. (1976)* reports

$$CNS^- + 2O_3 + 3OH^- \rightarrow CN^- + SO_3^{2-} + 3O_2 + H_2O \quad \ldots\ldots (2.21)$$

As the latter equation is not balanced, the former (Eqn. 2.20) was used later in this work.

Arsenic is also present in some gold barren waste streams. In particular, this is the case with the gold mines in the Yellowknife area where arsenic is present in the gangue ore minerals, such as arsenopyrite. In this case, *Eiring (1969)* suggests the common trivalent state of arsenic will convert to the pentavalent state. Although the pentavalent state is soluble, precipitation of arsenic may occur, with excess CaO, as a calcium arsenate.

$$As_2O_3 + O_3 + 2OH^- \rightarrow As_2O_5 + H_2O + O_2 \quad \ldots\ldots (2.22)$$

$$As_2O_5 + 3Ca(OH)_2 + 4O_3 \rightarrow Ca_3(AsO_4) + 6O_2 + 3H_2O \ldots (2.23)$$

The influence of ozone decomposition, mentioned in Section 2.3.1, on the reaction between ozone and cyanides has not been reported in the literature. Some papers *(Eiring (1969), Ikehata (1975), Balyanskii et al. (1972)* and *Sondak and Dodge (1961))* report the enhancement of the cyanide ozonation at high pH. Two principal influences could contribute to this increase in rate; the dissociation of hydrogen cyanide mentioned previously and/or the impact of ozone decomposition products on cyanide oxidation.

2.3.3.1 Mass Transfer Studies

*Heist (1973)* reviewed ozonation literature. Previous ozone cyanide research for the most part failed to properly account for the influence of mass transfer on the rate of reaction thus resulting in the generation of an overall "rate constant" combining mass transfer properties and reaction kinetics.

*Khandelwal et al. (1959)* studied cyanide depletion when ozone was bubbled into a 1500 mL batch reactor and absorption tower. They concluded that the cyanide reaction is slow in comparison to the rate of solution of ozone and hence, the rate of reaction was controlling (kinetic regime - see Section 2.4.2.1.2). Khandelwal assumed ozone saturated the bulk liquid. Since a one-third order dependence (with respect to cyanide) was found as well as a lack of a temperature effect on rate, it is likely that both mass transfer and chemical reaction were influencing the results.

*Selm (1957)* utilized redox potential to monitor cyanide depletion during ozonation. Results obtained did not provide sufficient detail to develop a rate expression.

*Balyanskii et al. (1972)* batch tested cyanide solutions by bubbling ozone into a 320 mL vessel. They report that the rate of oxidation of cyanide depended on the rate of bubbling, implying mass transfer controlled their experiment. The rate expressions, determined to be first order thus derived, did not give insights into the reaction kinetics.

*Sondak and Dodge (1961)*, using a bubble batch reactor with a capacity of 3.5 L, concluded that their results correlated to film theory absorption accompanied by instantaneous chemical reaction. Like *Khandelwal et al. (1959)*, they found the reaction to be independent of temperatures between 20° and 80°C. *Sondak and Dodge (1961)*, utilizing Hatta's theory of instantaneous reaction and simultaneous absorption, indicate the absorption rate in the absorption column is expressed by

$$\overline{V} = k_G a A h p_{av} \quad \ldots\ldots (2.24)$$

where $k_G$ is the gas phase transfer coefficient, a is the interfacial area per unit volume of absorber, A is the cross-sectional area of the absorber, h is the height of the absorber and $p_{av}$ is the logarithmic average of p, partial pressure. Whereas they did not provide sufficient experimental data to accurately establish $k_G a$, order of magnitude values were given as $4.46 \times 10^{-4}$ g mole/atm L s at a gas flow rate of $1.76 \times 10^{-5}$ L/s and $1.3 \times 10^{-3}$ g mole/atm L s at a flow rate of $4.12 \times 10^{-5}$ L/s.

More recent articles give some insights into the physical mass transfer coefficients for ozone uptake in tapwater. *McCarthy et al. (1978)* estimated a value of $k_L^o$ to be $1.0 \times 10^{-2}$ cm/s in a 6 stage countercurrent bubble column system and compared this favorably to the findings of *Hill and Spencer (1975)*. They measured a physical transfer coefficient of $1.7 \times 10^{-2}$ cm/s in a sparged reactor. The gas flow rate was 9.0 L/min and an average bubble diameter of 0.32 cm was obtained by photography. The determination of $k_L$ was based on the relative insolubility of ozone in the liquid phase, which results in the total resistance to mass transfer residing in the liquid phase. They assumed, based on the Henry's Law constant for ozone (3760 atm/mole fraction at 20°C), that the overall mass transfer coefficient was equal to the liquid phase transfer coefficient.

## 2.4 Mass Transfer Fundamentals

### 2.4.1 Physical Mass Transfer

When a solution is not uniform in concentration or when two or more phases do not exist in chemical equilibrium, molecular transfer occurs. This molecular transfer is termed diffusion. Steady state molecular diffusion is governed by Fick's first law.

$$V = \frac{-D_1 \partial c}{\partial z} \qquad \ldots\ldots (2.25)$$

In the absence of chemical reaction and physical currents within the mass, the equation of continuity yields Fick's second law for unsteady state molecular diffusion, namely,

$$\frac{\partial c}{\partial t} = D_1 \left( \frac{\partial^2 c}{\partial x^2} + \frac{\partial^2 c}{\partial y^2} + \frac{\partial^2 c}{\partial z^2} \right) \qquad \ldots\ldots (2.26)$$

For the one dimensional model in the z direction, this reduces to

$$\frac{\partial c}{\partial t} = D_1 \frac{\partial^2 c}{\partial z^2} \qquad \ldots\ldots (2.27)$$

The movement of material however, is not solely governed by molecular diffusion and in fact, when physical flow exists the diffusion caused by turbulence, or eddies, becomes the dominant method of transfer.

In the practical two phase transfer problem, as in the liquid-gas contacting system, the diffusion process between two stagnant phases is of little interest. In this case the unknowns of eddy and molecular diffusion and the pathway of diffusion can be combined into a mass transfer coefficient. The coefficients are defined by equations with the general form,

Flux = coefficient (concentration difference)

and the coefficient is dependent upon the manner of defining the concentration.

In the transfer of material across a phase boundary it can be visualized that a stagnant or relatively quiescient condition exists in both phases at the immediate interface. If this is the case, while realizing the remaining bulk phases are agitated or in turbulent flow, it is reasonable to assume that the molecular diffusion occurs in the imaginary stagnant zone while eddy diffusion dominates the bulk phase. Thus, the resistance to transfer lies at the phase boundary.

Predicated on these assumptions several hydrodynamic models of a gas-liquid interface have been developed and presented in the literature.

2.4.1.1 Film Theory

The first model was proposed by *Lewis and Whitman (1924)* and is known as the film theory. In a thin film of stagnant fluid at the phase boundary of two moving fluid phases molecular diffusion occurs. The concentration gradient in the film is assumed as is the transfer direction perpendicular to the interface. The conditions in the bulk phase are assumed to be constant. With the overall driving force characterized by molecular diffusion in the film, Fick's first law (equation 2.25) holds and upon integration,

$$\overline{V}^{o} = \frac{D_1}{\delta} (c_o' - c_o) \qquad \ldots\ldots (2.28)$$

Where $c_o'$ is the interfacial concentration of the absorbing gas, $c_o$ is the bulk liquid concentration of the absorbing gas and $\delta$ is the thickness of the fictitious film.

Since the general form for defining mass transfer coefficients has been previously established, equation 2.28 can be modified to;

$$\overline{V}^{o} = k^{o}_{L} (c_{o}' - c) \qquad \ldots\ldots (2.29)$$

The liquid phase mass transfer coefficient is $k_L^{o}$. Comparing equations 2.28 and 2.29, the following expression is derived for the transfer coefficient;

$$k_L^{o} = \frac{D_1}{\delta} \qquad \ldots\ldots (2.30)$$

2.4.1.2 Penetration Theory

*Higbie (1935)* questioned the film model assumption of a steady state concentration gradient in the film and proposed a model incorporating a continual renewal of the surface. When a fluid element is in contact with the gas phase over a time element, unsteady state diffusion or penetration was presumed to occur. The main aspects of this model are;

a) the length of time each fluid element is amenable for transfer is constant

b) transfer occurs by molecular diffusion in a direction perpendicular to the interface

c) the fluid element is assumed to be stagnant, much like the film of the film theory

d) the fluid element, when brought to the surface, has a uniform bulk liquid-gas concentration

e) the liquid is essentially infinite in depth

Under these conditions Fick's second law (Equation 2.26) applies with the following boundary conditions;

$$c[[z,o]] = c_o$$

$$c[[\infty,t]] = c_o$$

$$c[[o,t]] = c_o'$$

The solution of equation with these boundary conditions is;

$$\frac{c - c_o}{c_o' - c_o} = \text{erfc}\ \frac{z}{2\sqrt{Dt}} \qquad \ldots\ldots (2.31)$$

where

$$\text{erfc} = \frac{2}{\sqrt{\pi}} \int_z^\infty \exp(-z^2)dz \qquad \ldots\ldots (2.32)$$

and t is the time elapsed since the fluid element arrived at the surface.

The instantaneous mass flux crossing the interface is determined by integrating equation 2.31, with respect to z and evaluating the differential at z=o. Multipying the result by the molecular diffusivity yields;

$$V^o[[t]] = (c_o' - c_o)\ \sqrt{D_1/\pi t} \qquad \ldots\ldots (2.33)$$

If this is averaged over the entire life of the elements, which is constant at a time t*, then,

$$\overline{V}^o = (c_o' - c_o)\ 2\sqrt{D_1/\pi t^*} \qquad \ldots\ldots (2.34)$$

Comparing this to equation 2.29 gives

$$k_L^{\ o} = 2\sqrt{D_1/\pi t^*} \qquad \ldots\ldots (2.35)$$

2.4.1.3 Surface Renewal Theory

*Danckwerts (1951)* extended the Higbie model incorporating the concept that the fluid elements were exposed at the phase interface for varying lengths of time.

The average absorption rate would thus be given by,

$$\overline{V}^{o} = \int_{o}^{\infty} (c_o' - c_o) \sqrt{D_1/\pi t} \; \Psi[[t]]dt \qquad \ldots\ldots (2.36)$$

where $\Psi[[t]]dt$ is the fraction of the surface elements having exposure times between t and t+dt.

The total surface area becomes

$$\int_{o}^{\infty} \Psi[[t]]dt = 1 \qquad \ldots\ldots (2.37)$$

If it is assumed that a surface elements' interface life is independent of its age and s' is introduced as the fractional rate of replacement of elements in any age group, then *Danckwerts (1951)* determined,

$$\Psi = s' e^{-s't} \qquad \ldots\ldots (2.38)$$

Substituting equation 2.38 in to 2.36 yields;

$$\overline{V}^{o} = \sqrt{D_1 s'} \; (c_o' - c_o) \qquad \ldots\ldots (2.39)$$

Since s' is the rate of surface renewal, then 1/s' is the average life of the surface elements.

*Astarita (1967)* proposed to replace s' in equation 2.39 and t* in equation 2.35 by a term he denotes as an "equivalent diffusion time", $t_D$. Using this time and comparing equations 2.39 and 2.29 leads to,

$$k_L^{o} = \sqrt{D_1/t_D} \qquad \ldots\ldots (2.40)$$

## 2.4.2 Simultaneous Absorption & Chemical Reaction

When a chemical reaction occurs in the liquid phase a depletion term is added to the unsteady state diffusion equation 2.27. Thus,

$$D_1 \frac{\partial^2 c}{\partial z^2} = \frac{\partial c}{\partial t} + r \qquad \ldots\ldots (2.41)$$

is obtained where r is a reaction rate.

The success of analytically solving the equation is dependent upon the form of r. Asympotic solutions have been found when simple expressions of r and the concepts of reaction regimes are used. The reaction regime concept can be simplified using the two time parameters "diffusion time" (previously defined) and "reaction time".

The reaction time represents the amount of time required for the reaction to proceed appreciably. It is defined as,

$$t_r = (c-c')/r \qquad \ldots\ldots (2.42)$$

where c is the actual reactant concentration and c' is the equilibrium reactant concentration. The reaction rate is a function of $(c_o'-c')$. For a first order reaction equation 2.42 reduces to

$$t_r = 1/k' \qquad \ldots\ldots (2.43)$$

where k' is the kinetic constant.

In physical absorption the absorbing component continues to be transferred into the solute until saturation in the bulk phase is achieved. The rate of transfer is dependent upon the concentration gradient that exists at any time.

The effect of a reaction between the absorbing component and a component in the solute is to maintain a higher driving force,

or concentration gradient and thus enhance transfer from one phase to the other.

This enhancement has been quantified by *Astarita (1967)* through the identification of an enhancement factor defined as;

$$I = \frac{k_L}{k_L^o} \qquad \ldots\ldots (2.44)$$

where $k_L$ is the chemical absorption coefficient.

2.4.2.1 Slow Reaction Regime

In this case the condition which applies is

$$t_D \ll t_r \qquad \ldots\ldots (2.45)$$

for which the average life of the surface elements is much less than the time required by the reaction to occur. The depletion of the liquid reactant near the liquid surface is negligible and thus, the liquid reactant concentration can be assumed to be the bulk phase concentration throughout.

In the mathematical description of this regime the reaction is assumed not to occur during the diffusion time and thus, the r term is dropped from equation 2.41 and thus, $k_L$, the chemical absorption coefficient is equal to $k_L^o$, the physical absorption coefficient.

The average absorption rate is given by

$$\bar{V} = k_L^o (c_o' - c_o) \qquad \ldots\ldots (2.46)$$

If $\Phi$ is defined as the volume of liquid per unit interfacial area then,

$$\bar{V} = k_L^o (c_o' - c_o) = \Phi r \qquad \ldots\ldots (2.47)$$

The slow reaction regime may be analyzed and further subdivided if the overall driving force $(c_o' - c')$ is divided into a diffusion component $(c_o' - c_o)$ and a reaction component $(c_o - c')$.

2.4.2.1.1 Diffusional Sub-regime

In this case *Astarita (1967)* assumes,

$$\Phi r\,[[c_o'-c']] >> k_L^o\,(c_o'-c') \qquad \ldots\ldots (2.48)$$

which implies that the reaction rate per unit interface is much larger than the absorption rate. Recognizing that equation 2.45 still holds then,

$$t_D << \frac{c_o'-c'}{r[[c_o'-c']]} << \frac{1}{k_L^o a} \qquad \ldots\ldots (2.49)$$

where a is the interfacial area per unit volume of the absorber.

Thus, the reaction rate is sufficient to keep the unreacted gas concentration, $c_o$, practically equal to the equilibrium value c' and therefore,

$$c_o-c' << c_o'-c_o \qquad \ldots\ldots (2.50)$$

The absorption rate in the diffusional regime is given by,

$$\overline{V} = k_L^o\,(c_o'-c') \qquad \ldots\ldots (2.51)$$

Absorption occurs at a finite rate; the chemical reaction maintains the bulk liquid concentration at the equilibrium value c' and the value of $k_L^o$ is not influenced by the reaction.

2.4.2.1.2 Kinetic Sub-regime

When the reaction rate is such that,

$$\Phi r[[c_o'-c']] << k_L^o\,(c_o'-c') \qquad \ldots\ldots (2.52)$$

the overall driving force is almost depleted by the reaction: i.e.

$$c_o'-c_o << c_o-c'$$

This being the case, the liquid phase will be saturated with the absorbing gas, $c_o = c_o'$. Thus, the absorption rate is given by,

$$\overline{V} = \Phi r[[c_o'-c']] \qquad \ldots\ldots (2.53)$$

Equation 2.53 indicates the total absorption rate for the kinetic regime is;

i) independent of interfacial area

ii) proportional to liquid hold-up

iii) independent of $k_L^o$

iv) proportional to r, and

v) influenced by the overall driving force, $c_o'-c'$.

2.4.2.2 Fast Reaction Regime

In this case the reaction is fast enough to maintain the bulk-liquid concentration equal to its equilibrium value $c_o \simeq c'$ and $t_r << t_D$. The instantaneous and average absorption rates are equal and are expressed as:

$$V = \overline{V} = \sqrt{2D_l \int_{c_o}^{c_o'} r[[c]]dc} \qquad \ldots\ldots (2.54)$$

(for the penetration theory). A first order reaction yields,

$$\overline{V} = \sqrt{D_l k}\ (c_o'-c') \qquad \ldots\ldots (2.55)$$

thus,

$$k_L = \sqrt{D_l k} = \sqrt{D_l/t_r} \qquad \ldots\ldots (2.56)$$

while for any reaction order n,

$$\overline{V} = \sqrt{(2/(n+1))D_l k_n\ (c_o'-c')\exp(n-1)}\ (c_o'-c') \qquad \ldots\ldots (2.57)$$

In this case,

$$k_L = \sqrt{(2/(n+1))D_l k_n\ (c_o'-c')\exp(n-1)} \qquad \ldots\ldots (2.58)$$

Equation 2.57 implies the fast reaction regime average absorption rate is:

i) proportional to interfacial area

ii) independent of liquid hold-up

iii) independent of $k_L^o$

iv) proportional to $\sqrt{r}$, and

v) proportional to the overall driving force raised to the exponent (n+1)/2

The enhancement factor for the fast reaction regime can be found from equations 2.40 and 2.56 as,

$$I = \frac{k_L}{k_L{}^o} = \sqrt{t_D/t_r} \qquad \ldots\ldots (2.59)$$

2.4.2.3 Instantaneous Regime

When the reaction in the liquid phase is instantaneous the absorbing component cannot coexist with the liquid phase component and the overall absorption rate is influenced by the concentration distribution of the liquid-phase reactant. A reaction plane (being a distance, $\tau$, into the liquid phase from the gas-liquid interface), can be envisioned where both b and c are zero, each having diffused from the respective sides of their origin. Two differential equations describe the process, namely,

$$D_1 \frac{\partial^2 c}{\partial x^2} = \frac{\partial c}{\partial t} \qquad \ldots\ldots (2.60)$$

$$D_2 \frac{\partial^2 b}{\partial x^2} = \frac{\partial b}{\partial t} \qquad \ldots\ldots (2.61)$$

where the boundary conditions are:

$t=o \quad c=o \quad b=b_o$

$x=o \quad c=c_o'$

$b=b_o \quad \frac{\partial b}{\partial x} = o$

$x=\tau \quad b=c=o$

$$\frac{\partial \tau}{\partial t} = -\left(\frac{\partial c/dt}{\partial c/dx}\right)_{x=\tau}$$

and the stoichiometric relationship at the reaction plane is,

$$-D_1\left(\frac{\partial c}{\partial x}\right)_{x=\tau} = \frac{1}{q} D_2\left(\frac{\partial b}{\partial x}\right)_{x=\tau} \qquad \ldots\ldots (2.62)$$

where q is the stoichiometric coefficient (q moles of liquid phase reactant per mole of absorbing reactant).

The solution, when based on the film theory *(Hatta (1928))*, is given as,

$$\frac{k_L}{k_L^o} = 1 + \frac{D_2}{D_1}\frac{b_o}{qc_o'} \qquad \ldots\ldots (2.63)$$

The general solution to the moving boundary problem has been given by *Astarita (1967)* (penetration theory):

$$V = \sqrt{\frac{D_1}{\pi t}}\ \text{erf}\sqrt{\alpha/D_1}\ \frac{c_o'}{} \qquad \ldots\ldots (2.64)$$

where $\alpha$ can be obtained from,

$$\frac{q\sqrt{D_1}\ c_o'}{\text{erf}\sqrt{\alpha/D_1}}\ \exp\left(\frac{-\alpha}{D_1}\right) = \frac{\sqrt{D_2 b_o}}{\text{erfc}\sqrt{\alpha/D_2}}\ \exp\left(\frac{-\alpha}{D_2}\right) \qquad \ldots\ldots (2.65)$$

and,

$$\bar{V} = k_L^o\ c_o' \ /\ \text{erf}\sqrt{\alpha/D_1} \qquad \ldots\ldots (2.66)$$

The evaluation of the constant $\alpha$ is not simple and hence, a simplification was described by *Nijsing (1957)* when $b_o/qc_o'$ is large. When this is assumed, which corresponds to most practical cases, then

$$\frac{1}{\text{erf}\sqrt{\alpha/D_1}} = \frac{k_L}{k_L^o} = \left(1 + \frac{D_2}{D_1}\frac{b_o}{qc_o'}\right) / \sqrt{D_2/D_1} \qquad \ldots\ldots (2.67)$$

hence,

$$\bar{V} \simeq k_L^o\ c_o'\ \left(1 + \frac{D_2}{D_1}\frac{b_o}{qc_o'}\right) / \sqrt{D_2/D_1} \qquad \ldots\ldots (2.68)$$

The total absorption rate of the instantaneous reaction regime is;

i) proportional to the area of the interface

ii) independent of liquid hold-up

iii) proportional to $k_L^o$

iv) independent of r, and,

v) almost independent of $c_o'$.

The absorption rate of the fast reaction regime (equation 2.57) and the instantaneous reaction regime (equation 2.68) can be analysed to ascertain which theory is applicable to the case being considered. Since the absorption rate has a finite limit, as the reaction rate approaches infinity the diffusion of the liquid phase reactant can become limiting. This would not be predicted by the fast reaction theory which neglects diffusion of the liquid phase reactant. Thus, it is necessary to utilize the theory which predicts the lower absorption rate. As a result, the instantaneous reaction regime is applicable when

$$\sqrt{t_D/t_r} \gg b_o/qc_o' \qquad \ldots\ldots (2.69)$$

and the fast reaction regime condition is

$$1 \ll \sqrt{t_D/t_r} \ll \frac{b_o}{qc_o'} \qquad \ldots\ldots (2.70)$$

2.4.2.4 Transition from Fast to Instantaneous Reaction

It may well be that $(t_D/t_r)^{\frac{1}{2}}$ is the same order of magnitude as $b_o/qc_o'$ namely the rate of reaction is a function of both absorbing and liquid phase reactants and that both can coexist in a reaction zone. Mathematically there is no rigorous analytical solutions available to this situation. Numerical solutions have been obtained by *Van Krevelen and Hofttizer (1948)*, using simplified hypotheses based on the film theory model and second order irreversible reaction

kinetics. The solution given was

$$I = \left(\frac{t_D}{t_r}\frac{I_\infty - I}{I_\infty - 1}\right)^{.5} / \text{tgh}\left(\frac{t_D}{t_r}\frac{I_\infty - I}{I_\infty - 1}\right)^{.5} \qquad \ldots\ldots (2.71)$$

and has been plotted with an ordinate of I and an abscissa of $\sqrt{t_D/t_r}$, sometimes referred to as a diffusion reaction modulus *(Sada et al. (1978))*. Here $I_\infty$ is given as

$$I_\infty = 1 + \frac{D_2}{D_1}\frac{b_o}{qc_o}, \qquad \ldots\ldots (2.72)$$

Further use of equation 2.71 has been made by *Gilliland et al. (1958)* by substituting the penetration theory $I_\infty$ value defined in equation 2.67.

## 2.5 Summary

A high degree of uncertainty exists in the literature with respect to stoichiometry of ozone-cyanides reactions, relative rates of reaction and catalysis of the same, and mass transfer aspects of previous studies. However, the following conclusions can be made:

(1) The rate of the ozone-cyanide reaction is sufficiently fast that it is not possible to operate in the kinetic regime.

(2) The most probable stoichiometric relationships for the cyanide and cyanate reaction with ozone are expressed in equation (2.8) and (2.12), respectively.

(3) *Balyanskii et al. (1972)* and *Sondak* and *Dodge (1961)* report that the cyanate reaction appears approximately 5.1 times slower than the cyanide reaction.

(4) The reactions are pH dependent.

(5) The reactions have been found to be independent of temperature over the anticipated operating range, however, this may have been due to experimental design whereby individual components of mass transfer and kinetic effects were not adequately assessed.

(6) The rate of reaction may be of sufficient rapidity that gas phase resistance to mass transfer is significant. Gas phase resistance to mass transfer was assumed controlling by *Sondak* and *Dodge (1961)*.

(7) Both cyanide and ozone are toxic and safety precautions should be incorporated into equipment design and experimental procedures.

The difficulty experienced in previous works could be overcome through the design of a gas liquid contactor operated such that the gas liquid interfacial area is known. If experiments could be designed operating in the fast reaction regime, the separation of mass transfer and reaction kinetics may be accomplished and kinetic constants determined by application of fast reaction regime theory coupled with a given reaction mechanism.

# 3 EXPERIMENTAL

## 3.1 Choice of System

As the rate of reaction has been shown by others to be rapid, a system was required which had a limited, yet known, surface area. Both mass transfer/kinetic studies on synthetic cyanide solutions and treatability studies on a barren bleed solution were planned. As this was the case the system chosen was designed to be flexible and convertible to facilitate both experimental phases.

The reactor system required the following characteristics;

(1) Batch and continuous operating capability.

(2) Liquid phase residence time for continuous flow of up to one hour.

(3) Variable stirring speed to enable changes to $t_D$.

(4) Capability to assess area of gas-liquid contact.

(5) Sufficient size to generate the required liquid volume for cyanide determination for treatability studies (≃ 500 mL).

(6) No temperature bath and no excessive pressure requirements.

(7) Corrosion resistance to ozone and alkaline environments.

(8) Ease of cleaning and construction.

(9) Maintenance of constant inlet gas and liquid compositions.

The gas liquid contactor chosen was that specified in *Danckwerts* and *Gillham (1966)*, sometimes called the Danckwerts cell. The reactor was a quiescent surface stirred vessel which provided the degree of liquid and gas residence time control as well as a variety of operating modes. Since a quiescent interface could be maintained for the mass transfer studies the area for mass transfer was established equal to the column cross-sectional area less that of the stirrer and stirring blades.

One of the objectives of the study was to measure fundamental design parameters, namely the overall mass transfer coefficient and kinetic constant for a cyanide-ozone reaction system. To do so, the reactor system, previously identified, had to be operated in a reaction regime which was dependent upon the kinetic constant. If both physical and chemical mass transfer coefficients were measured, an enhancement factor could be generated, which would be independent of reactor operating conditions. The enhancement factor could then be related through a reaction regime to the kinetic constant. In this way the problem of combining mass transfer and kinetic data in an unspecific way could be overcome.

## 3.2 Description of Apparatus

### 3.2.1 Reactor

A diagram of the reactor used is shown on Figure 2. A 10.6 cm center diameter, 17.8 cm in length Pyrex glass column section was used sealed by Teflon gaskets between stainless steel plates.

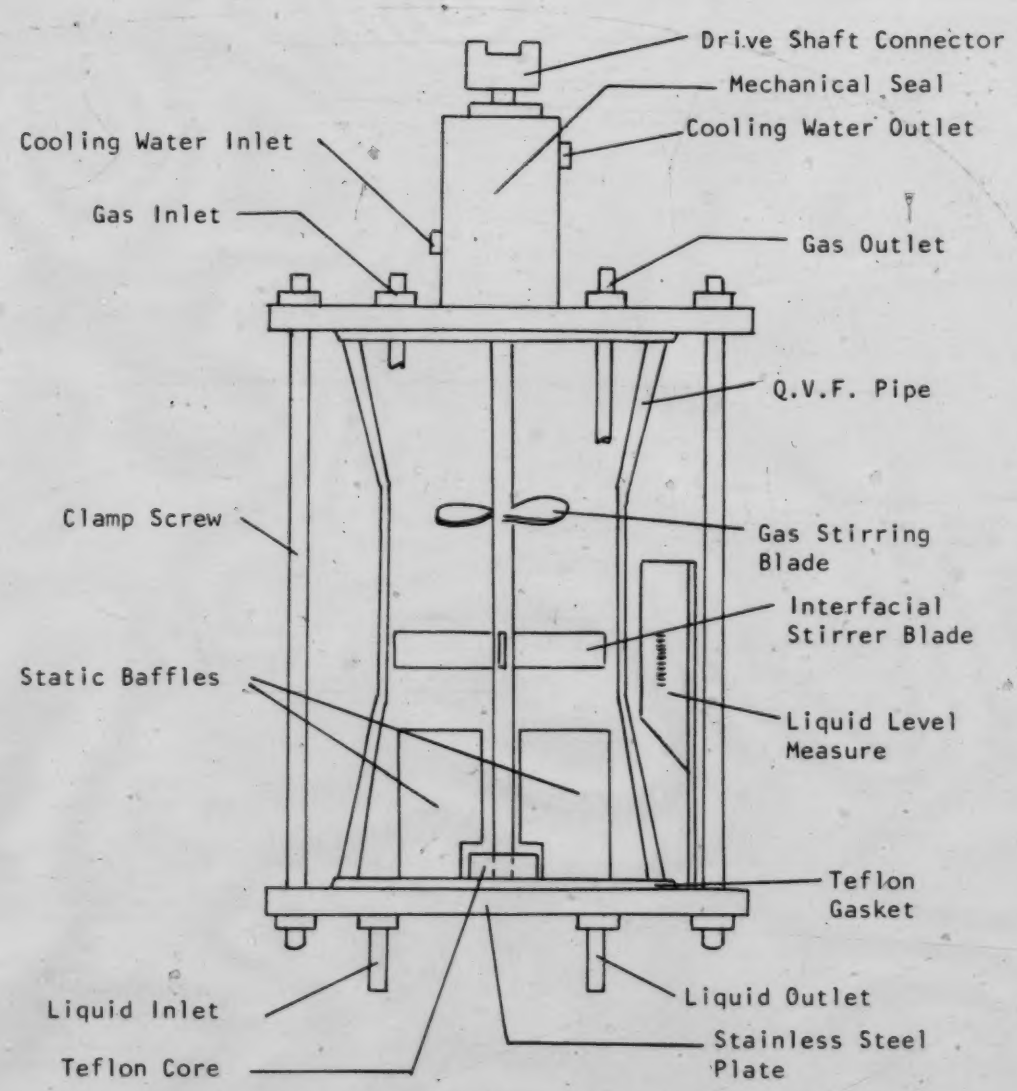


Figure 2 Quiescent Surface Reactor

The stirrer which was constructed of stainless steel had two sets of blades attached to its shaft. The upper blades consisted of two stainless steel propellers and were provided to aid in maintaining uniform gas characteristics. The lower blades were formed by four stainless steel strips set perpendicular to the stirrer shaft. These blades were immersed 1 mm into the liquid and were used to vary the liquid phase mass transfer characteristics and to aid in mixing of liquid. The shaft was sealed at the top by a water cooled mechanical seal while the bottom was slotted into a Teflon core. The rotating mechanical seal was constructed from two carbon faces rotating on two ceramic faces in a stainless steel jacket.

Static baffles, also stainless steel, were press fit into a slot in the bottom plate. Completely mixed liquid conditions were anticipated to be accomplished primarily by liquid flow rate and baffle placement to minimize short circuiting.

A scale was fixed to one of the clamp rods with its base on the bottom plate. This enabled accurate liquid level monitoring.

The reactor was mounted by flanges on a rigid free standing support and housed in a fume cabinet. The support was designed to be capable of being levelled.

The precatuion of housing the reactor assembly in a fume cabinet was initially intended as a safety precaution while using cyanide. Fortunately, no difficulties were experienced using cyanide solutions and the fume cabinet proved to be more valuable in reducing ozone concentrations when occasional gas system failures occurred.

The gas flow lines were nylon which became brittle with time and cracked usually on a bend close to a connector.

3.2.2 Auxiliary Equipment

3.2.2.1 Ozone-Cyanide Studies

A schematic diagram of the equipment is shown in Figure 3. Liquid from the charge liquid reservoir (approximately 20 L capacity) was pumped by a positive displacement pump (7) through a damper (9) and a rotameter (11) into the reactor (5). The damper served to minimize the pulsing effect of the pump so that an accurate flow reading could be taken. Also, the pressure gauge on each damper was utilized as a warning indicator for a line blockage. Outlet liquid was pumped by another positive displacement pump (8) through a damper (10), rotameter (12) and a backpressure valve (13) into a pair of monitoring chambers (16) and (19).

The chambers, of approximately 80 mL capacity, were constructed from glass tubing with two short lengths of glass tubing serving as connectors to flow lines. The chambers were stirred by magnetic stirrers (20) and (21).

The two pumps (7) and (8) (Milton Roy. Co. Mini-Pump 2-C-96R) were connected via the same driveshaft to a common motor. As it was important to maintain a constant liquid level, the duplication of pumps and rotameters (Matheson glass No. 604) provided system control.

All flow lines were 0.635 cm (1/4") 'Poly-flo' nylon tubing. All connectors and fittings were Swagelok 316 while all valves were stainless steel Whitey valves.

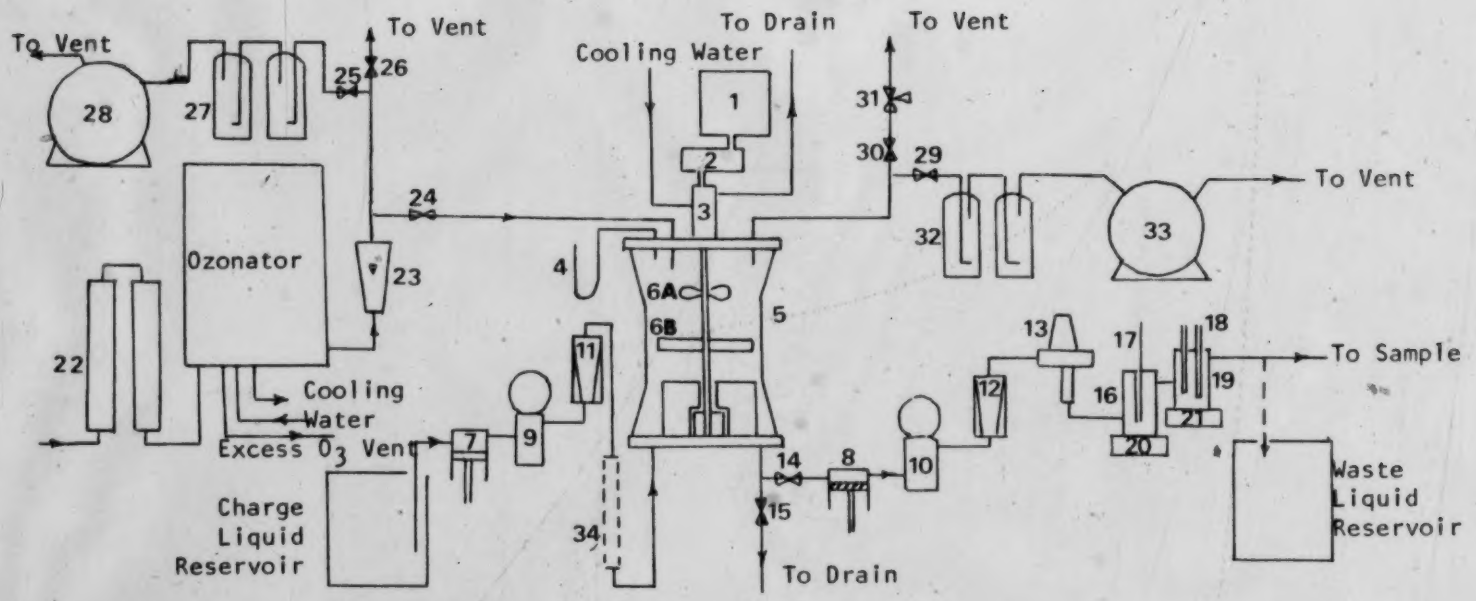


LEGEND

| | | | | | | | |
|---|---|---|---|---|---|---|---|
| 1 | Motor | 8 | Outlet Liquid Pump | 18 | Selective Ion Electrode ($CN^-$) | 29 | Gate Valve |
| 2 | Gear Box | 9 | Surge Damping Chamber | 19 | Monitoring Chamber | 30 | Gate Valve |
| 3 | Mechanical Seal | 10 | Surge Damping Chamber | 20 | Magnetic Stirrer | 31 | Needle Valve |
| 4 | Manometer | 11 | Rotameter | 21 | Magnetic Stirrer | 32 | Outlet Gas Bubblers |
| 5 | Reactor | 12 | Rotameter | 22 | Desiccator | 33 | Wet Test Meter |
| 6A | Gas Stirring Blade | 13 | Back-Pressure Valve | 23 | Rotameter | 34 | Heat Exchanger |
| 6B | Liquid Stirring Blade | 14 | Gate Valve | 24,25,26 | Gate Valves | | |
| 7 | Charge Liquid Pump | 15 | Gate Valve | 27 | Inlet Gas Bubblers | | |
| | | 16 | Monitoring Chamber | 28 | Wet Test Meter | | |
| | | 17 | pH Probe | | | | |

Figure 3 Equipment Configuration - Mass Transfer Studies

The cyanide feed liquid stream was pumped from the reactor to the two monitoring chambers (16) and (19). An on line Fisher Accumet Model 520 Digital pH/Ion Meter was used to monitor when the free cyanide concentration had attained a steady-state level. A cyanide activity electrode (Orion Research Model 94-06A), and reference Ag/AgCl electrode (Orion Model 90-01) were mounted in chamber (16). The other chamber (19) housed a pH and reference probes which were connected to a Metrion II pH Meter. The pH was found not to vary over the course of most runs, however, the capability for monitoring remained primarily for safety reasons.

Liquid leaving the system had varying quantities of cyanide remaining in solution; hence, all liquids were collected in a 10 litre waste liquid reservoir. Upon filling, the reservoir contents were extensively ozonated prior to disposal.

A sample of the outlet liquid stream was taken by directing the discharge line output from the monitoring chamber (19) to a 100 mL round bottom flask. Upon filling the flask the discharge line was inserted into a liquid waste reservoir. The valve on drain line from the outlet port of the reactor was utilized to perform slight adjustments to the liquid level or to drain the reactor.

Building air, metered through a regulator valve, passed through two drying columns (22) assembled in series filled with Drierite, to dry the air to a frost point of approximately -50$^{o}$C. This dried air entered a Welsbach T-816 ozonator set to the manufacturers' suggested operating pressure of 8 psig by the built-in

pressure regulating valve and passed through a Brooks type 2-1110 rotameter (R-2 15C tube) (23) prior to distribution to sampling bubblers (27), vent or the reactor (5) whichever was the desired operation mode.

The outlet gas line was equipped with a micrometer needle (31) valve serving as a backpressure valve for the system. The sample bubblers (27) and (32) were two 500 mL glass bubblers connected in series fitted with medium coarse glass fitted disks. The pair of bubblers were snapped into the flow stream using Quick Connect Poly-flo connectors. Hence, removal from and replacement to the system was easily facilitated. The micrometer needle valve (31) was set to exert a backpressure approximately equal to the pressure drop across the set of bubblers and wet test meter. This was required to keep the reactor system at the same pressure while sampling the outlet gas ozone concentration and flow rate. Brass and stainless steel valves were suitable for the gas line hardware.

Mixing of both phases was accomplished by starting the 1/4 hp Wagner-Leland motor (1) and setting the impeller speed (6A & B) by adjustment of a 'Zero-Max' gear box (2).

3.2.2.2 Treatability System

The flow diagram for the equipment used for studying the treatment of cyanide wastes is shown in Figure 4.

For this configuration, the reactor was operated as a gas phase continuous flow, liquid phase batch type reactor. The gas phase equipment flow scheme was identical to that described in section

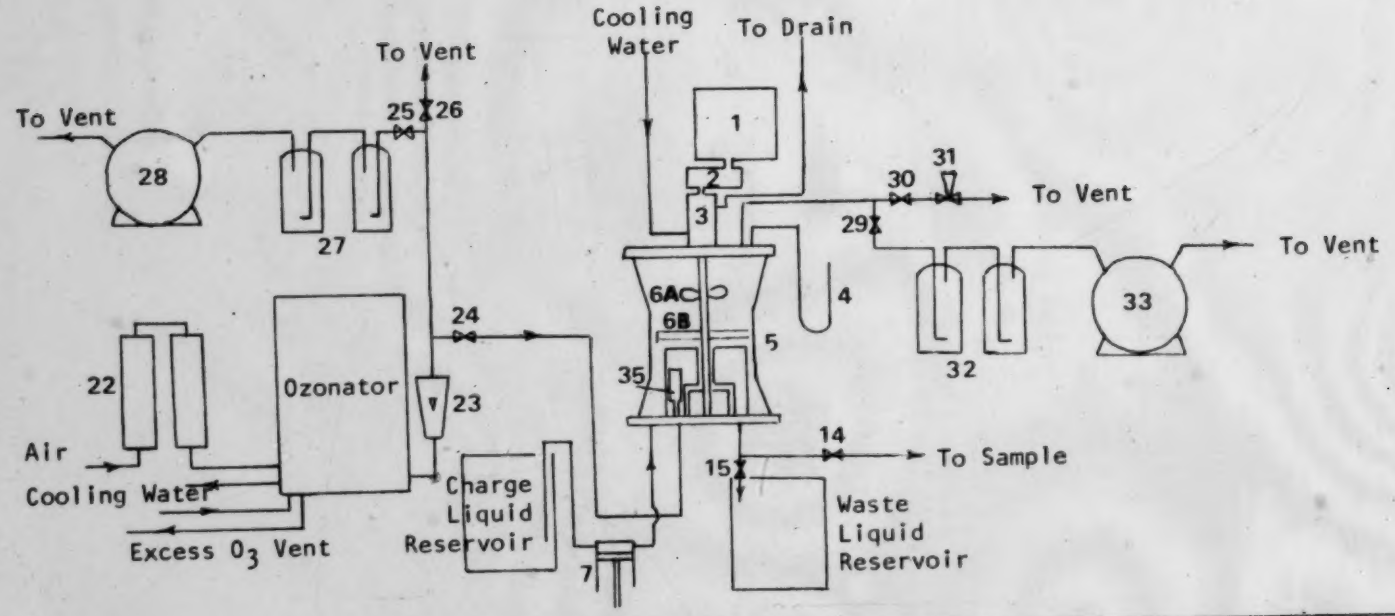


| LEGEND | | | | | | | |
|---|---|---|---|---|---|---|---|
| 1 | Motor | 8 | Outlet Liquid Pump | 18 | Selective Ion Electrode ($CN^-$) | 29 | Gate Valve |
| 2 | Gear Box | 9 | Surge Damping Chamber | 19 | Monitoring Chamber | 30 | Gate Valve |
| 3 | Mechanical Seal | 10 | Surge Damping Chamber | 20 | Magnetic Stirrer | 31 | Needle Valve |
| 4 | Manometer | 11 | Rotameter | 21 | Magnetic Stirrer | 32 | Outlet Gas Bubblers |
| 5 | Reactor | 12 | Rotameter | 22 | Desiccator | 33 | Wet Test Meter |
| 6A | Gas Stirring Blade | 13 | Back-Pressure Valve | 23 | Rotameter | 35 | Gas Sparger |
| 6B | Liquid Stirring Blade | 14 | Gate Valve | 24,25,26 | Gate Valves | | |
| 7 | Charge Liquid Pump | 15 | Gate Valve | 27 | Inlet Gas Bubblers | | |
| | | 16 | Monitoring Chamber | 28 | Wet Test Meter | | |
| | | 17 | pH Probe | | | | |

Figure 4 Equipment Configuration - Treatability Studies

3.2.2.1 except the gas was delivered to an additional 0.95 cm port on the bottom reactor plate, allowing for the introduction of gas. Gas was bubbled either directly into the reactor through the port or sparged using a medium coarse stainless steel fitted desk.

Barren bleed from Giant Yellowknife Mines Ltd., stored in the charge liquid reservoir, was pumped into the reactor via the positive displacement pump (7). In order for filling to occur valve (15) remained closed. The reactor contents could be drained by gravity into a waste liquid reservoir by opening valve (15).

## 3.3 Quantification of Reactor Characteristics

The reactor chosen, as previously stated, was a quiescent surface, stirred vessel. The area available for mass transfer was known using this reactor type and the system could be readily quantified using well documented methods.

This quantification of the reactor system was accomplished in three phases. These were:

(1) the evaluation of the residence time distribution. This was required because mixing was to be achieved by liquid flow through and stirring facilitated by a stirring blade only slightly immersed in the liquid. Stirring speeds yielding ideal mixing while maintaining a flat liquid surface had to be ascertained. The system chosen, primarily for ease of measurement, was the introduction of a step function of saline solution to a distilled water system. The influence of increased

chloride in the reactor outlet liquid on the specific conductivity was the monitoring principle.

(2) the determination of the liquid phase absorption coefficients at various stirring speeds. The carbon dioxide-distilled water system was used and corrected for ozone by comparison of the respective gas diffusivities. The carbon dioxide-distilled water system was used primarily because the solubility of carbon dioxide in water under atmospheric conditions is small and hence, liquid phase mass transfer resistance can be assumed.

(3) verification of the assumption that the liquid phase resistance to mass transfer was equivalent to the overall resistance to mass transfer. The sulphur dioxide-nitrogen-aqueous sodium hydroxide system was used because the sulphur dioxide-sodium hydroxide reaction is instantaneous *(Sharma and Danckwerts (1970))*, exhibiting no liquid phase resistance. The nitrogen carrier gas provided gas phase transfer resistance while its liquid phase transfer can be neglected.

### 3.3.1 Equipment Modifications For Reactor Quantification

#### 3.3.1.1 Residence Time Distribution System

For the residence time distribution studies, a dilute solution of salt water was charged in a similar manner as that described in section 3.2.2 to the reactor filled initially with distilled deionized water. The resulting change in conductance of the reactor effluent was monitored at sample chamber (16) using a conductivity probe and a YSI Model 33 Salinity-Conductivity-Temperature Meter. The temperature could be monitored by either the thermometer (45) in chamber (19) (Figure 5) or by the above mentioned meter.

#### 3.3.1.2 Carbon Dioxide-Water System

Figure 5 is a schematic diagram of the system used. The reactor was operated as a continuous flow type in both gas and liquid phases. Equipment for the liquid phase remained the same as that outlined in section 3.2.2; however, instead of utilizing chamber (16) as a monitoring chamber, samples of liquid were withdrawn from this point by pipette.

Carbon dioxide flow was regulated by a pressure regulating valve (46) on the gas cylinder. Gas passed through a Brooks Type 2-1110 rotameter (R-2 15C tube) into the reactor (5). Pressure in the reactor was read on a mercury manometer (4).

#### 3.3.1.3 Sulphur Dioxide-Sodium Hydroxide System

The schematic diagram of the experimental design is shown on Figure 5.

The liquid, in this case a 2M NaOH solution, charge and discharge was the same as for section 3.3.1.2. The flow of sulphur

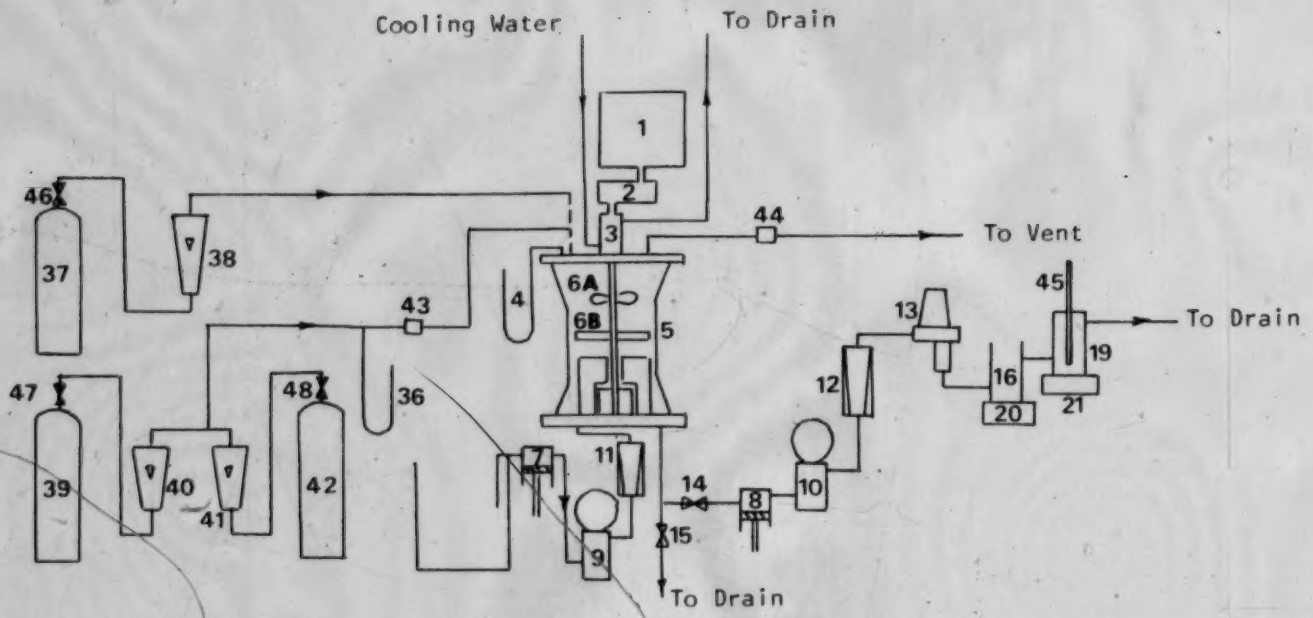


LEGEND

| | |
|---|---|
| 1-21 | As Per Figure 3 |
| 36 | Manometer |
| 37 | $CO_2$ Cylinder |
| 38 | Rotameter |
| 39 | $SO_2$ Cylinder |
| 40 | Rotameter |
| 41 | Rotameter |
| 42 | $N_2$ Cylinder |
| 43 | Inlet Gas Sample Port |
| 44 | Outlet Gas Sample Port |
| 45 | Thermometer |
| 46 | $CO_2$ Regulator Valve |
| 47 | $SO_2$ Regulator Valve |
| 48 | $N_2$ Regulator Valve |

Figure 5 Equipment Modifications - Reactor Quantification Studies

dioxide and nitrogen, regulated by the pressure regulating valves (47) and (48) on the respective cylinders and monitored by the rotameters (40) and (41), mixed and entered the reactor (5). The pressure reading of the mixture was taken on a mercury manometer (36) and when necessary sampling using a glass syringe could be performed at the sample port (43).

Since the gas flow rate was very important in subsequent calculations, two manometers (36) and (4) were utilized to assess the pressure drop between the point of mixing and the reactor.

3.4 Procedure

3.4.1 Equipment Operation

3.4.1.1 Procedure Common to Residence Time Distribution, $CO_2$ Absorption, Ozone-Cyanide & Sulphur Dioxide Study Phases

Refer to Figure 3.

1. Prior to the commencement of a series of runs the reactor (5) was dismantled and all inner surfaces and components were washed thoroughly with detergent and rinsed with distilled water.
2. The inlet liquid line was placed into a distilled water reservoir and the reactor and system was flushed for 30 minutes prior to an experimental run. The inlet line was replaced into the charge liquid reservoir.
3. The cooling water to the mechanical seal (3) was turned on and the motor (1) was started.

4. The stirring speed of the twin blades (6A) and (6B) was set by adjusting the gear ratio in the gear box (2).
5. The inlet liquid pump (7) and outlet pump (8) was started.
6. The positive displacement pumps were connected to the same motor hence, in order to facilitate filling of the reactor the valves (14) and (15) were closed. The desired height of the liquid was determined by visual assessment of the liquid surface against the level indicator. The objective of maintaining a horizontal surface (no gas entrainment) was accomplished by stirring with the blades (6B) immersed to a depth of 1 mm.
7. Upon filling the reactor to the liquid height desired, the valve (14) was opened and the inlet/outlet flow was adjusted by altering the stroke length of either the inlet or outlet pump piston.
8. After the flow rates were equalized the liquid level was adjusted to regain the desired height by closing valves (14) and (15) or opening valve (15) while closing (14).

3.4.1.2 Ozone-Cyanide System Procedure

Refer to Figure 3 for flow schematic. The liquid feed was either an aqueous solution of NaCN-NaOH or barren bleed.

1. The cooling water flow to the ozonator was started. Flow was maintained at over 20 L/hr.
2. The air flow rate was set utilizing the gas rotameter in the ozonator and air was allowed to purge the ozonator for 15 to 30 minutes prior to each run. To do so, valves (24) and (25)

were closed and valve (26) opened. All air entering the ozonator was dried.

3. The needle valve (31) was set such that the gauge pressure in the reactor (5), as monitored by the manometer (4), was approximately the same as the pressure drop across the sample bubblers (27) and (32). This ensured that only a minute pressure change occurred in the reactor over the sampling period.

4. The ozonator was switched on and the proper operating pressure (as specified in the Welsbach operating manual) was set using the outlet gas rotameter valve. As there were two ozone-air outlet lines from the ozonator the desired air flow and proper pressure could be maintained by adjusting the proportion of the gas stream to the excess ozone line. At the commencement of each run, valves (24) and (30) were open while (25), (26) and (29) were closed.

5. Using the $CN^-$ selective ion electrode and the pH meter steady-state conditions were assessed when no change in reading occurred. This condition was typically obtained within 45 minutes.

6. Slight adjustments to gas flow rate and liquid height were occasionally required and this was accomplished as previously described.

7. Liquid inlet cyanide concentration was obtained by taking at least two samples of feed stock from the charge reservoir in 100 mL volumetric flasks. Upon collection these flasks were stoppered.

8. Outlet liquid samples were obtained by redirecting the flexible

tube leading to the waste liquid reservoir to fill a 100 mL volumetric flask. The flask was then stoppered.

9. In order to obtain a ozone concentration in inlet and outlet gases, two 500 mL bubblers connected in series and fitted with medium coarse fritted disks, were clipped into the sample line using connecting couplings. The bubblers were each filled with approximately 400 mL of a 2% KI solution. The outlet gas was sampled by closing valve (30) and opening valve (29). The bubbling time, period of flow and volume of flow were recorded. The flow volume was obtained using a wet test meter. After approximately 3 L had flowed through the bubbler the flow pattern was returned to the starting configuration by closing valve (29) and opening valve (30).

10. The inlet ozone concentration was monitored in a similar procedure to step 9 by leaving valve (26) closed and opening valve (25) and closing valve (24) simultaneously. The flow of gas to the reactor was temporarily curtailed over the sampling period and hence, a possible disruption to steady state conditions resulted.

11. A period of restabilization was allowed prior to repeating the sampling procedure of steps 8, 9 and 10. Approximately 5 outlet liquid samples and 3 inlet and outlet gas samples were taken.

12. Some runs were performed at temperatures greater than room temperature. In these cases, a 30 cm long stainless steel tube (34) wrapped with treating tape was installed in the line between the inlet liquid rotameter (12) and the reactor (5). A variac con-

trol was used to adjust the liquid temperature. The temperature was monitored in the outlet liquid samples collected.

3.4.1.3 Treatability Studies Procedure

Refer to Figure 4 for flow schematic.

1. The charged liquid reservoir was filled with barren bleed solution from a Giant Yellowknife Mines, Ltd.
2. The reactor was filled with charge solution by pumping to the desired height which was just covering the top stirring blade (6A).
3. After proper preparation of the ozone system, described in section 3.4.1.2, the ozone-air mixture was directed through valve (26) to the vent.
4. The inlet ozone concentration was monitored by simultaneously closing valve (26) and opening valve (25) in a similar fashion, as described in section 3.4.1.2.
5. The gas was charged to the reactor through valve (24) (closing valve (26)) and the time was recorded.
6. The outlet gas was directed to either a sampler or to vent through a needle valve (31) which established the necessary pressure (step 3, section 3.4.1.2). The outlet gas concentration was monitored similar to step 4.
7. As the liquid was batch reacted, the cyanide concentration changed with time. The cyanide concentration was monitored at specified intervals by draining a portion of the reactor liquid into a polyethylene sample bottle. Ten mL of concentrated sodium hydroxide were added to preserve the sample.
8. Excess liquid waste was bled to the waste liquid reservoir.

9. Prior to commencement of another run the reactor was filled to the top with distilled water, drained, and filled again with a weak solution of HCl to remove any residual metal hydroxide or sulphide sludge. The solution was mixed, drained and the reactor was again flushed with distilled water.

10. Safety precautions were necessary when handling cyanide or cyanide solutions. Segregation of acid solutions from those containing cyanide was performed by using separate benches dedicated to either alkali or acidic chemicals. This avoided the possibility of accidentally adding acid to cyanide thereby generating the highly toxic gas HCN.

    In order to avoid possible exposure to ozone and cyanide vapors the equipment was housed in a fume cabinet, however, this was not completely effective as ozone could be detected when a leak occurred in the gas system.

3.4.1.4 Residence Time Distribution Procedure

Only the liquid phase schematic diagram of Figure 5 is pertinent for this phase of the study.

1. The conductivity meter probe was immersed in the liquid in the sampling chamber (16). The magnetic stirrers were switched on as was the meter. The conductivity of the circulating distilled water was recorded.

2. The inlet liquid flow line was quickly removed from the distilled water reservoir and placed into a reservoir filled with a NaCl-distilled water solution of known conductivity.

3. The conductivity of the outlet liquid passing through the sam-

pling chamber (16) was continuously monitored and upon conductivity response the time was set at t=o.

4. Conductivity measurements were recorded at frequent intervals until the reading had attained a value within 10% of the original saline solution.
5. The salt solution was very weak to minimize density gradients which could affect the results.
6. The procedure was repeated for various flow rates and stirring speeds.
7. One run was conducted using an acid solution monitoring the response using a pH probe and meter.

3.4.1.5 $CO_2$ Absorption Into Water Procedure

Refer to Figure 5 for flow schematic.

1. The flow of carbon dioxide was controlled by adjusting the cylinder regulator valves (46).
2. Atmospheric pressure was recorded from the barometer installed in the laboratory and the reactor pressure was taken by reading the manometer (4).
3. The magnetic stirrers (20) and (21) were started.
4. Steady-state was allowed to develop.
5. The liquid was sampled by pipetting a known volume from sample chamber (16) and immediately adding the pipette contents to a known volume of standard sodium hydroxide solution.
6. The temperature of the liquid was recorded using the thermometer (17) immersed in the monitoring chamber (19).

7. Steps (5) and (6) were repeated to ensure steady state conditions had been achieved.
8. Frequent checks of liquid level were necessary and the level was occasionally adjusted.

3.4.1.6 $SO_2$ Absorption Into NaOH Solution Procedure

Refer to Figure 5 for flow schematic.

1. The carrier gas ($N_2$) flow was initiated by opening the cylinder regulator valves (48) and adjusted using the nitrogen rotameter (41). Similarly the $SO_2$ flow was adjusted using the cylinder regulator (47).
2. After a lengthy period for steady-state development the inlet gas concentration was sampled using a 5 mL glass syringe inserted into the sampling port (43). The extracted gas was immediately injected into a gas chromatograph column for analysis. The pressure of the gas mixutre was recorded by reading the manometer (36).
3. The outlet gas was similarly sampled using the sampling port (44). The outlet gas pressure was assumed to be the reactor pressure as measured by the manometer (4).
4. The sampling procedure of 2 and 3 was repeated five or six times.

3.4.2 Analytical Procedures

3.4.2.1 Ozone-Cyanide and Treatability System

Analysis of cyanide and ozone was required for these systems.

3.4.2.1.1 Cyanide

The analytical methods for cyanide determination vary considerably depending on the forms of cyanide present in the sample. In

general cyanide complexes can be represented in two classes; simple, those defined by the formula $A(CN)_x$ and complex, those defined by the formula $AyM(CN)_x$. Here A refers to an alkali or metal with the valance of A determining the number of cyanide groups for simple cyanides. For complex cyanides M represents a heavy metal and the anion formed upon solution is not $CN^-$ but is the radical $M(CN)_x^-$.

i) For the runs using sodium cyanide it was assumed that all the cyanide was present as sodium cyanide and hence, could be considered a simple cyanide. The method of analysis used is described in detail in *APHA (1971)*.

The solution was titrated with a standard solution of silver nitrate, $AgNO_3$. This converted the cyanide present to a silver cyanide complex, $Ag(CN)_2^-$ and small excesses of $Ag^+$ were detected by the silver sensitive indicator, para-dimethylaminobenzalrhodanine. The color changes from yellow to salmon pink indicated the completion of titration. A blank silver nitrate sample was titrated also.

Details of the method are given in Appendix A.1.

ii) The cyanide in the barren bleed was present in a multiple of simple and complexed forms. As this was the case, a more complex method of analysis was required to determine the total amount of cyanide present. To further confuse the situation the cyanides present as $CNS^-$ and $CNO^-$ would not be included in the typical cyanide methods. Thiocyanate and cyanate are not considered as part of the total cyanide determination, and in some runs these were monitored separately.

The method used to monitor complex cyanides was a destruction technique which converted complex cyanides into simple cyanides to facilitate colourimetric determination. The capability to do the analysis, although attempted, was not attained on site. Samples preserved with 1N NaOH to a pH greater than 12 were shipped to the Can Met, Department of Energy, Mines and Resources Laboratory in Ottawa for analysis.

The technique used was described in *Barkley and Ingles (1970)*. The procedure utilized picric acid (trinitrophenol) combined with sodium carbonate reagent to produce a cyanide-picrate color. The color intensity was measured using a spectrophotometer and the absorbance was compared to a calibration graph generated from standard cyanide solutions to obtain the amount of cyanide present in the effluent. The method relied on ethylenediamine tetraacetic acid (EDTA) to release cyanide contained in the metal complexes.

The method has been found *(Barkley and Ingles (1970))* to be free from thiocyanate and cyanate interferences; however, the method is insensitive to the very stable metal cyanide complexes of ferrocyanide or cobalticyanide.

The insensitivity to cobalticyanide is considered to be unimportant as it is not normally present in gold mining effluents *(Barkley and Ingles (1970))*. The ferrocyanide analytical insensitivity did affect the treatability study program. The cyanide rich waste streams from gold mining operations may contain ferrocyanide in varying amounts dependent upon what uses are made of

these streams for washing purposes and pyrite and other iron compounds in the ores to name two sources. In the case of Giant Yellowknife Mines the samples received were analyzed for metal content using flame atomic absorption and 10 mg/L iron was found. This value is lower than subsequent testing conducted by the Wastewater Technology Centre in Burlington, Ontario. Values of 25-29 mg/L Fe were obtained. It can be assumed due to the very stable nature of the iron cyanide complex that all the iron was present as some complex of cyanide. If ferrocyanide was not detected using the CanMet method errors would result in the initial and subsequent samples for "total cyanide" content.

Cyanate ($CNO^-$) and thiocyanate ($CNS^-$) were also determined by the Energy, Mines and Resources CanMet Laboratory in the treatability phase of the work. The cyanate method used is based on the cyanate hydrolysis to ammonia upon heating at low pH according to the reaction;

$$2NaCNO + H_2SO_4 + 4H_2O \rightarrow (NH_4)^2\ SO_4 + 2NaHCO_3 \quad \ldots\ldots (3.1)$$

The ammonia concentration, before and after hydrolysis of cyanate, was measured by direct nesslerization.

Solutions containing thiocyanate form an intense red colour when ferric iron is added at an acidic pH. Colouroimetric determinations of thiocyanate concentrations were found using a spectrophotometer set at 480 nm.

Methods for cyanate, ammonia and thiocyanate are given in detail in *APHA (1975)*.

3.4.2.1.2 Ozone in Air

The iodometeric method was used to determine the ozone concentration in air. The method is based on ozone absorption in alkaline potassium iodide solution

$$O_3 + 2I^- + H_2O \rightleftarrows O_2 + I_2 + 2OH^- \quad \ldots\ldots (3.2)$$

After absorption the iodide solution was acidified and the liberated iodine titrated with standard sodium thiosulphate using starch as an indicator. Measurement of thiosulphate used can be related to the iodine generated according to the following reaction

$$2Na_2S_2O_3 + I_2 \rightarrow Na_2S_4O_6 + 2NaI \quad \ldots\ldots (3.3)$$

3.4.2.2 Residence Time Distribution

As previously mentioned, a tracer step change introduced to the reactor was monitored from sample locations on the effluent liquid stream. The tracer used was a dilute solution of sodium chloride or hydrochloric acid. The sodium chloride concentration was monitored using a YSI Model 33 Salinity Conductivity-Temperature Meter.

Conductivity is the numerical expression of the ability of water to transport an electric current. As this number is linearly dependent upon the total concentration of ionized substances dissolved in the water at a given temperature, the conductivity could be utilized directly to give a measure of the degree of mixing.

When using HCl as the trace constituent the pH, as a function of time, of the resulting liquid effluent stream from the reactor was monitored. The concentration of hydrogen ions, as a function of time, was then calculated and the difference from the initial concentration was obtained.

3.4.2.3 Carbon Dioxide - Water System

Carbon dioxide transfer into distilled water was monitored by analysis of $CO_2$ in the liquid phase. Pure carbon dioxide was used as the gas phase. A known quantity of liquid, usually 10 mL, was procured from the base of the sample chamber (16) shown on Figure 5, using a volumetric pipette. This was immediately added to a known volume of NaOH. The mixture was titrated under a nitrogen atmosphere using HCl and the pH was monitored as a function of the amount of HCl added. A phenolphthalein indicator was also used to denote the end point. Inflection points could thus be obtained from a graph of HCl added versus pH.

A blank titration with NaOH against HCl in a nitrogen atmosphere was performed for each experimental run.

The concentration of $CO_2$ in the water sample was calculated in the manner detailed in Appendix A.2

3.4.2.4 Sulphur Dioxide Absorption into Sodium Hydroxide System

The amount of $SO_2$ present in the inlet and outlet gas streams was measured using a Hewlitt-Packard gas chromatograph.

Sulphur dioxide was metered from a cylinder of 100% sulphur dioxide into a nitrogen carrier stream utilizing two Matheson rotameters. It was assumed that nitrogen did not transfer into the liquid and as such a reference flow rate was established. Measuring the relative proportions of $SO_2$ to $N_2$ in the inlet and outlet gas phase streams would enable the calculation of the number of moles of $SO_2$ transferred.

The sample was obtained via two sample ports using a 5 $cm^3$ syringe. The syringe was flushed in the stream at least 10 times prior to drawing the sample. The sample was immediately discharged into the G.C.

This was repeated several times until the inlet and outlet $SO_2$ levels were established to be constant.

## 3.5 Treatment of Data

The objective of the experimental studies was to attempt to operate the reactor in the fast reaction regime so that an understanding of the kinetics of the cyanide ozone reaction could be assessed. The quantification of the enhancement of physical mass transfer by a chemical reaction in the liquid phase was also an objective. To realize these objectives the physical mass transfer of ozone into water, the evaluation of the significance of gas phase resistance and the measurement of residence time distribution to assess the mixing characteristics of the reactor had to be measured. The following section describes the evaluation techniques used for the data obtained.

### 3.5.1 Residence Time Distribution

The residence time distribution was measured employing a conductivity or hydrogen ion concentration measurement to a step function of a NaCl tracer or HCl tracer, respectively.

Prior to recording the response of the system to the tracer, the transport lag in the system was taken into account. The time of t=0 was noted when deviations from the starting pH or conductivity

were noted. The flow of a fluid element from the reactor through the 0.635 cm nylon line was assumed to be free from backmixing.

The sample chamber held approximately 45 mL of liquid when the conductivity probe was immersed. It was assumed that the chamber was ideally mixed and as such a series of tanks analysis was required to evaluate the results.

Using salt solution tracer of $C_o$ the resulting concentration, C, was monitored as a function of time. For n tanks the response curve is described by equation 3.4.

$$(C_n/C_o)\text{step} = J_n(t) = 1\text{-}e^{-nt/\bar{\theta}}\ (1 + nt/\bar{\theta} + (1/2!)\ (nt/\bar{\theta})^2 + \ldots\ldots + (1/(n-1)!)(nt/\bar{\theta})^{n-1}) \quad \ldots\ldots (3.4)$$

where

$$\bar{\theta} = \sum_{i=1}^{n} (v/Q)i$$

Thus for two tanks

$$(C/C_o)\text{step} = J_2(t) = 1\text{-}e^{-2t/\bar{\theta}}(1 + nt/\bar{\theta}) \quad \ldots\ldots (3.5)$$

When hydrogen ion concentration was the trace material, measured via pH, the concentration was directly obtainable since the equipment was modified so that the effluent spilled over the probes into a waste receptical. In this case a tracer concentration, C, was introduced to the reactor filled with distilled water of hydrogen ion concentration $C_o$. The resulting concentration was monitored with time and is mathmatically expressed as

$$\frac{dc}{dt} = \frac{1}{\bar{\theta}}\ (C_F\text{-}C) \quad \ldots\ldots (3.6)$$

The solution to equation 3.6 with boundary conditions $C=C_o$ at $t \leq 0$ is

$$\ln((C_F-C) / (C_F-C_o)) = t/\bar{\theta} \quad \ldots\ldots (3.7)$$

where $\bar{\theta} = \frac{v}{Q}$

Consequently, a plot of $\ln((C_F-C) / (C_F-C_o))$ versus t should yield a straight line of slope $\bar{\theta}$ if completely mixed conditions exist.

3.5.2 Physical Mass Transfer Measurement

The physical absorption of ozone in distilled water was estimated from measurements of carbon dioxide uptake in water. This indirect method was used since analyses of ozone in water has been suggested to be subject to error *(Kinman (1975))* partly because ozone decomposes in aqueous solutions.

The uptake of $CO_2$ in the liquid phase was measured and an liquid phase mass transfer coefficient generated using

$$\bar{V}a^o = k_L{}^o a\ (c_o'-c_o) \quad \ldots\ldots (3.8)$$

where a is the interfacial area and $c_o$ is the concentration of the absorbing component. Since

$$\bar{V}^o = Q(c_o-c_{oi})/a \quad \ldots\ldots (3.9)$$

equation 3.8 could be rearranged to

$$k_L{}^o{}_{CO_2} = \frac{Q}{a}\frac{(c_o-c_{oi})}{(c_o'-c_o)} \quad \ldots\ldots (3.10)$$

The transfer coefficient for ozone could then be calculated assuming that under similar hydrodynamic conditions (same stirring rate and ideal mixed conditions), the time available for diffusion was equivalent for the two systems. That is;

$$t_{D\ CO_2} = \frac{D_{CO_2}}{k_L{}^{o2}{}_{CO_2}} = t_{D\ O_3} = \frac{D_{O_3}}{k_L{}^{o2}{}_{O_3}} \quad \ldots\ldots (3.11)$$

Thus, $$k_L^o{}_{O_3} = k_L^o{}_{CO_2} (D_{O_3}/D_{CO_2})^{.5} \quad \ldots\ldots (3.12)$$

The diffusivity of carbon dioxide was obtained from the literature while that of ozone was calculated using the *Wilke and Chang (1955)* correlation. This method has been used by other investigators, including *Hill and Spenser (1975)*, and the diffusivity was found to be $1.984 \times 10^{-5}$ cm/s at 25°C. Details of the calculation can be found in Appendix C.1.

3.5.3 Measurement of Gas Phase Resistance

In order to determine if the gas phase resistance to absorption was significant a system was required in which the liquid resistance could be eliminated. This could be accomplished by absorbing a gas into a solution of a reagent with which it instantaneously reacts. This has been reviewed by *Sharma and Danckwerts (1970)* and should the condition

$$k_G p < k_L b_o \quad \ldots\ldots (3.13)$$

be satisfied the rate of absorption can be expressed as

$$\bar{V} = k_G p \quad \ldots\ldots (3.14)$$

where $k_G$ is the gas phase mass transfer coefficient expressed in gmole/cm$^2$ s atm. The $SO_2$ absorption into a 1-4 M NaOH solution has been identified to be such a system *(Vidwans and Sharma (1967))*. The generated value of $k_G$ could be converted to that of ozone using a relationship similar to equation 3.12.

To convert $k_G$ to the same units as $k_L^o$ it is multiplied by the gas constant and temperature;

$$k_g = k_G RT \qquad \ldots\ldots (3.15)$$

where R is expressed in atm $cm^3$/gmole K. The proportion of liquid phase to total mass transfer resistance can be determined from equation 3.16.

$$\frac{1}{K_L} = \frac{1}{k_L} + \frac{RT}{Hk_g} \qquad \ldots\ldots (3.16)$$

where H is the Henry's law coefficient expressed in atm $cm^3$/gmole. The liquid phase resistance is defined as

$$\frac{1/k_L}{1/K_L} \qquad \ldots\ldots (3.17)$$

and if

$$1/k_L >> RT/Hk_g \qquad \ldots\ldots (3.18)$$

$$k_L \simeq K_L \qquad \ldots\ldots (3.19)$$

3.5.4 Absorption with Simultaneous Chemical Reaction - Simple Cyanide Reactions

3.5.4.1 Mass Transfer Characteristics

The method of calculating the chemical mass transfer coefficient of ozone absorption for the reacting system with cyanide is similar to equation 3.10. For ozone

$$K_L = \frac{\text{Ozone Consumed in Gas Phase}}{ap/H} \qquad \ldots\ldots (3.20)$$

Knowing $k_g$ and $K_L$, $k_L$ can be determined from equation 3.16. If the gas phase resistance to mass transfer is negligible equation 3.19 can be substituted into equation 3.20 resulting in

$$k_L = \frac{\text{Ozone Consumed in Gas Phase}}{a(c_o' - c_o)} \qquad \ldots\ldots (3.21)$$

It was assumed, based on the review of the literature, that the time required for reaction, $t_r$ was much less than that for diffusion, $t_D$. This implies that the bulk liquid ozone concentration approached zero and was immeasurable. It was therefore necessary to obtain a value for $c_o - c_{oi}$ in an indirect manner. Two possibilities existed

a. Measure the change in the gas phase concentration of ozone and assume that this amount was completely absorbed into the liquid and reacted with cyanide.

b. Assume a stoichiometry and monitor cyanides depletion, and as such calculate a value for the ozone consumed in the gas phase by the following relationship

$$\text{Ozone Consumed in Gas Phase} = (b_i - b_o)/q \quad \ldots\ldots (3.22)$$

where q is the stoichiometric coefficient.

In that the stoichiometry was not completely understood it was desirable to obtain the amount of ozone reacted by measuring the depletion of ozone in the gas phase. However the very small concentrations of ozone in the inlet (1.6%) and outlet (1.5%) streams coupled with the small change in concentration led to considerable uncertainty in the measured amount of ozone consumed. Cyanide and ozone depletion was measured and a $\Delta O_3/\Delta CN^-$ value was generated which varied for each run.

Equating cyanide depletion in the liquid phase to an equivalent molar amount of ozone absorbed was equally inaccurate in that the cyanate reaction has been suggested by *Tang (1978)* to be significant. Due to an experimental design assumption to

the contrary, the cyanate concentration was not monitored so the influence of the ozone-cyanate reaction on the total absorption of ozone between phases is unknown.

Due to these difficulties, the average measured ratio of ozone absorption to cyanide depletion (1/q) was used to calculate a measured value of $K_L$. A stoichiometry for an overall reaction could be obtained by using this average, namely

$$O_3 + q(\text{reactants}) \rightarrow \text{products} \quad \ldots\ldots (3.23)$$

where the reactants are cyanide and cyanate for the simple cyanide runs and include thiocyanate for the barren bleed runs and the products are those described earlier in section 2.3.3.

Substitution of equation 3.22 into 3.20 and assuming $c_o$ is equal to zero in the denominator results in

$$K_L = \frac{Q(b_i - b_o)}{ap/H} \quad \ldots\ldots (3.24)$$

Correcting for gas phase resistance yields a value for $k_L$.

3.5.4.2 Calculation of Kinetic Constants

An attempt to approximate kinetic constants for the reactions could be made if the experimental results indicated operating conditions in the fast or transition from fast to instantaneous (transition) reaction regimes.

3.5.4.2.1 Transition Regime

For the transition regime the reduction of cyanide and cyanate concentration occurs in the vicinity of the interface. As the reaction rate increases the extent of this depletion approaches a situation described in the instantaneous reaction regime where two

differential equations are solved using boundary conditions representing a distinct stationary reaction plane.

The moving boundary solution for the transition regime has not been solved analytically; however, simplifying hypotheses and numerical computation has been shown by *Astarita (1967)* for a two reactant system. In this case the original model assumed, namely the cyanide-ozone, cyanate-ozone reactions would not allow for a solution. Three simultaneous dependent differential equations are involved,

$$D_1 \frac{\partial^2 c}{\partial x^2} = kcb + 1.5k_2 cb_N \quad \ldots\ldots (3.25)$$

$$D_2 \frac{\partial^2 c}{\partial x^2} = kcb \quad \ldots\ldots (3.26)$$

$$D_3 \frac{\partial^2 b_N}{\partial x^2} = -kcb + k_2 cb_N \quad \ldots\ldots (3.27)$$

where c, b and $b_N$ and subscripts 1, 2 and 3 refer to ozone, cyanide and cyanate, respectively.

As has been shown, q moles of liquid phase reactant were depleted for each mole of ozone absorbed. An alternate reaction mechanism possibly could be used to overcome the difficulty of using a three component system in the transition regime. This simplification assumes;

$$qCN^- + O_3 \rightarrow CNO^- + \text{other products} \quad \ldots\ldots (3.28)$$

The two component assessment of transition regime theory can then be utilized as described in section 2.4.2.4.

The relationship between I and the transition regime model is given in equation 2.71. It will be shown that for all the runs the operating conditions allowed for a significant simplification of equation 2.71 to

$$I^2 = \frac{t_D}{t_r} \frac{(I_\infty - I)}{(I_\infty - 1)} \quad \ldots\ldots (3.29)$$

Substituting the expression for $t_r$ (given in equation 2.43) into equation 3.29 and rearranging yields

$$k = \frac{I^2}{t_D b_o} \left(\frac{I_\infty - 1}{I_\infty - I}\right) \quad \ldots\ldots (3.30)$$

3.5.4.2.2 Fast Reaction Regime

If the cyanide and cyanate reactions occurred in the fast reaction regime the material balances for $CN^-$, $CNO^-$ and $O_3$ could be reduced to one differential equation, namely,

$$D_1 \frac{\partial^2 c}{\partial x^2} = kcb + 1.5\, k_2 c b_N \quad \ldots\ldots (3.31)$$

where c, b and $b_N$ refer to ozone, cyanide and cyanate, respectively. The boundary conditions are

$$x=o \rightarrow c=c_o'$$

$$c=c_o \rightarrow \frac{\partial c}{\partial x} = o$$

This is possible since it is assumed that b and $b_N$ were constant through the film. The above equation can be simplified to

$$D_1 \frac{\partial^2 c}{\partial x^2} = k_1 c \quad \ldots\ldots (3.32)$$

where

$$k_1 = kb + 1.5\, k_2 b_N \quad \ldots\ldots (3.33)$$

The general solution to equation 3.32 can be found in the literature for the psuedo first order reaction. This solution is given as

equation 2.55. Since ozone was assumed not to be able to co-exist with cyanide in the liquid phase, c' is equal to zero and equation 2.55 becomes

$$\overline{V} = \sqrt{D_1 k_1}\, c_o' \qquad \ldots\ldots (3.34)$$

Utilizing equation 2.56, the chemical absorption coefficient is expressed as

$$k_L = \sqrt{D_1 k_1} = \frac{\overline{V}}{c_o'} \qquad \ldots\ldots (3.35)$$

Equation 3.35 is dependent on the cyanate concentration, $b_N$, which was unknown. In order to obtain an expression for the cyanate concentration, material balances for a continuous stirred tank reactor (CSTR) were used.

For cyanide;

$$Q(b_i - b_o) = k b_o c_o' \nu_\ell \qquad \ldots\ldots (3.36)$$

where $\nu_\ell$ is the volume of liquid in the reactor.

For cyanate;

$$Q(-b_N) = (k_2 b_{N_o} c_o' - k b_o c_o')\, \nu_\ell \qquad \ldots\ldots (3.37)$$

Substituting $c_o'$ derived from equation 3.36 into equation 3.37 the steady state bulk liquid concentration of cyanate is expressed as

$$b_{No} = \left(\frac{k_2}{k b_o} + \frac{1}{b_i - b_o}\right)^{-1} \qquad \ldots\ldots (3.38)$$

Instead of using the average measured ratio of ozone absorption to cyanide destruction, the expression

$$1/q = 1 + 1.5\, k_2 b_{No}/k b_o \qquad \ldots\ldots (3.39)$$

can be used where the latter term on the right hand side is the influence of the cyanate reaction. Substituting equation 3.39 into equation 3.24 results in

$$k_L = \left(1 + \frac{1.5\, k_2 b_{No}}{k b_o}\right) \frac{Q(b_i - b_o)}{a c_o'} \qquad \ldots\ldots (3.40)$$

assuming the gas phase resistance is negligible.

The solution of the above equation can be made through trial and error procedure by;

1) Assume a value for k

2) Calculate $k_2$ by using the relationship found in *Baiyanskii et al. (1972)* where $k/k_2 = 5.1$

3) Use equation 3.38 to calculate $b_N$

4) Calculate $k_L$ from equation 3.40

5) Calculate value of $k_1$ from equation 3.35 and check with assumed value using equation 3.33.

### 3.5.5 Complex Cyanide Reactions

#### 3.5.5.1 Mass Transfer Studies

When ozone was absorbed by the barren bleed many complex cyanide reactions occurred. Apart from the cyanide ion, cyanide complexes, cyanate and thiocyanate were present in the liquid phase. Since many of the metallic cyanide species have been suggested to react as ionic cyanide after dissociation of the complex (section 2.3.3), three principal species can be assumed as reactants with ozone; $CN^-$, $CNO^-$ and $CNS^-$.

For the barren bleed runs all three were measured however delays in shipping and analysis may have resulted in deterioration of the preserved samples, especially through hydrolysis of cyanate. An estimate of the total ozone absorption could be obtained directly by gas phase measurement or by assuming reaction stoichiometrics for the cyanide (equation 2.8), cyanate (equation 2.12) and

thiocyanate (equation 2.20) reactions. The measured value could be compared to a theoretical value in order to determine the significance of the sample deterioration and to provide some indication as to the validity of the assumed stoichiometrics. Once a method for calculating the ozone absorption rate was determined the overall liquid phase mass transfer coefficient could be calculated in a similar fashion to equation 3.24.

3.5.5.2 Treatability Studies

Previous studies outlined in section 2.3.3 indicate the effectiveness of ozone to destroy most of the cyanide species present in electroplating and gold mining wastes. Thus, only several runs were required to verify the effectiveness of ozone on treating the barren bleed solution from Giant Yellowknife Mines, Ltd. Of primary interest in this experiment was the measurement of ozone use and residual cyanide concentration.

# 4 RESULTS

## 4.1 Residence Time Distribution

Results for the conductivity response measurement as analysed using equation 3.5 are shown in Figure 6.

Deviation from ideal mixing behavior was noted at the stirring speed of 82 rpm yet at 150 rpm ideal behavior was satisfied. At 150 rpm the liquid surface was unacceptably wavy and hence, a lower stirring speed range of 90-120 rpm was used for the mass transfer runs.

Residence time distribution studies were conducted in this range and initially assessed to indicate near-perfect mixing. Upon completion of the experimental work further assessment indicated a deviation from ideality.

One possible explanation for this deviation could have been due to the monitoring configuration of the conductivity probe. The probe was a cylinder with two internal cylindrical channels running its full length. These channels may not have been well mixed, as was assumed, due to the shielding afforded by the probe and as such verification of residence time distribution by a different method, the HCl trace, was employed.

The results of this trace conducted at a stirring speed of 106 rpm, which was the speed for the majority of mass transfer runs, were plotted reflecting equation 3.7 and are shown in Figure 7.

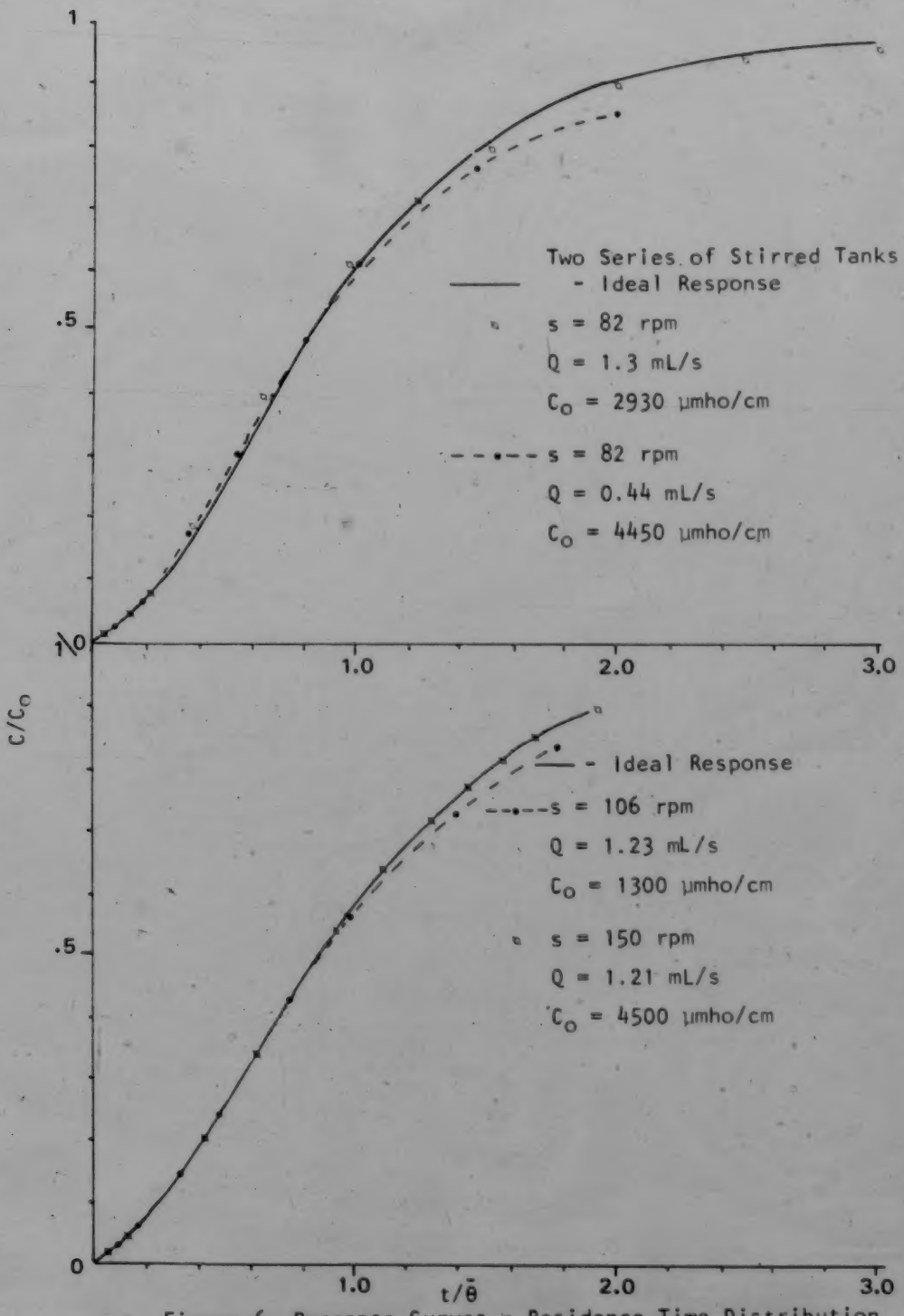


Figure 6 Response Curves - Residence Time Distribution
Sodium Chloride Tracer

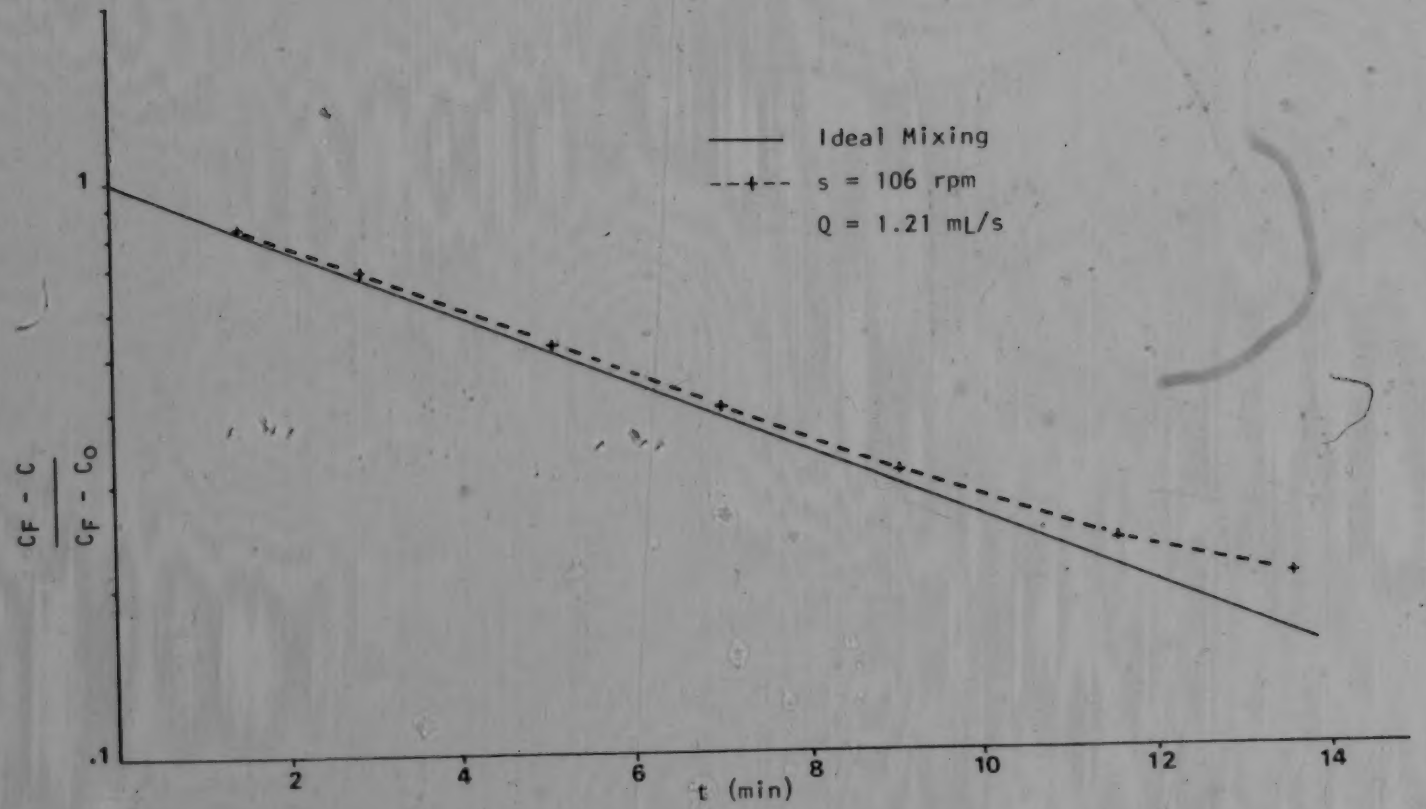


Figure 7 Residence Time Distribution - Hydrochloric Acid Tracer

Deviation from ideality was still evident and hence, it was concluded that continuous stirred tank reactor conditions did not apply. The deviation, however, was considered small and as such, analysis of the absorption results found later in this report are based on ideal stirred reactor conditions.

## 4.2 Carbon Dioxide Absorption

The liquid side mass transfer coefficient for the physical absorption of carbon dioxide into water at 25°C ranged between $5.2 \times 10^{-3}$ and $7.2 \times 10^{-3}$ cm/s over the stirring speed range of 99 to 121 revolutions per minute. This range of stirring speeds was used for the ozone cyanide system.

The results of the experimental runs are shown in Figure 8, along with the line representing the least mean squares fit. Details of associated reactor conditions are given in Appendix B.1 and a sample calculation is given in Appendix C.2.

The value of $k_L^o$ graphically depicted is the carbon dioxide absorption coefficient adjusted to 25°C. No temperature control features were incorporated into the design of the equipment. The liquid temperature varied with room temperature and ranged between 20.8 and 23.8°C. The relationship

$$k_{L_{T_2}}^{o} = k_{L_{T_1}}^{o} \left(D_{T_2} / D_{T_1}\right)^{0.5} \qquad \ldots\ldots (4.1)$$

where $D_{T_2}$ and $D_{T_1}$ are the diffusivities of carbon dioxide or ozone in water evaluated at $T_2$ and $T_1$, respectively, was used to correct the absorption coefficient for temperature. Diffusivities were adjusted to the desired temperature using the Nernst-Einstein relationship;

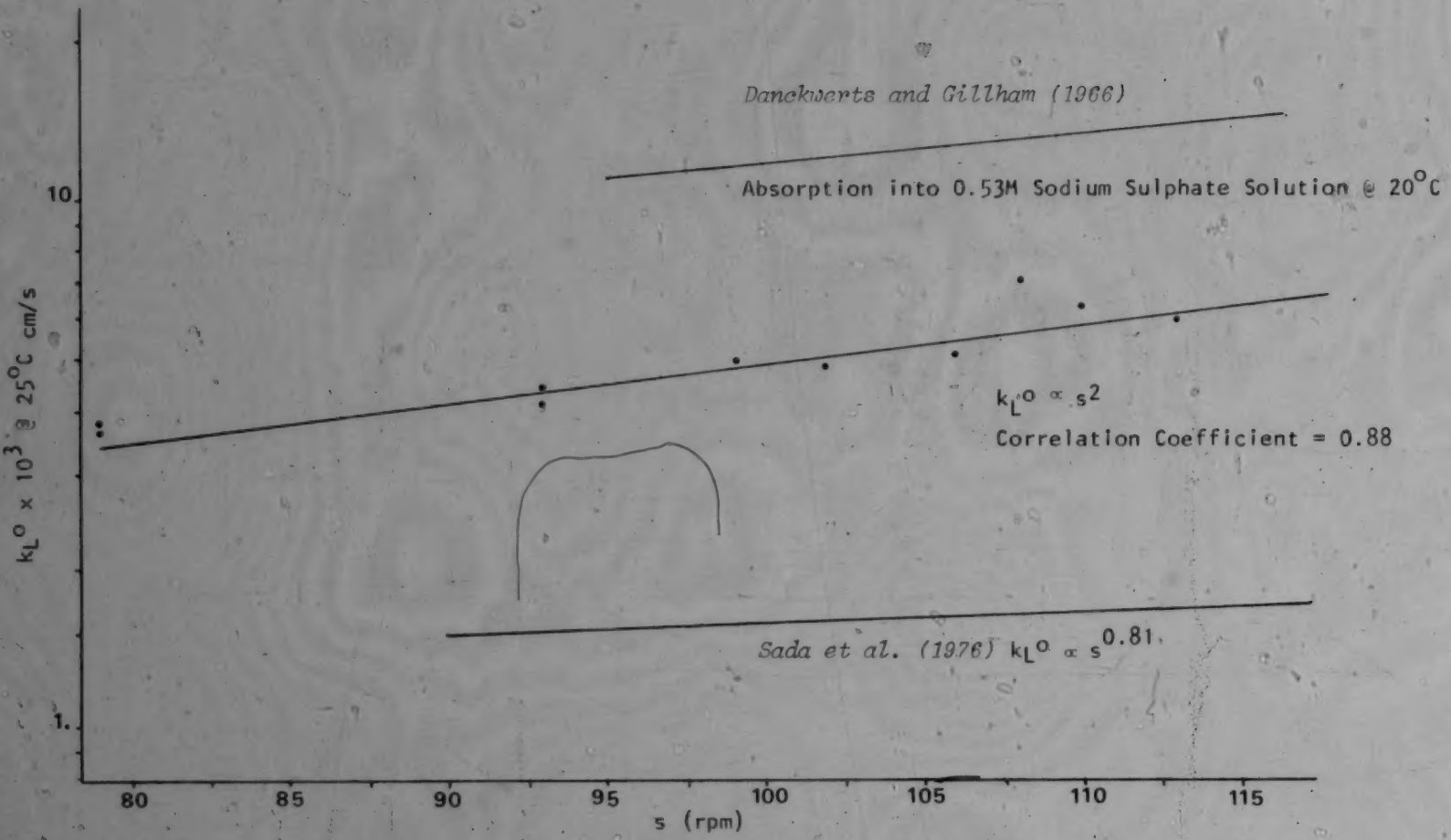


Figure 8 Liquid Side Mass Transfer Coefficient of Carbon Dioxide Absorption into Water Versus Stirring Speed

$$\frac{D\mu}{T} = \text{constant} \qquad \ldots\ldots (4.2)$$

where $\mu$ is the viscosity of water. The temperature dependence of the carbon dioxide diffusivity has been demonstrated by *Nijsing et al. (1959)* to follow this relationship.

The distilled water used, although not monitored for pH prior to each run, commonly exhibited slightly acidic quality in the range of 5.0-6.0. *Nijsing et al. (1959)* and *Sada et al. (1976)* report that this absorption may be considered purely physical.

4.2.1 Ozone-Water Physical Transfer Coefficients

Table I shows the calculated values of $k^{o}_{L_{O_3}}$ for those stirring speeds used in the cyanide-ozone experiments. Since the calculated diffusivity of ozone is approximately equal to that of carbon dioxide at 25°C, the values of $k^{o}_{L_{O_3}}$ were calculated to be equal to $k^{o}_{L_{CO2}}$.

4.3 Sulphur Dioxide Absorption Into Sodium Hydroxide

Two runs were conducted to measure gas phase resistance using the $SO_2$ absorption from a $SO_2$- $N_2$ gas into a caustic solution. The results of the two experiments conducted are found in Table 2. The diffusivities applied to both systems were calculated using the Wilke-Lee modification of the Hirschfelder-Bird-Spotz method *(Hirschfelder et al. (1949))*. Details of the calculations are given in Appendix C.3.

TABLE I

MASS TRANSFER COEFFICIENT
FOR OZONE - WATER SYSTEM @ 25°C

| RPM | $k^{o}_{L_{CO_2}}$ @ 25°C cm/s | $k^{o}_{L_{O_3}}$ @ 25°C * cm/s |
|---|---|---|
| 99 | 0.0052 | 0.0052 |
| 100 | 0.0053 | 0.0053 |
| 106 | 0.0058 | 0.0058 |
| 110 | 0.0062 | 0.0062 |
| 115+ | 0.0066 | 0.0066 |
| 121+ | 0.0072 | 0.0072 |

$D_{O_3} = 1.984 \times 10^{-5}$ cm$^2$/s @ 25°C

$D_{CO_2} = 1.96 \times 10^{-5}$ cm$^2$/s @ 25°C

* As calculated using equation (3.12)

\+ Extrapolated values from Figure 8

TABLE 2

GAS PHASE MASS TRANSFER COEFFICIENTS

| Stirring Speed | Temp | $D_{SO_2-N_2}$ | $D_{O_3-air}$ | $k_{GSO_2}$ | $k_{gSO_2}$ | $k_{gO_3}$ |
|---|---|---|---|---|---|---|
| | | | | gmole | | |
| RPM | °C | $cm^2/s$ | $cm^2/s$ | $cm^2$ s atm | cm/s | cm/s |
| 106 | 20.5 | 0.109 | 0.124 | $5.25 \times 10^{-5}$ | 1.26 | 1.34 |
| 106 | 21.1 | 0.113 | 0.125 | $6.8 \times 10^{-5}$ | 1.64 | 1.72 |

The average of the two runs, 1.53 cm/s, was used as the value of the gas phase mass transfer coefficient.

4.4 Ozone Absorption and Simultaneous Reaction with Cyanide

4.4.1 Simple Cyanide Reactions

System operating conditions for each mass transfer run are given in Tables 3 and 4 for the gas and liquid phases, respectively. Gas flow rates for all runs were near 1.80 sL/ min and the average ozone concentration was approximately 1.6%. The range of liquid flow rates was 0.17 to 1.37 mL/s which equates to an average residence time range between 379 to 2971 s. The stirring speed was varied for several runs, however the majority of experimental runs were conducted at 106 rpm.

The ozone uptake expressed as a fraction of the cyanide depletion was found to average 1.2 with a standard deviation of 0.42 (Table 5). From this result a stoichiometric coefficient (1/q) of 1.2 gmole $O_3$/gmole $CN^-$ was used for calculating $k_L$.

TABLE 3

GAS PHASE OPERATING CONDITIONS

FOR $O_3$ ABSORPTION INTO NaCN SOLUTIONS

| Run No. | Gas Temperature °C | Outlet Flow Rate sL/min | Outlet % $O_3$ | $C_o$* (mg/L) | Inlet Flow Rate sL/min | Inlet % $O_3$ |
|---|---|---|---|---|---|---|
| 1 | 22.8 | 1.75 | 1.52 | 11.62 | 1.75 | 1.57 |
| 2 | 23.7 | 1.72 | 1.53 | 11.13 | 1.72 | 1.63 |
| 3 | 22.3 | 1.76 | 1.5 | 11.5 | 1.76 | 1.59 |
| 4 | 23.3 | 1.73 | 1.55 | 11.44 | 1.73 | 1.61 |
| 5 | 22.5 | 1.68 | 1.57 | 11.72 | 1.68 | 1.64 |
| 6 | 22.8 | 1.80 | 1.58 | 12.32 | 1.80 | 1.72 |
| 7 | 22 | 1.83 | 1.55 | 12.18 | 1.83 | 1.57 |
| 8 | 22.4 | 1.84 | 1.52 | 11.83 | 1.83 | 1.59 |
| 9 | 22.8 | 1.80 | 1.64 | 12.63 | 1.80 | 1.70 |
| 10 | 23.3 | 1.80 | 1.45 | 11.01 | 1.80 | 1.51 |
| 11 | 23.3 | 1.83 | 1.57 | 11.71 | 1.83 | 1.63 |
| 12 | 22.3 | 1.85 | 1.57 | 12.08 | 1.83 | 1.63 |
| 13 | 22.8 | 1.84 | 1.46 | 11.2 | 1.82 | 1.62 |
| 14 | 23.1 | 1.82 | 1.62 | 12.47 | 1.82 | 1.64 |
| 15 | 22.8 | 1.89 | 1.55 | 11.95 | 1.85 | 1.60 |
| 16 | 22.1 | 1.88 | 1.54 | 12.26 | 1.85 | 1.63 |
| 17 | 22.9 | 1.84 | 1.57 | 12.01 | 1.84 | 1.60 |
| 18 | 21.7 | 1.83 | 1.59 | 12.7 | 1.83 | 1.61 |
| 19 | 21.5 | 1.80 | 1.58 | 12.81 | - | - |
| 20 | 21.7 | 1.80 | 1.59 | 12.88 | 1.82 | 1.61 |
| 21 | 22.3 | 1.81 | 1.62 | 12.79 | 1.81 | 1.67 |
| 22 | 22.2 | 1.84 | 1.58 | 12.71 | 1.84 | 1.67 |
| 23 | 22 | 1.84 | 1.59 | 12.78 | 1.82 | 1.66 |
| 24 | 21.8 | 1.84 | 1.59 | 12.9 | 1.83 | 1.65 |
| 25 | 22.3 | 1.84 | 1.60 | 12.9 | - | - |
| 26 | 21.6 | 1.85 | 1.56 | 13.0 | - | - |
| 27 | 22.8 | 1.78 | 1.67 | 13.1 | - | - |
| 28 | 21.7 | 1.81 | 1.61 | 6.16 | 1.79 | 1.69 |
| 29 | 22.2 | 1.81 | 1.61 | 3.52 | - | - |
| 30 | 21.9 | 1.83 | 1.60 | 6.35 | 1.82 | 1.66 |
| 31 | 21.9 | 1.81 | 1.61 | 6.06 | - | - |
| 32 | 22.4 | 1.81 | 1.6 | 3.08 | - | - |

Gas phase reactor volume = 0.96L

$\bar{\theta}$ = 0.5 min

* dry basis

TABLE 4

LIQUID PHASE REACTOR CONDITIONS

FOR $O_3$ ABSORPTION INTO NaCN SOLUTIONS

| Run No. | $CN_i$ | $CN_b$ | Molarity $OH^-$ | Temp of Liquid | Stirring Rate | Liquid Average Residence Time (s)** | $D_{O_3} \times 10^{-5}$ @ T |
|---|---|---|---|---|---|---|---|
| | mg/L | mg/L | gmole/L | °C | (RPM) | | $cm^2/s$ |
| 1 | 53.3 | 41.4 | 0.05 | 22.8 | 106 | 409 | 1.87 |
| 2 | 54.0 | 42.4 | 0.05 | 23.6 | 106 | 422 | 1.91 |
| 3 | 54.3 | 40.5 | 0.05 | 22.3 | 106 | 541 | 1.84 |
| 4 | 54.4 | 33.1 | 0.05 | 23.3 | 106 | 981 | 1.90 |
| 5 | 54.4 | 7.3 | 0.05 | 22.8 | 106 | 2971 | 1.87 |
| 6 | 41.6 | 28.0 | 0.05 | 23 | 106 | 642 | 1.88 |
| 7 | 38.9 | 26.2 | 0.05 | 23.2 | 106 | 642 | 1.87 |
| 8 | 90.6 | 68.3 | 0.05 | 22.7 | 106 | 642 | 1.87 |
| 9 | 90.6 | 67.7 | 0.05 | 22.8 | 106 | 642 | 1.87 |
| 10 | 90.6 | 68.7 | 0.05 | 22.8 | 106 | 642 | 1.87 |
| 11 | 101.3 | 77.9 | 0.05 | 23.5 | 106 | 626 | 1.91 |
| 12 | 51.2 | 34.6 | 0.05 | 23 | 115 | 634 | 1.88 |
| 13 | 58.1 | 38.4 | 0.05 | 23 | 121 | 634 | 1.88 |
| 14 | 58.1 | 38.9 | 0.05 | 23 | 110 | 634 | 1.88 |
| 15 | 122.2 | 98.3 | 0.05 | 23 | 99 | 634 | 1.88 |
| 16 | 77.8 | 60.5 | 0.05 | 22.4 | 99 | 634 | 1.85 |
| 17 | 19.0 | 8.3 | 0.025 | 23.2 | 106 | 642 | 1.89 |
| 18 | 24.3 | 17.2 | 0.025 | 22 | 100 | 642 | 1.83 |
| 19 | 68.3 | 56.8 | 0.003* | 21.6 | 106 | 388 | 1.81 |
| 20 | 59.7 | 48.5 | 0.003* | 21.7 | 106 | 394 | 1.82 |
| 21 | 65.5 | 53.7 | 0.003 | 22.4 | 106 | 394 | 1.85 |
| 22 | 101.8 | 84.6 | 0.03 | 22.2 | 106 | 388 | 1.84 |
| 23 | 40.2 | 27.7 | 0.03 | 22.1 | 106 | 388 | 1.84 |
| 24 | 37.5 | 28.6 | 0.006 | 21.8 | 106 | 394 | 1.82 |
| 25 | 34.1 | 22.7 | 0.07 | 22 | 106 | 394 | 1.83 |
| 26 | 35.7 | 25.7 | 0.025 | 21.3 | 106 | 400 | 1.8 |
| 27 | 43.5 | 32.5 | 0.05 | 22.5 | 106 | 388 | 1.86 |
| 28 | 43.5 | 23.3 | 0.05 | 35.5 | 106 | 385 | 2.57 |
| 29 | 42.6 | 27.6 | 0.05 | 42 | 106 | 385 | 2.97 |
| 30 | 42.5 | 31.8 | 0.05 | 35.5 | 106 | 382 | 2.57 |
| 31 | 43.0 | 32.6 | 0.05 | 35.7 | 106 | 388 | 2.58 |
| 32 | 42.6 | 27.1 | 0.05 | 43.3 | 106 | 379 | 3.05 |

* CaO used as base; all other runs NaOH used

** Based on liquid volume of 520 mL

TABLE 5

MEASURED LIQUID PHASE MASS TRANSFER COEFFICIENT AND ASSOCIATED ENHANCEMENT FACTORS

| Run | $b_o$ mg/L | $k_L^o \times 10^3$ cm/s | $k_L \times 10^3$ cm/s | I | $q^{-1}$ gmole/gmole |
|---|---|---|---|---|---|
| 1 | 41.4 | 5.63 | 36.84 | 6.6 | 0.86 |
| 2 | 42.4 | 5.67 | 36.12 | 6.4 | 2.16 |
| 3 | 40.5 | 5.58 | 31.92 | 5.8 | 1.67 |
| 4 | 33.1 | 5.67 | 27.36 | 4.8 | 2.39 |
| 5 | 7.3 | 5.63 | 19.44 | 3.5 | 1.74 |
| 6 | 28.0 | 5.64 | 25.20 | 4.4 | 1.22 |
| 7 | 26.2 | 5.63 | 23.64 | 4.2 | 1.14 |
| 8 | 68.3 | 5.63 | 42.60 | 7.6 | 1.08 |
| 9 | 67.7 | 5.63 | 41.28 | 7.3 | 1.0 |
| 10 | 68.7 | 5.63 | 45.12 | 8.0 | 1.29 |
| 11 | 77.9 | 5.69 | 45.72 | 8.0 | 1.02 |
| 12 | 34.6 | 6.42 | 31.68 | 4.9 | 1.01 |
| 13 | 38.4 | 7.0 | 39.60 | 5.6 | 1.32 |
| 14 | 38.9 | 6.03 | 34.68 | 5.8 | 1.03 |
| 15 | 98.3 | 5.06 | 44.88 | 8.9 | 0.61 |
| 16 | 60.5 | 5.02 | 32.88 | 6.5 | 1.53 |
| 17 | 8.3 | 5.66 | 20.28 | 3.6 | 0.96 |
| 18 | 17.2 | 5.09 | 12.72 | 2.5 | 0.99 |
| 19 | 56.8 | 5.54 | 33.72 | 6.1 | - |
| 20 | 48.5 | 5.55 | 32.16 | 5.8 | 1.1 |
| 21 | 53.7 | 5.60 | 34.08 | 6.1 | 1.02 |
| 22 | 84.6 | 5.58 | 50.88 | 9.1 | 1.04 |
| 23 | 27.7 | 5.58 | 36.72 | 6.6 | 0.89 |
| 24 | 28.6 | 5.55 | 25.56 | 4.6 | 0.84 |
| 25 | 22.7 | 5.56 | 32.64 | 5.9 | - |
| 26 | 25.7 | 5.52 | 28.08 | 5.2 | - |
| 27 | 32.5 | 5.62 | 30.36 | 5.4 | - |
| 28 | 23.3 | 6.60 | 122.28 | 18.5 | 0.91 |
| 29 | 27.6 | 7.07 | 161.28 | 22.8 | - |
| 30 | 31.8 | 6.06 | 63.60 | 9.6 | 1.02 |
| 31 | 32.6 | 6.61 | 64.44 | 8.6 | - |
| 32 | 27.1 | 7.19 | 193.2 | 26.9 | - |
| | | | | Mean | 1.20 |
| | | | | Std. Dev. | 0.42 |

4.4.1.1. Mass Transfer Coefficients

Table 5 shows the measured liquid phase mass transfer coefficient and the associated value of I for each run. The value of $k_L$ has not been corrected for gas phase resistance since it can be shown that the measured gas phase transfer coefficient (section 4.3) represents approximately less than one percent of the total mass transfer resistance. A detailed calculation verifying this is given in Appendix C.4. Since the standard deviation for the measured value of q is 35 percent of the mean, correcting for the gas phase resistance is not warranted.

4.4.1.1.1 Affect of Changing Hydrodynamics

A variety of operating modes were used to generate different bulk liquid cyanide concentrations. Whereas the primary method was the alteration of the inlet cyanide concentration, other methods including changing the liquid average residence time and the stirring speed; namely changing the hydrodynamic conditions.

Figure 9 presents the enhancement factor versus $k_L^o$ in an attempt to show the affect of changing hydrodynamics on the results. Groupings for similiar bulk cyanide concentrations are shown. It is not possible to identify the relationship or independence of $k_L^o$ on I given the limited data and the small range of $k_L^o$ investigated. It appears that changing hydrodynamics do not influence the results from the pairs of runs 13 and 14, 12 and 27, 15 and 22, and 16 and 19. However, considerable scatter was experienced for the same hydrodynamic condition ($k_L^o = 5.5 \times 10^{-3}$ cm/s) for similiar bulk cyanide concentrations as is evidenced by the identification of runs with $b_o$ approx-

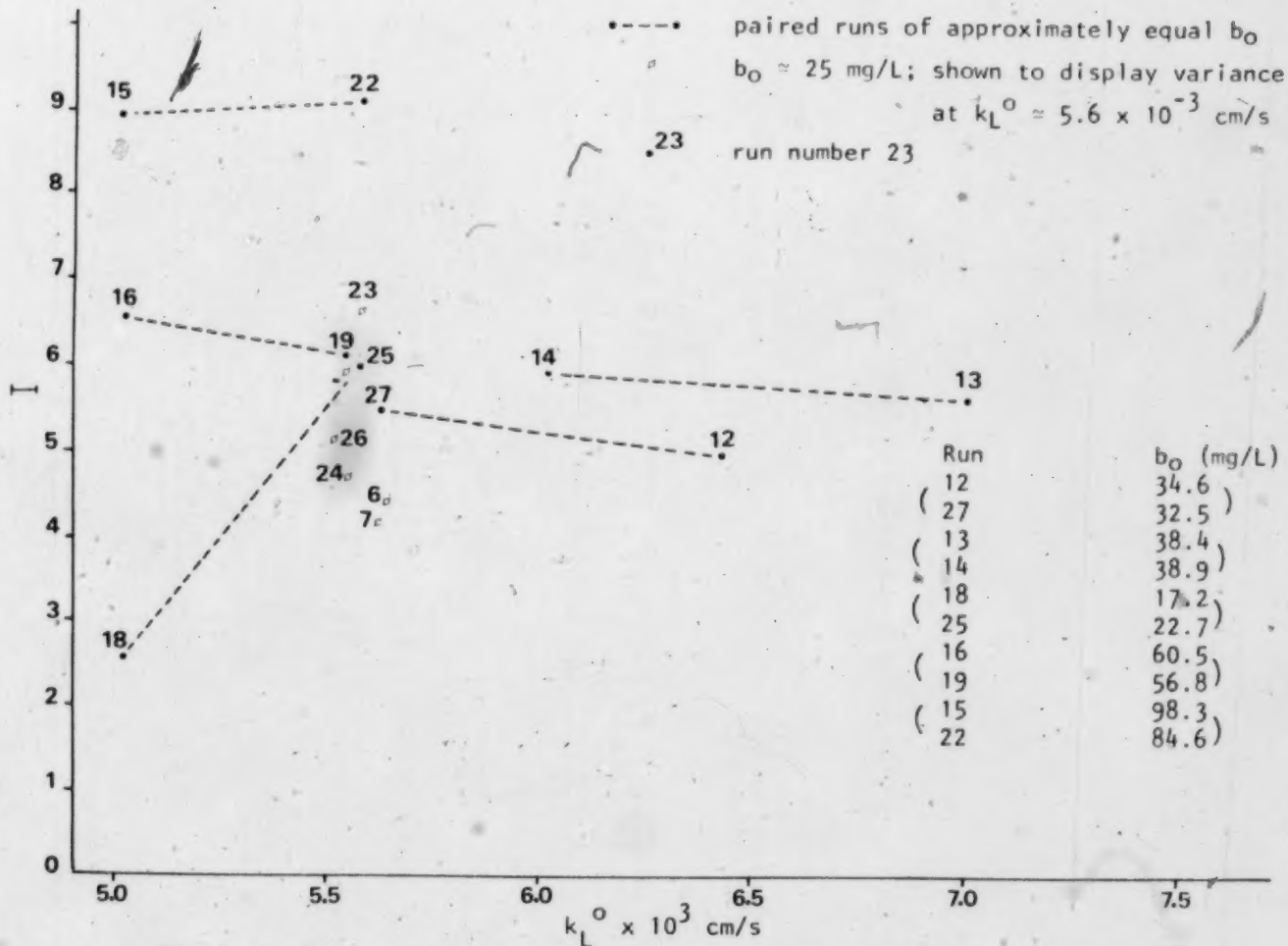
paired runs of approximately equal $b_o$
$b_o \approx 25$ mg/L; shown to display variance of I
at $k_L^o \approx 5.6 \times 10^{-3}$ cm/s
23 run number 23
I
$k_L^o \times 10^3$ cm/s
Run $b_o$ (mg/L)
( 12 34.6 )
( 27 32.5 )
( 13 38.4 )
( 14 38.9 )
( 18 17.2 )
( 25 22.7 )
( 16 60.5 )
( 19 56.8 )
( 15 98.3 )
( 22 84.6 )

Figure 9 I versus $k_L^o$ for several runs showing pairing based on the same value of $b_o$ (approximately)

imately equal to 25 mg/L shown on Figure 9. It is thus not possible to establish whether the instantaneous reaction regime applies (I independent of $k_L^o$).

Wave creation at the stirring interface may account for some of this scatter. As $k_L$ and $k_L^o$ are dependent on the inverse of the interfacial area the enhancement factors given would be influenced by different areas created by wave action. *Danckwerts and Gillham (1966)* show the influence of stirring speed on the apparent interfacial area of a similar absorber; however, they do not discuss the reproducibility of the "apparent area" by successive runs at the same stirring speed. Over a stirring speed range of 95 to 160 rpm, the apparent interfacial area varied 14% when established by chemical reaction methods. Using the same diameter reactor as this work, they demonstrated at 106 rpm a 2.5% increase in apparent area over cross-sectional area. The experimental variation thus cannot be solely attributed to wave action and in fact the reporting of enhancement factor rather than mass transfer coefficient could reduce the significance of this increase.

4.4.1.2 Kinetic Constants

4.4.1.2.1 Transition Regime Model

The lack of a definite relationship or independence of $k_L^o$ to the enhancement factor, I, suggests the reactions involved could be modelled using the transition from fast to instantaneous regimes (transition regime) for the experimental conditions used.

The transition regime requires the use of the instantaneous reaction regime enhancement factor, $I_\infty$, which in turn requires values for the diffusivities of ozone and the liquid phase reactant, assumed to be cyanide, in water. $I_\infty$ is defined as per equation (2.72) as,

$$I_\infty = 1 + D_2/D_1 \; b_o/qc_o' \qquad \ldots\ldots (2.72)$$

where the subscripts 2 and 1 refer to cyanide and ozone, respectively.

The diffusivity could be calculated as if the compound behaved as a single salt and the diffusion could be assumed to be molecular diffusion. The diffusion coefficient would then be given by the Nernst equation (Nernst (1888)), namely;

$$D = (RT/F_2)^2 ((1/n+ + 1/n-)/(1/\lambda_+^o + 1/\lambda_-^o)) \qquad \ldots (4.23)$$

where F is the Faraday, $n\pm$ is the valance of the cation or anion and $\lambda\pm$ is the limiting ionic conductances of the same. Data for the latter are very scarce for cyanide and thiocyanate and non-existant for cyanate. Nevertheless, calculations given in Appendix C.1 utilize these limited data taken from the International Critical Tables. Although cyanate and thiocyanate are now not assumed to react, values for their diffusivities were also calculated.

The calculated molecular diffusivities for the sodium cyanide and sodium thiocyanate salts in water are $1.3 \times 10^{-5}$ $cm^2/s$ and $1.26 \times 10^{-5}$ $cm^2/s$ at $18^oC$. The diffusion coefficients for free $CN^-$ and $CNS^-$ ions ($RT\lambda-/F^2$) are $1.6 \times 10^{-5}$ $cm^2/s$ and $1.48 \times 10^{-5}$ $cm^2/s$ at $18^oC$. It was assumed that the ion diffusion coefficient for cyanate would be similar and since the diffusivity of ozone was calculated to be $1.63 \times 10^{-5}$ $cm^2/s$ ($18^oC$), a value of unity was

assumed for $D_2/D_1$, $D_3/D_1$ and $D_4/D_1$, where the subscripts 3 and 4 refer to thiocyanate and cyanate.

It is recognized that since the experimental runs were conducted using solutions of sodium hydroxide the above generated values may be subject to error. *Sherwood and Wei (1955)* and *Vinograd and McBain (1941)* indicate that for diffusion in mixed electrolytes ions may move ahead of their "partners" so long as the electric current is maintained at zero by the lagging behind of slower ions of other molecular partners. For instance, in the simultaneous diffusion of HCl and NaCl in water the faster-moving $H^+$ ion may move ahead of its $Cl^-$ partner, as long as $Na^+$ lag behind to maintain electrical neutrality in the reaction film. *Sherwood and Wei (1955)* demonstrated that the allowance for ion diffusion may considerably influence the rate of transfer from those predicted by molecular diffusion.

The kinetic constants generated from transition regime theory are found in Table 6 together with the calculated value of $I_\infty$ and the value of I (from Table 5). Appendix C.5 details the approach taken. Values obtained vary widely, however, a mean value of 91600 L/gmole s was obtained for all room temperature runs (1-27) excluding those where analyses indicated $I_\infty > I$ and number 5.

4.4.1.2.2 Fast Reaction Regime Model

The foregoing approach was based on an average measured stoichiometric coefficient of 1.2 (1/q). Given the literature value of the relationship between the cyanide and cyanate rate and assuming fast reaction regime behaviour it was possible to calculate kinetic

TABLE 6

ENHANCEMENT FACTORS AND CALACULATED KINETIC CONSTANTS

USING TRANSITION REGIME

| Run No. | I | $I_\infty$ | $I_\infty - I$ | k(L/gmole s) |
|---|---|---|---|---|
| 1 | 6.6 | 9.0 | 2.4 | 154000 |
| 2 | 6.4 | 9.2 | 2.8 | 124700 |
| 3 | 5.8 | 8.8 | 3.0 | 95200 |
| 4 | 4.8 | 7.4 | 2.6 | 75500 |
| 5 | 3.5 | 4.0 | 0.5 | 443000 |
| 6 | 4.4 | 6.0 | 1.6 | 95200 |
| 7 | 4.2 | 5.8 | 1.6 | 89000 |
| 8 | 7.6 | 13.8 | 6.2 | 76900 |
| 9 | 7.3 | 12.9 | 5.6 | 73700 |
| 10 | 8.0 | 14.8 | 6.8 | 83300 |
| 11 | 8.0 | 15.6 | 7.6 | 69600 |
| 12 | 4.9 | 7.3 | 2.4 | 103800 |
| 13 | 5.6 | 7.8 | 2.2 | 171000 |
| 14 | 5.8 | 7.8 | 2.0 | 58500 |
| 15 | 8.9 | 19.2 | 10.3 | 50400 |
| 16 | 6.5 | 11.9 | 5.4 | 49900 |
| 17 | 3.6 | 2.5 | -1.1 | |
| 18 | 2.5 | 4.0 | 1.5 | 26700 |
| 19 | 6.1 | 10.8 | 4.7 | 60200 |
| 20 | 5.8 | 9.3 | 3.5 | 72500 |
| 21 | 6.5 | 10.3 | 4.2 | 67600 |
| 22 | 9.1 | 15.7 | 6.6 | 96100 |
| 23 | 6.6 | 5.8 | -0.8 | |
| 24 | 4.6 | 5.9 | 1.3 | 122900 |
| 25 | 5.9 | 4.9 | -1.0 | |
| 26 | 5.2 | 5.4 | 0.2 | |
| 27 | 5.4 | 6.5 | 1.1 | 197700 |
| | Mean All Runs (except 5, 25) | | | 91600 ± 41300 |
| 28 | 18.5 | 9.4 | - | |
| 29 | 22.8 | 18.3 | - | |
| 30 | 9.6 | 12.2 | 2.6 | 545000 |
| 31 | 8.6 | 12.9 | 4.3 | 292000 |
| 32 | 26.9 | 20.5 | - | |

constants for the cyanide and cyanate reactions, the bulk liquid cyanate concentration and a derived mass transfer coefficient. The approach discussed in section 3.5.4.2.2 is shown in Appendix C.5.

The calculated values for $k_L$ and I using the fast reaction regime assessment are shown in Table 7. For comparison, values of $k_L$ and I calculated based on measured ozone uptake (Section 4.4.1.1) are on average greater by 1.20/1.13, namely the ratio of the average measured $q^{-1}$ and the average calculated $q^{-1}$.

In order to graphically display the results a review of previous similar studies was conducted. *Astarita (1967)*, *Gilliland et al. (1958)* and *Sada et al. (1976)* displayed enhancement factors in log-log plots versus the square root of the reaction modulus as defined by;

$$M = t_D/t_r = k_1 D_1/(k_L^o)^2 \qquad \ldots\ldots (4.4)$$

The $k_1$ term must be expanded to incorporate both the cyanide and cyanate reaction (equation 3.33).

$$k_1 = k[CN] + 1.5k_2[CNO] \qquad \ldots\ldots (3.33)$$

Assuming $k_2 = k/5.1$, this can be simplified to

$$k_1 = k([CN] + 1.5[CNO]/5.1) \qquad \ldots\ldots (4.5)$$

Therefore,

$$M = \frac{t_D}{t_r} = k\,\frac{([CN] + 1.5[CNO]/5.1)D_1}{(k_L^o)^2} \qquad \ldots\ldots (4.6)$$

Since k was unknown and, by virtue of the fast reaction regime model, forced to fit the value of I obtained from the experiments, it is meaningless to plot I versus $\sqrt{M}$, for this work. However, in that runs 1-27 and were at approximately the same temperature k should be

TABLE 7

FAST REACTION REGIME CALCULATED RESULTS

| Run | $b_o$ mg/L | $\Delta b$ mg/L | $b_{Nmax}^*$ mg/L | $b_{No}$ mg/L | $b_{No}/b_{Nmax}$ x 100 | $k_L \times 10^3$ cm/s | I | Calculated q | k L/gmole s |
|---|---|---|---|---|---|---|---|---|---|
| 1 | 41.4 | 11.9 | 19.2 | 18.2 | 94.8 | 32.8 | 5.8 | 1.08 | 33600 |
| 2 | 42.4 | 11.6 | 18.7 | 17.2 | 95.0 | 32.3 | 5.7 | 1.08 | 31100 |
| 3 | 40.5 | 13.8 | 22.3 | 20.8 | 93.3 | 29.3 | 5.2 | 1.09 | 27500 |
| 4 | 33.1 | 21.3 | 34.4 | 30.5 | 88.6 | 26.8 | 4.7 | 1.17 | 25500 |
| 5 | 7.3 | 47.1 | 76.1 | 33.4 | 43.9 | 29.9 | 5.3 | 1.83 | 92700 |
| 6 | 28.0 | 13.6 | 22.0 | 20.0 | 91.0 | 23.5 | 4.2 | 1.13 | 24100 |
| 7 | 26.2 | 12.7 | 20.5 | 18.7 | 91.1 | 22.2 | 3.9 | 1.13 | 23100 |
| 8 | 68.3 | 22.3 | 36.0 | 33.8 | 93.8 | 38.8 | 6.9 | 1.09 | 28100 |
| 9 | 67.7 | 22.9 | 37.0 | 34.6 | 93.5 | 37.4 | 6.6 | 1.09 | 26300 |
| 10 | 68.7 | 21.9 | 35.4 | 33.2 | 93.8 | 40.9 | 7.2 | 1.09 | 31100 |
| 11 | 77.9 | 23.4 | 37.8 | 35.4 | 93.7 | 41.3 | 7.3 | 1.08 | 27600 |
| 12 | 34.6 | 16.6 | 26.8 | 24.6 | 91.7 | 29.8 | 4.6 | 1.13 | 31400 |
| 13 | 38.4 | 19.7 | 31.8 | 28.9 | 90.8 | 38.4 | 5.5 | 1.14 | 46700 |
| 14 | 38.9 | 19.2 | 31.0 | 28.3 | 91.2 | 33.5 | 5.5 | 1.13 | 35200 |
| 15 | 98.3 | 23.9 | 38.6 | 36.8 | 95.3 | 40.9 | 8.1 | 1.07 | 22000 |
| 16 | 60.5 | 17.3 | 27.9 | 26.4 | 94.5 | 29.9 | 5.8 | 1.08 | 18300 |
| 17 | 8.3 | 10.7 | 17.3 | 13.8 | 79.8 | 22.0 | 3.9 | 1.30 | 61500 |
| 18 | 17.2 | 7.1 | 11.5 | 10.6 | 92.4 | 11.8 | 2.3 | 1.11 | 10300 |
| 19 | 56.8 | 11.5 | 18.6 | 17.8 | 95.8 | 29.7 | 5.4 | 1.06 | 21100 |
| 20 | 48.5 | 1.2 | 18.1 | 17.3 | 95.8 | 28.6 | 5.2 | 1.06 | 22600 |
| 21 | 53.7 | 1.8 | 19.1 | 18.3 | 96.0 | 30.2 | 5.4 | 1.06 | 22500 |
| 22 | 84.6 | 7.2 | 27.8 | 26.7 | 96.1 | 44.8 | 8.0 | 1.06 | 31700 |
| 23 | 27.7 | 2.5 | 20.2 | 18.5 | 91.6 | 34.4 | 6.2 | 1.12 | 53800 |
| 24 | 28.6 | 8.9 | 14.4 | 13.5 | 93.9 | 23.1 | 4.2 | 1.09 | 24500 |
| 25 | 22.7 | 1.4 | 18.4 | 16.7 | 90.7 | 30.9 | 5.6 | 1.13 | 52600 |
| 26 | 25.7 | 0.0 | 16.1 | 15.1 | 93.5 | 26.0 | 4.7 | 1.11 | 34300 |
| 27 | 32.5 | 1.0 | 17.8 | 16.6 | 93.4 | 28.7 | 5.1 | 1.09 | 32500 |
| 28+ | 23.3 | 20.2 | 32.6 | 27.9 | 85.5 | 126.0 | 19.1 | 1.22 | 56600 |
| 29+ | 27.6 | 15.0 | 24.2 | 21.9 | 90.4 | 153.8 | 21.8 | 1.14 | 65700 |
| 30+ | 31.8 | 10.7 | 17.3 | 16.0 | 92.6 | 57.5 | 8.71 | 1.09 | 95600 |
| 31+ | 32.6 | 10.4 | 16.8 | 15.1 | 90.0 | 55.5 | 8.4 | 1.08 | 87800 |
| 32+ | 27.1 | 15.5 | 25.0 | 22.5 | 90.0 | 185.4 | 25.8 | 1.15 | 940000 |
| | | | | | | | Mean | 1.13 | |
| | | | | | | | Std. Dev. | 0.14 | |

+Runs at elevated temperature

*Assuming $b_{Noi} = 0$

**Calculated ozone usage/measured cyanide depletion

constant and $D_2$ is essentially constant. As all runs were not conducted at the same stirring speed, $k_L^o$ was not constant and thus, the enhancement factor is proportional to;

$$I \propto \frac{\sqrt{([CN]+1.5[CNO]/5.1)}}{k_L^o}$$

$$\propto \frac{\sqrt{\text{equivalent cyanide concentration}}}{k_L^o} \qquad \ldots\ldots (4.7)$$

A plot of the results is shown on Figure 10 for runs 1-28. Runs 28-32 were conducted at elevated temperatures thus changes to the kinetic constant and diffusivity invalidate this proportionality.

4.4.2 Ozonation of Giant Yellowknife Mines' Barren Bleed

4.4.2.1 Treatability Studies

Figure 11 shows the concentration of reacting cyanide species versus contact time, determined using time zero as the commencement of ozone introduction to the reactor. The two modes of ozonation are denoted by:

(a) "B" for the system where ozone was bubbled into a stirred liquid; or

(b) "S" for the system where ozone was sparged through a medium course stainless steel fritted desk.

For comparison, the destruction of a sodium cyanide solution is also shown along with some of Sondak and Dodge's *(Sondak and Dodge (1961))* results for metal plating wastes and KCN. A tabulation of test results is given in Appendix B.2.

Free cyanide was destroyed to below detectability in less than 60 minutes of contact. Total cyanide was reduced to less than

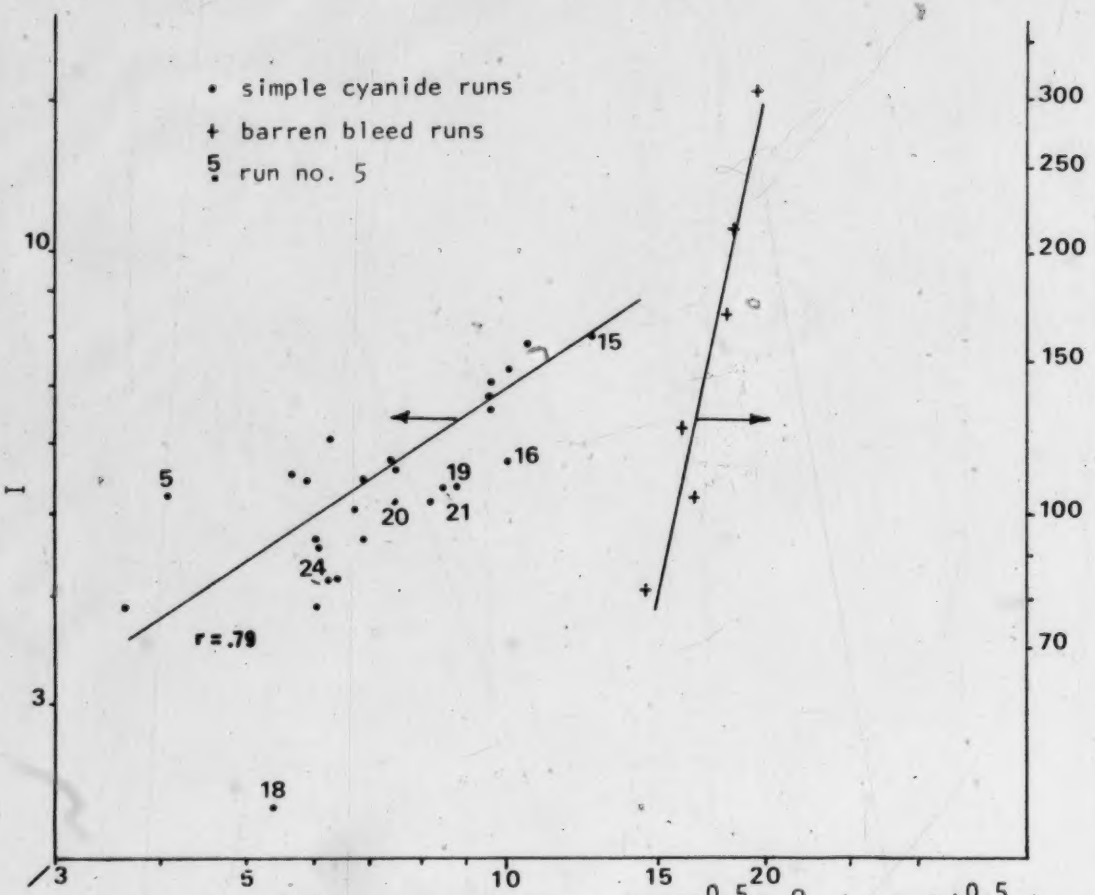


Figure 10 I versus modified reaction modulus

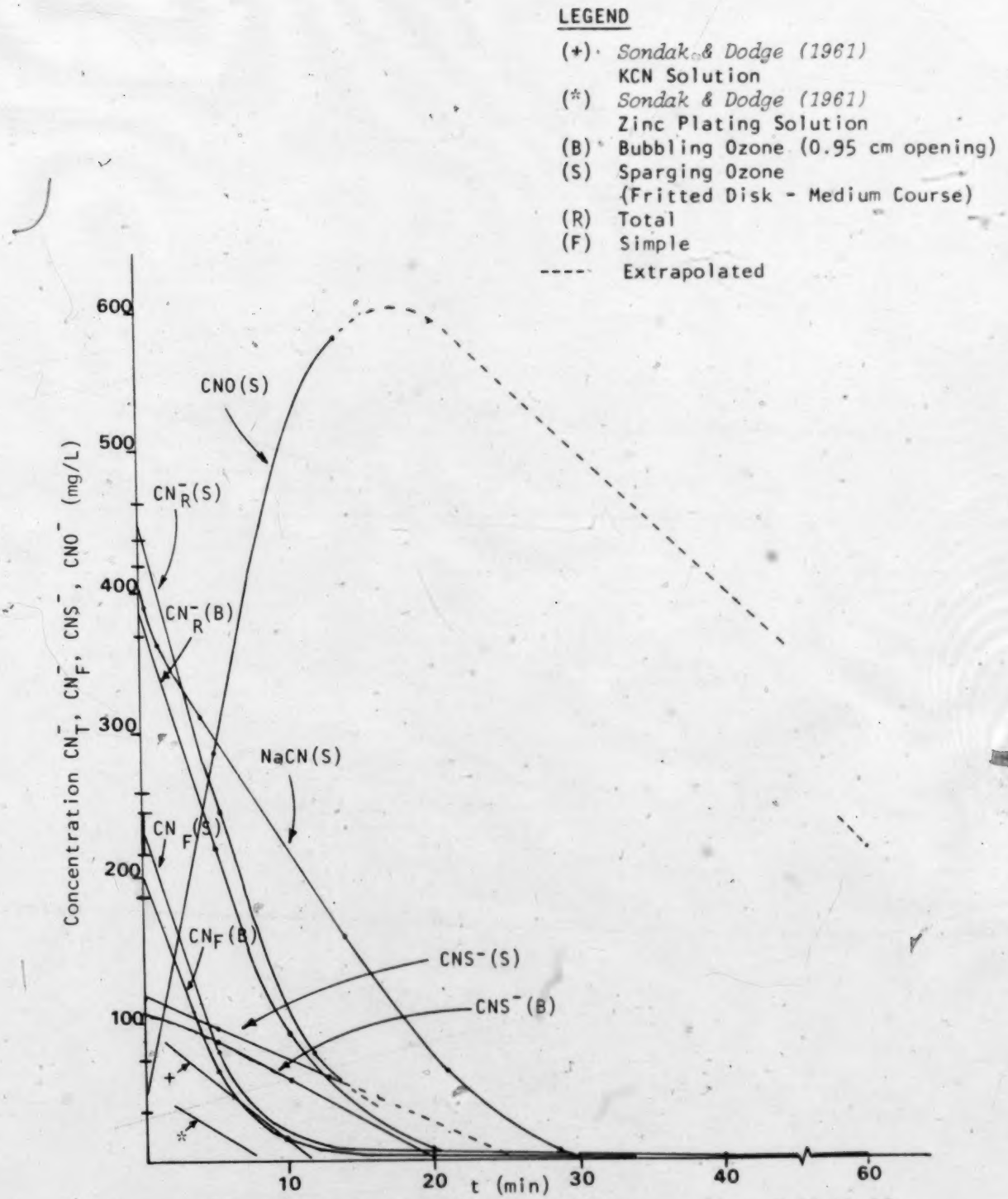


Figure 11 Rate of Ozonation of Cyanides - Giant Yellowknife Mines Barren Bleed

2.0 mg/L, however continued ozonation did not prove effective in reducing this concentration further. It must be noted that the method for cyanide analysis did not include all of the iron complexed cyanide and hence, a residual higher than 2 mg/L may have been determined if a cyanide detection technique had been used which included all the iron cyanides. It is suspected that the residual cyanides, seemingly unaffected by ozonation, are iron cyanide complexes (i.e. ferricyanide, ferrocyanide, ferriferrocyanide, cupric/cuprous ferri/ferro cyanides etc.). Many researchers, including *Hardisty and Rosen (1978)*, have documented the inability of ozone (by itself) to remove iron complexed cyanides in wastewaters.

Ozone reduced thiocyanate to less than detectable levels after 20 to 40 minutes of bubbling. The concentration of cyanate was found to increase, as cyanide was destroyed, after which, the cyanate was in turn oxidized.

The cyanate measurement appeared to have been affected by sample deterioration prior to analysis, in that the measured cyanate concentrations were appreciably less than that which could be calculated from the measured cyanide and thiocyanate depletion. The short contact time for runs 49 and 52 showed the measured cyanate concentration was only 75 and 78 percent, respectively, of that expected from the measured depletion of cyanide and thiocyanate. Thus, the cyanate curve depicted on Figure 11, is intended as an indication of the behavior of cyanate growth/depletion relative to the cyanide/thiocyanate reactions.

4.4.2.1.1 Ozone Uptake

Sparging the ozone into the liquid did not appreciably improve the rate of cyanide destruction over the bubbled ozone results. The ozone uptake was measured as the difference between the concentration of inlet and outlet gas. Approximately $2.2 \times 10^{-5}$ gmole/s of ozone were bubbled or sparged into the reactor. Ozone was not detected in the off-gas for the first 11.5-15 minutes of contact for the sparged system and first 5 minutes for the bubbled system. After breakthrough the uptake diminished with time, as shown in Figure 12, for both sparged and bubbled systems.

Evaluation of ozone demand is complicated due to the poor reliability of cyanate measurements. Runs 39, 49 and 52 (Appendix B) can be used to give some indication of ozone usage since it was likely that all the ozone was absorbed during the runs. The ratio of the measured amount of ozone used to the theoretical amount necessary to oxidize the measured cyanide and thiocyanate depleted was found to be 0.97, 0.86 and 0.94, respectively. Since the cyanate reaction likely was occurring values slightly higher than unity were anticipated. These results seemed to confirm the assumed ozone stoichiometry for the cyanide and thiocyanate reactants.

4.4.2.1.2 Observed Solution Changes During Ozonation

During the ozonation process the pH dropped from near 11.0 to approximately 7.6. Based on previous discussion, this drop in pH could affect the rate of cyanide oxidation. Ozonation of the barren bleed solution, initially clear and slightly greenish, resulted in the

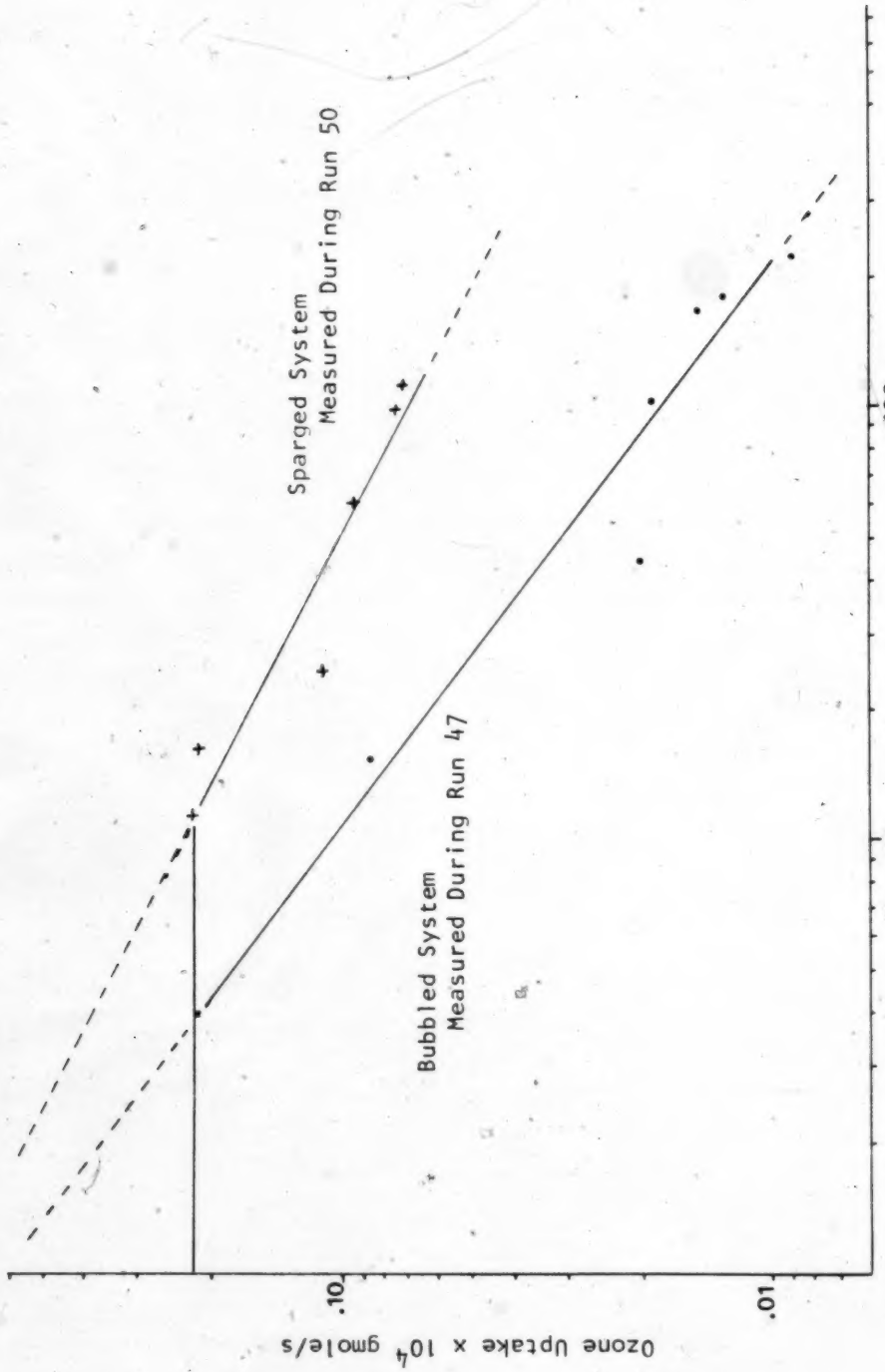


Figure 12 Ozone Uptake During Ozonation of Barren Bleed

formation of precipitates. These precipitates displayed a variety of colours dependent upon the length of the period of ozonation. The change was from clear to whitish green opaque at 5 minutes contact to black after 20 minutes.

Samples of the barren solution were acidified and analysed for copper, zinc, iron and arsenic. The stock solution contained 135 mg/L Cu, 80 mg/L Zn, 10 mg/L Fe and 4.6 mg/L As. Even with acidification to a pH near 1.0 a reddish purple precipitate formed. This precipitate would not allow for an accurate metal analysis as all metals likely were not in the dissolved form. The reddish precipitate was believed to be a copper iron complex as addition of ammonium hydroxide turned air dried samples of the precipitate deep blue. As copper cyanide has been found to readily dissociate under ozonation *(Hardisty and Rosen (1978))* and is unstable in an acidic medium, the copper must be associated with a very stable cyanide complex. A review of a list of physical properties of inorganic complexes in *Perry et al. (1963)* indicated that copper iron cyanide complexes are brownish red in color.

Liquid from the run 42 (contacted for 40 minutes) was filtered through a 0.45 micron filter. The filtrate was analysed for metals. The metal concentrations were found to be 2.5 mg/L Cu, 2.4 mg/L Zn, 1.15 mg/L Fe and 0.95 mg/L As. Thus, cyanide destruction resulted in metal liberation and precipitation, likely in hydroxide form. Since iron cyanides are not affected by ozonation, possibly absorption with co-precipitation accounted for the drop in iron concentration.

4.4.2.2 Mass Transfer Studies

Table 8 shows the reactor conditions for runs 33-38, namely controlled ozone absorption into the barren bleed solution of Giant Yellowknife Mines (G.Y.M.) Ltd. Outlet cyanide concentrations were varied by changing the inlet flow rate since the concentrations of reactants in the barren bleed was essentially constant for all of the runs.

4.4.2.2.1 Ozone Uptake

The ozone demand for each run varied depending on the relative amounts of cyanide, cyanate and thiocyanate depleted. The molar ratio of measured ozone used to a theoretical amount required to achieve the measured reduction of cyanate, thiocyanate, and cyanide was calculated to vary between 0.69 and 1.12 for runs 33-38 (Table 9). The average measured molar ratio of ozone used to the sum of cyanide and thiocyanate depleted was measured to be 0.94 (Table 9). This was calculated assuming thiocyanate is converted to cyanide (equation 2.20), hence adding to the total amount of cyanide destroyed (i.e. cyanide destroyed is $b_i - b_o + b_{Ti} - b_T$). These ratios should be 1.0 for the former and slightly greater than one for the cyanide and thiocyanate based theoretical value if the assumed stoichiometric coefficients of 1.0, 1.5 and 3 are valid for the cyanide, cyanate and thiocyanate reactions. The calculated ratios are lower than expected. Since previous runs (1-27) seem to verify the assumed stoichiometric coefficients of cyanide and cyanate reactions the possible reasons for the low measured uptake ratios may possibly be attributed to 1) too

TABLE 8

REACTOR CONDITIONS FOR $O_3$ ABSORPTION INTO BARREN BLEED SOLUTION

| Run No. | 33 | 34 | 35 | 36 | 37 | 38 |
|---|---|---|---|---|---|---|
| $[CN_T]_i$ mg/L | 350/370 | 350/370 | 350/380 | 380/380 | 390/380 | 380/390 |
| $[CN_R]_i$ mg/L | 190/230 | 190/230 | 220/230 | 200/190 | 200/200 | 190/150 |
| $[CNS]_i$ mg/L | 110 | 110 | 110 | 110 | 115 | 120 |
| $[CNO]_i$ mg/L | 110 | 110 | - | 93 | 60 | 68 |
| $pH_i$ | | | | 10.72 | | |
| $[CN_T]_b$ mg/L | 180/210 | 150/160 | 140/160 | 110/110 | 120/110 | 83/83 |
| $[CN_R]_b$ mg/L | 36/48 | 48/36 | 42/12 | 48/36 | 35/25 | 18/18 |
| $[CNS]_b$ mg/L | 70/70 | 68/67 | 64/60 | 52/53 | 49/52 | 34/35 |
| $[CNO]_b$ mg/L | 430/430 | 420/450 | 490/380 | 420/420 | 390/430 | 390/390 |
| $pH_b$ | | | | 9.37 | | |
| $\bar{\theta}$ s | 390 | 481 | 590 | 846 | 882 | 1274 |
| Liquid T °C | 22.2 | 22.5 | 21.8 | 23.5 | 21.8 | 22.3 |
| $D_{O_3}$ @ T $cm^2/s$ | 1.84 | 1.85 | 1.82 | 1.91 | 1.82 | 1.85 |
| $K_L^o$ @ T x $10^3$ cm/s | 5.59 | 5.6 | 5.55 | 5.69 | 5.55 | 5.59 |
| Outlet flow rate (dry basis) L/min | 1.85 | 1.81 | 1.84 | 1.84 | 1.83 | 1.83 |
| Gas T °C | 21.5 | 22.4 | 21.8 | 23.2 | 21.5 | 21.9 |
| % $O_3$ Inlet (dry basis) | 1.65 | 1.68 | 1.62 | 1.66 | 1.68 | 1.67 |
| % $O_3$ Outlet (dry basis) | 0.75 | 0.85 | 0.91 | 1.06 | 1.10 | 1.18 |
| $c_o'$ mg/L | 6.0 | 6.72 | 7.34 | 7.94 | 8.94 | 9.42 |
| V x $10^5$ gmole/s | 1.23 | 1.12 | 0.96 | 0.82 | 0.77 | 0.66 |

$\bar{\theta}$ based on liquid volume of 520 mL

/ duplicate sample result

$CN_T$ complex cyanide

$CN_R$ simple cyanide

TABLE 9

RESULTS OF $O_3$ ABSORPTION INTO BARREN BLEED SOLUTION

| Run | Measured $O_3$ Uptake * / Theoretical $O_3$ Uptake | Measured $O_3$ Uptake ** / Component of Theoretical $O_3$ Uptake | Theoretical $O_3$ Uptake *** / reactant depletion | $k_L$ † | I |
|---|---|---|---|---|---|
| 33 | 1.12 | 1.02 | 1.15 | 1.71 | 306 |
| 34 | 0.85 | 0.96 | 1.18 | 1.20 | 214 |
| 35 | 0.80 | 0.94 | 1.20 | 0.95 | 171 |
| 36 | 0.68 | 0.93 | 1.24 | 0.72 | 127 |
| 37 | 0.67 | 0.88 | 1.24 | 0.59 | 106 |
| 38 | 0.69 | 0.92 | 1.28 | 0.47 | 82 |

* Calculated from $\overline{V}/(2.5\Delta[CN] + 5.5\Delta[CNS] + 1.5\Delta[CNO])Qa^{-1}$ based on cyanide, cyanate and thiocyanate stoichiometrics of 1, 1.5 and 3.0 respectively.

** Calculated from $\overline{V}/(\Delta[CN] + 4\Delta[CNS])Qa^{-1}$

*** Equivalent to the average theoretical reactant stoichiometry; calculated using $(2.5\Delta CN + 5.5\Delta CNS + 1.5\Delta CNO)/(2\Delta CN + 3\Delta CNS + \Delta CNO)$

† Based on measured ozone uptake rate, $\overline{V}$, and corrected for gas phase resistance.

high an assumed stoichiometric coefficient for the thiocyanate reaction 2) a reduction of reactant concentrations in the bulk liquid not attributed to ozone oxidation and/or other chemicals were present in the sample and were oxidized by ozone. The average ratio based on the cyanide and thiocyanide reactions, being 0.94, indicated that the assumed stoichiometric coefficient of 3 or the conversion of thiocyanate to cyanide may be in error. Assuming a coefficient of 1.0 changes the average ratio to 1.12, a more reasonable figure. The ratio based on all three reactants varies considerably and the deterioration of cyanate concentrations, thus falsely increasing the theoretical ozone consumption, seems likely to have occured. Since samples were shipped to CanMet the lag between sampling and analysis likely resulted in deterioration of cyanate concentrations, possibly by hydrolysis *(Selm (1957))*. The error in cyanate measurement also influences the theoretical ozone demand, skewing it so as to yield higher demands since the cyanate reaction would become significant (increasing from 33-38). The measured bulk liquid cyanate concentration of runs 34-38 was less than the calculated amount based on cyanide depletion, thus, notwithstanding the above observation, the cyanate reaction was likely occurring. A theoretical overall stoichiometric ratio was calculated by dividing the theoretical ozone uptake by the measured depletion of the three reactants. Whereas previously mentioned errors could affect this figure, the tendency shown on Table 10 is to increasing values from near 1.0 toward 1.5. The cyanate reaction became more significant for the runs with longer contact time as was expected.

In order to compare the value of I to those obtained for the simple cyanide runs, an approach similar to that used in section 4.4.1.2.2 was used. Equation 4.7 was expanded to include the thiocyanate reaction. Without knowing the relationship of the rate of cyanide to that of thiocyanate, coupled with the uncertainty of the thiocyanate stoichiometric coefficient and the deterioration of cyanate samples the proportionality was only approximated using

$$I \propto ([CN] + 1.5[CNO]/5.1 + [CNS])^{0.5}/k_L^o \quad \ldots\ldots (4.8)$$

The results of this evaluation are plotted on Figure 10.

4.4.2.2.2 Mass Transfer Coefficient

The measured ozone uptake was used to calculate the overall mass transfer coefficient due to difficulties of establishing ozone use by measuring liquid phase reactants. The reactions were extremely fast resulting in an order of magnitude increase over the values measure for the simple cyanide system. Gas phase resistance was no longer insignificant and hence a correction was made accounting for its influence. The resulting value of $k_L$ and the associated enhancement factor are reported in Table 9. Details of the calculations are given in Appendix C.6.

4.4.2.2.3 Instantaneous Reaction Regime

The other asymptotic solution to the transition regime is the instantaneous regime. Whereas no kinetic data can be gleaned from the use of this model, a verification of the calculated ratio of the diffusivity of cyanide and ozone can be obtained. By rearrange-

ing equation (2.72) to solve for $D_2$ and substituting the measured enhancement factor for $I_\infty$ and q equal to 0.83 it was found that the average cyanide diffusivity was $1.37 \times 10^{-5} \pm 0.65 \times 10^{-5}$ $cm^2/s$ for runs 1-27 measured at an average temperature of 22.4°C. The average diffusivity of cyanide used in the section 4.4.1.2.1 was $1.8 \times 10^{-5}$ cm/s, equal to that of ozone.

# 5 DISCUSSION

## 5.1 Treatability

It is apparent from the results that achievement of the original objective of 0.1 mg/L total cyanide was not attained in this set of experiments. Residual cyanides, likely in the iron cyanide complexed form, did not appear to be amménable to direct ozonation. This has been found by other investigators *(Prober et al. (1978))* and has lead to investigations on enhancement of oxidation methods using ultraviolet irradiation or ultrasound in combination with ozone.

The results do show however, that the majority of cyanides are quickly reduced to below detection. It is hypothesized that those residual cyanides are not toxic to fish *per se*, except possibly for cyanate which, depending on the total contact time, may be present in ozonated barren bleed effluent at 600-700 mg/L. The lethal concentration (killing 50% of the test fish within 96 hours) is between 100-200 mg/L cyanate *(Serfass and Muraca (1956))*. The cyanate concentration, however, would be reduced upon dilution with other non-cyanide bearing wastewaters common to mine-mill complexes and the long retention time within tailings ponds would allow for the further oxidation or hydrolysis of cyanate. The resulting concentrations and lethality characteristics of the tailings pond decant are unknown at this time.

It has been previously mentioned that the method used to analyse for total cyanide was insensitive to iron cyanides. It may be that further quantification using a more "complete" cyanide

analytical method would increase the residual cyanide present in the ozonated effluent. The significance of the possible increase in residual would be somewhat overcome by dilution as the total barren bleed stream represents less than 10% of the total liquid discharge from Giant Yellowknife Mines, Ltd.

5.2 Ozone Uptake

The literature does not provide a definite stoichiometry of the two ozonation reactions. The measured average ozone demand per mole of simple cyanide depleted for runs 1-32 was 1.20 moles $O_3$/mole $CN^-$. The theoretical ozone demand per mole of cyanide destroyed with the associated cyanate destruction was 1.13 moles $O_3$/mole $CN^-$. In spite of the degree of difficulty in measuring the ozone change in the gas phase, the two agree favorably and support the concept that the cyanate reaction competes with the cyanide ozonation. The measured value also supports the assumed stoichiometric coefficient of 1.0 and 1.5 for the cyanide and cyanate reactions, respectively. Possibly, the difference between the theoretical demand and that measured could be attributed to ineffective (products not entering into oxidation reactions) ozone decomposition; however, the difference is less than the standard deviations of each average and thus no statistically valid conclusions can be drawn regarding ozone reactions other than those with cyanide and cyanate.

Theoretically the ratio of 1.1-1.3 moles of ozone per mole of reactant can be used in treating the barren bleed. This ratio of oxidant use would accomplish thiocyanate and cyanide destruction

to the residual levels previously discussed. The measured ozone use per mole of reactant depleted was less than the proposed value but this was influenced by sample deterioration prior to analyses.

## 5.3 Enhancement Factors

### 5.3.1 Affect of Physical Mass Transfer Coefficient

The enhancement of physical mass transfer by a liquid phase chemical reaction has been quantified for the cyanide ozonation study. In the range of simple cyanide concentrations studied the enhancement was found to approximately 2 to 9 times that of the physical mass transfer coefficient for the simple cyanide system.

Apart from the errors inherent in monitoring the value of $k_L$ by way of assuming a reaction stoichiometry, the main source of uncertainty of the resulting I is likely to originate from the estimation of physical mass transfer for the ozone system using carbon dioxide absorption into water. Figure 8 shows the results of $CO_2$ - water absorption experiments. It is evident that scatter did occur. Normalized values, used for subsequent calculations of I, were taken from the fitted line. If the individual values of $k_L^o$ used for the calculations deviated 15% from those used the value of enhancement factor would deviate by a similar percentage. As can be seen however, the absorption coefficients for carbon dioxide appear reasonable considering the results obtained by *Danckwerts and Gillham (1966)* and *Sada et al. (1976)* under similar conditions using the same type of absorber.

The data on Figure 10 are correlated using a least squares linear regression analysis. The line y=0.5 x -1.81 is generated from all available data, runs 1-27, and has a correlation coefficient of 0.79. Omitting runs 5 and 18 improves the correlation (coefficient 0.85) but this does not substantially change the expression for the line which now becomes y=.5 x -1.96. The scatter evidenced in Figure 10 does not allow any definitive differentiaion of results with changing hydrodynamics. A stirring speed of 99 rpm was used for runs 15 and 16, and run 18's stirring speed was 100 rpm. Although runs 15 and 16 appear to be consistent with other runs the results from 18 may demonstrate deviations from ideal mixing. This explanation may also apply to the results from run 5 since the low flow rate may have detrimentally influenced mixing.

5.3.2 Affect of Ozone Decomposition

Ozone decomposition did not appear to significantly affect measured ozone uptake. Liquid feed solutions were alkaline with initial pH values usually over 10.5. These conditions are ideal for ozone decomposition (section 2.3.1).

The simple cyanide runs were conducted with solutions containing 0.025-0.07 M hydroxide ion however, runs 19, 20, 21 and 24 were in solutions of 0.002-0.006 M hydroxide concentration. As seen in Figure 10 the enhancement factors for each of these runs is less than the generated least mean squares fit and considering the scatter of the other runs only limited conclusions can be made

regarding the effect of hydroxide concentration on the rate of reaction. It appears that pH may directly influence the reaction not inversely as it would if decomposition produced non-reactive constituents, as suggested by *Shambaugh* and *Melnyk (1970)*. *Ritcey (1977)* stated that runs at pH of 12-13 increased the rate of reaction by 50% over that achieved at pH 9-11. It is thus hypothesized that the products of ozone decomposition at elevated pH form part of the mechanism for cyanide destruction.

Regardless of this suggested mechanism where both ozone and its decomposition products impact on cyanide destruction rate the calculations embodied herein have utilized only dissolved ozone as the absorbing reactant for the reactions with cyanide, cyanate and, for the barren bleed mass transfer runs #33-38, thiocyanate. Complexity of the set of diffusion differential equations precludes detailed solutions.

The increase in enhancement factor for the mass transfer runs using a mixture of complexed cyanides (barren bleed) over those recorded for the simple cyanide system cannot be quantitatively explained. An order of magnitude increase over that expected for the same reactant concentrations was found. Possible explanations are the catalysis of the cyanide reaction by copper and the multiplicity of reactions occurring in the liquid phase. Catalysis by copper, found in the barren bleed sample at 135 mg/L, has been suggested by other investigators *(Mathieu (1977))*. *Ritcey (1977)* reported that copper doubles the ozonation rate.

### 5.3.3 Affect of Gas Phase Resistance

Gas phase resistance to mass transfer was not significant for the simple cyanide runs. The calculated liquid phase mass transfer coefficient, when derived incorporating gas phase resistance, was found to be less than one percent higher than the measured overall mass transfer coefficient. As the reaction rate increased, as was the case for the complex cyanide ozonation studies, the significance of gas phase resistance increased. The calculated liquid phase mass transfer coefficients were 10-25% higher than the measured overall transfer coefficient, once correction was made for gas phase resistance.

## 5.4 Kinetic Data

The value of the kinetic constant for the cyanide reaction with ozone has been found by two methods to be in the range of $3 \times 10^4$ to $9 \times 10^4$ L/gmole s. The cyanate reaction has been reported to be approximately 5 times slower in which case, assuming first order with respect to the reactants the value of k would be $6 \times 10^3$ to $1.7 \times 10^4$ L/gmole s.

These kinetic constants represent very fast reaction conditions and given the hypothesis that the reaction occurs through free radical development the values obtained are reasonable. The results are intended to give an estimate of kinetic constant order of magnitude.

As discussed, the value of $k_L^o$ would have direct influence on the value of I. The enhancement factor is used in the transition regime to calculate the kinetic constant and as such, changes in $k_L^o$ would result in variation of the values of $t_D$ and I. For example, a 15% increase or decrease in $k_L^o$ would change the kinetic constant of

run 11 (Appendix C) to $1.9 \times 10^4$ L/gmole s and $1.1 \times 10^5$ L/gmole s, respectively, from the value reported of $6.96 \times 10^4$ L/gmole s.

Another influence on the magnitude of the kinetic constant is the ratio of the diffusivities used in calculating the asymptotic value of I, $I_\infty$. For the same run, a 10% deviation from the assumed value of unity would result in a range of k from $6.3 \times 10^4$ to $8.38 \times 10^4$ L/gmole s.

It appears from the values of the kinetic constant obtained that runs 5, 17, 23 and 25 are uncharacteristically high in comparison to the other runs. Using the fast reaction regime the average rate constant for the cyanide reaction at approximately 22.4°C (average temperature) was found to be 33000 ± 16400 L/gmole s using data from runs 1-27. Excluding the above mentioned "high" runs the average dropped to 27500 ± 7400 L/gmole s. The value of $I_\infty$ calculated for the application of the transition regime was found to be nearly equivalent or less than the measured value of I for these runs (Table 6). Thus the reactions were effectively instantaneous and no kinetic information can be derived from these cases. There is no explanation available to describe why these runs were different from the majority.

5.4.1 Temperature Effects

Runs 28-32 were conducted at temperature 10-20°C over the average temperature of runs 1-27. Kinetic constants evaluated using both the fast reaction regime model (Table 7) and the transition regime model (Table 6) are unrealistically elevated for the associated temperature differences from the room temperature runs. Evaluation of

an activation energy and frequency factor for the cyanide reaction through plotting ln k versus the inverse of absolute temperature did not provide reasonable values.

It was concluded that the transition regime does not adequately describe the experimental conditions of runs 28-32 and it is hypothesized that the reaction conditions were those of the instantaneous reaction regime. Evaluation of a kinetic constant cannot be achieved in this regime as the absorption rate is independent of the kinetics of the reaction.

5.4.2 Verification of Reaction Regime Applicability

The fast reaction regime was utilized to generate the rate constant for the cyanide and cyanate reaction model. An evaluation of the conditions, namely the relationship between $b_o/qc_o'$ and $\sqrt{t_D/t_r}$, can be used to give an indication of the applicability of this model. The range of cyanide concentrations for runs 1-27 was 7.3 mg/L ($2.81 \times 10^{-4}$ gmole/L) to 98.3 mg/L ($3.7 \times 10^{-3}$ gmole/L), while the typical solubility concentration of ozone at the interface was 12 mg/L ($2.5 \times 10^{-4}$ gmole/L). Assuming q equals 1.0 $b_o/qc_o'$ for the cyanide reaction ranged from a minimum of 1.1 to a maximum 15. Using calculated kinetic constants averaging near 30,000 L/s gmole for the cyanide reaction and a typical $t_D$ of 0.6 s, the approximate range of values for $\sqrt{t_D/t_r}$ (or $\sqrt{t_D k b_o}$) is 2.2-8.2. The calculated bulk liquid cyanate concentrations and the associated cyanate rate constant of approximately 5400 L/gmoles do not appreciably affect the comparison of $b_o/qc_o'$ versus $\sqrt{t_D/t_r}$ if added to the cyanide figures. The calculated constraints

are thus approximately equal. As this is the case the transition regime may more adequately apply to the reactor conditions of runs 1-27.

The reaction constant generated from transition regime theory is three times greater than that generated from the fast reaction regime. The value of $\sqrt{t_D/t_r}$ is thus increased by $\sqrt{3}$ over the range previously identified. The value of $b_o/qc_o'$ increased by 1.2 namely the value of $q^{-1}$. Thus both $b_o/qc_o'$ and $\sqrt{t_D/t_r}$ are increased by nearly the same amount. The resulting lack of a definitive inequality between the two confirms transition theory behavior assuming the reaction mechanism is valid.

5.4.3 Ratio of the Cyanide to Cyanate Rate Constants

The applicability of the fast reaction regime and the generation of kinetic constants using that regime with a two reaction model was based on accepting the literature reported value of $k/k_2$ *(Balyanskii et al. (1972))*. Since this ratio was derived from studies which did not allow for the segregation of mass transfer from kinetic effects on ozone absorption the ratio may be invalid. It was possible to generate a ratio of kinetic constants from the experimental information by a trial and error process. Details of the method are given in Appendix C.5. Several runs were randomly selected and the resulting calculated ratio was found to vary considerably (range of 1.6-8.4) however a value close to 2 appeared to be more applicable than the value of 5.1 obtained from *Balyanskii et al. (1972)*. By using a value of 2 for run II results the kinetic constant for the cyanide reaction changed from 27600 L/gmole s to 25000 L/gmole s.

Obviously a significant change occurred in the resulting derived cyanate rate constant. Thus the change in the kinetic constant of the cyanide reaction associated with a change in rate constant ratio was not significant for the purposes of this work. The same conclusions regarding reaction regime applicability can be drawn (section 5.4.2).

5.4.4 Affect of $D_2/D_1$

The instantaneous reaction regime asympotic evaluation of data of section 4.4.1.2.3 identifies a value of $D_2$ of $1.37 \times 10^{-5}$ cm/s. This value is closer to the calculated molecular diffusivity of sodium cyanide, $1.3 \times 10^{-5}$ cm/s, (section 4.4.1.2.1) than to the ionic diffusion coefficient used in evaluating kinetic constants from the transition regime. The impact of using a lower value for the ratio of $D_2/D_1$ would be an increase in the calculated value of k. For example for run II the value of k would increase to $9.73 \times 10^4$ L/gmole s from $6.96 \times 10^4$ L/gmole s if a $D_2/D_1$ ratio of 0.76 (1.37/1.80) was used. More importantly the value of $I_\infty$ approaches that of the measured I, namely, the instantaneous reaction regime would be approached. With $D_2/D_1$ equal to unity three values of $I_\infty$-I (Table 6) were negative. Lowering $D_2/D_1$ increases the number of negative values, thereby precluding the usefulness of the transition regime evaluation.

5.5 Economic Evaluation

*Wiskel and Erkku (1978)* conducted alkaline chlorination pilot studies for treating cyanide wastes from Giant Yellowknife Mines Ltd. Typical reactor feed analysis from a flow proportioned stream of the two cyanide source streams at G.Y.M. is shown in Table 10. Analy-

TABLE 10

BARREN BLEED CHARACTERISTICS OF GIANT YELLOWKNIFE MINE

| | Flow L/day | Total Suspended Solids mg/L | As mg/L | $CN_R$ mg/L | $CN_F$ mg/L | CNS mg/L | Cu mg/L | Fe mg/L | Zn mg/L |
|---|---|---|---|---|---|---|---|---|---|
| Typical Feed to Reactor (1) | | | | | | | | | |
| Mean | $3.0 \times 10^5$ | | | 340 | | | 159 | | 209 |
| Std. Dev. | | | | 15 | | | 26 | | 45.7 |
| Barren Bleed Analysis (2) | $2.7 \times 10^5$ | | < 3 | 280-320 | 190-200 | 63-64 | 77-83 | | 93-96 |
| Average of Samples for this work | | | 4.6 | 430 | 250 | 120 | 135 | 10 | 80 |

(1) *Wiskel and Erkku (1978)*

(2) *Ritcey (1977)*

ses of the barren bleed as reported by *Ritcey (1977)* and of the sample used in this work are also shown in Table 10.

In order to estimate the economics of cyanide waste treatment 400 mg/L total cyanide and 100 mg/L thiocyanate will be used for a flow rate of $3.0 \times 10^5$ L/day. This amounts to 120 kg/day of cyanide and 30 kg/day of thiocyanate which must be destroyed. A conservative ozone/reactant ratio of 1.2 has been found to effectively oxidize the cyanide species and hence an ozone plant capacity of 294 kg/day would be required.

Canvassing of the major ozone generator suppliers indicated a wide range of capital costs for a generator and contact system of the size required. Values of an installed system between $750,000 and $1,200,000 were quoted. The following economic evaluation will be conducted using the pessimistic capital cost figure of 1.2 million dollars.

Typical equipment needs for an ozone contacting system using an air feed include an air compressor, air cooler, dessicant dryers, ozonator, contactor, associated reagent mixing tanks, pumps etc. and O/R and pH control equipment. Since a precipitate forms, considered to be principally metal hydroxides, a system of solids liquid separation is required to selectively manage the generated solids. The hydroxide sludges are not stable and if they are not adequately contained metals can redissolve.

As shown on Table 11 the capital and first year annual operating costs were found to be approximately $1.2 million and $241,700, respectively. The operating costs are based on a 3¢ per kwh charge and straight line depreciation over a 10 year life.

If Giant Yellowknife Mines Ltd. borrowed funds to purchase the equipment installation at 12% with a repayment period of 10 years the cost of financing would be as shown on Table 12. The after tax loss and the after tax cash flow required to finance pollution control is shown on Table 13. This evaluation includes an 8% annual inflation rate in operating costs. A tax shield of 46% has been applied to the mining industry and the accelerated capital cost allowance provides for the write-off of pollution control capital expenditures within two years. These two factors heavily impact on the results of both tax loss and cash flow evaluations.

The cost of producing a kilogram of ozone was found to be $2.35. *Mathieu (1977)* reviewed the literature pertaining to ozonation of cyanide wastes and reported a downward trend in treatment costs from a 1961 figure of $2.79/kg, taken from *Sondak and Dodge (1961)* to less than $1.76/kg in 1976 reported by *Goldstein (1976)*. Costs generated through this evaluation do not support the most recent costs reported in the literature.

The costs reflected herein do not include the necessary filtration equipment since possible excess equipment on site could serve this function. Also the cost is based on a 300 kg/day ozonation plant. Since table 10 indicates cyanide levels lower than 400 mg/L can be expected, the costs thus provide adequate contingency for lower than maximum ozone production from the unit. It is quite possible that the extent of ozonation could be controlled by the acceptability of re-cycling the barren (after filtration) rather than discharge, thereby negating the need to reduce cyanide to the minimum levels.

TABLE 11

ECONOMIC EVALUATION

| | | |
|---|---|---|
| CAPITAL COSTS | | |
| Capital costs for an installed fully instrumented 294 kg/day ozone generation and contacting system were obtained from Union Carbide Ltd., Toronto, Ontario. The ozone generators marketed by Union Carbide are air cooled Lowther type generators. | | $1,200,000 |
| ESTIMATED ANNUAL OPERATING COST CALCULATION | | |
| Chemicals | | |
| Lime @ $0.02 per lb (taken from *Craigen and Kelly (1977)*) | | 1,000 |
| Utilities | | |
| Electrical power @ $.03 per kwh (Northern Canada Power Commission commercial Yellowknife rate) | | |
| 26 kwh/kg $O_3$ - 24 hr/day - 350 day/year | | 80,200 |
| Labor | | |
| Direct labor @ $6.00/hr - 4 hr/day | | 8,400 |
| Supervision - 15 percent of labor | | 1,300 |
| | Total | 9,700 |
| Maintenance | | |
| Maintenance Labor | | 1,200 |
| Maintenance Supervision, 20 percent of labor | | 200 |
| Materials | | 1,000 |
| Payroll Overhead | | |
| 35 percent of above payroll (direct and maintenance) | | 3,900 |
| Supplies & Miscellaneous | | |
| 20 percent of plant maintenance | | 500 |
| Fixed Costs | | |
| Taxes and Insurance 2% of plant cost | | 24,000 |
| Depreciation 10 year life straight line | | 120,000 |
| TOTAL OPERATING COST | | $ 241,700 |

TABLE 12

COST OF FINANCING AND REPAYMENT SCHEDULE

FOR A LOAN OF $1,200,000 @ 12% OVER 10 YEARS

| Year | Beginning Balance | Interest Charge | Principal Repayment | Annual Payment |
|---|---|---|---|---|
| 1 | 1,200,000 | 143,993 | 68,387 | 212,380 |
| 2 | 1,131,613 | 135,794 | 76,586 | 212,380 |
| 3 | 1,055,027 | 126,603 | 85,777 | 212,380 |
| 4 | 969,250 | 116,310 | 96,070 | 212,380 |
| 5 | 873,180 | 104,782 | 107,598 | 212,380 |
| 6 | 765,582 | 91,870 | 120,510 | 212,380 |
| 7 | 645,072 | 77,408 | 134,972 | 212,380 |
| 8 | 510,100 | 61,213 | 151,167 | 212,380 |
| 9 | 358,933 | 43,072 | 169,308 | 212,380 |
| 10 | 189,625 | 22,755 | 189,625 | 212,380 |
| | TOTAL | 923,800 | 1,200,000 | 2,123,800 |

TABLE 13

PROFIT/LOSS SCHEDULE AND CASH FLOW STATEMENT

Capital Cost: $1,200,000 Operating Cost: $241,700/year

| YEAR | 1 | 2 | 3 | 4 | 5 | 6 | 7 | 8 | 9 | 10 |
|---|---|---|---|---|---|---|---|---|---|---|
| Revenue $ ,000 | | | | | | | | | | |
| Interest | -144 | -136 | -127 | -116 | -105 | - 92 | - 77 | - 61 | - 43 | - 23 |
| Operating Cost* | -242 | -251 | -262 | -273 | -286 | -299 | -313 | -329 | -345 | -363 |
| Depreciation | 120 | 120 | 120 | 120 | 120 | 120 | 120 | 120 | 120 | 120 |
| Capital Cost Allowance @ 50% | -600 | -600 | - | - | - | - | - | - | - | - |
| Pre-tax Loss | -866 | -867 | -269 | -269 | -271 | -271 | -270 | -270 | -268 | -266 |
| Tax Shield (46%) | +398 | 399 | 124 | 124 | 125 | 125 | 124 | 124 | 123 | 122 |
| After Tax Loss | -468 | -468 | -145 | -145 | -146 | -146 | -146 | -146 | -145 | -144 |
| Cash Flow Schedule $ ,000 | | | | | | | | | | |
| After Tax Loss | -468 | -468 | -145 | -145 | -146 | -146 | -146 | -146 | -145 | -144 |
| Plus: CCA | 600 | 600 | - | - | - | - | - | - | - | - |
| Less: Principal Repayment | - 68 | - 76 | - 86 | - 96 | -107 | -120 | -135 | -152 | -169 | -190 |
| After Tax Cash Flow Required to Support Pollution Control | 64 | 60 | -231 | -241 | -253 | -266 | -281 | -298 | -341 | -334 |

*Operating Costs from Table 11 adjusted by an annual inflation rate of 8% (not including depreciation).

# 6 CONCLUSIONS AND RECOMMENDATIONS

## 6.1 Conclusions

Aspects of ozonation of aqueous solutions of cyanide were studied under controlled reactor conditions in order to assess the nature of mass transfer enhanced by chemical reaction and quantify residual levels of cyanide which could be achieved by ozonation. The following was found:

(1) The use of a quiescent surface Danckwerts cell system was found effective for studying the cyanide reaction with ozone. Long gas liquid diffusion times in the order of 0.6 s could be achieved with a known area of transfer.

(2) The chemical transfer coefficient of ozone absorbing into a simple cyanide solution (NaCN) at room temperature was found to vary between $1.27 \times 10^{-2}$ and $5.09 \times 10^{-2}$ cm/s. The bulk liquid cyanide concentration was altered for each experimental run by changing the hydrodynamics of the liquid phase or the inlet cyanide concentration. The range of bulk liquid cyanide concentration, pertinent to the above values of $k_L$, was 7.3 to 98.3 mg/L.

(3) The enhancement of physical mass transfer due to the chemical reaction in the liquid phase was found to be between 2.5 to 9.1, as measured by an enhancement factor ($I = k_L/k_L^{o}$).

(4) The transition from fast to instantaneous regimes was found to apply at room temperature to a simplified

reaction mechanism where all cyanide species ($CN^-$ and $CNO^-$) collectively react to give products. Using this model an order of magnitude kinetic constant for the cyanide reaction was found to be $10^4$ to $10^5$ L/gmole s. The fast reaction regime was also used to attempt to define a more complex, yet more realistic reaction mechanism where ozone reacts by way of individual irreversible reactions with cyanide and cyanate. Although the reaction regime could not be confirmed, the generated kinetic constant for the cyanide reaction was lower than the transition regime (as expected), but remained in the same order of magnitude, $10^4$ L/gmole s.

(5) In order to use the fast reaction regime a rate constant for the cyanate reaction was required. The one used in this report was taken from *Balyanskii et al. (1972)* as being 5.1 times less than that of cyanide. Checks on this assumed figure using experimental results gave an approximate range of the ratio $k/k_2$ from 1.6 to 8.4.

(6) The ionic diffusion coefficient for cyanide in water was calculated from theory to be $1.63 \times 10^{-5}$ $cm^2/s$ at 18°C. Using the measured value of I and instantaneous reaction regime theory the average cyanide diffusivity was calculated to be $1.37 \times 10^{-5} \pm 0.65 \times 10^{-5}$ cm/s at 22.4°C (average).

(7) The measured ozone uptake supports the following overall reaction scheme

$$CN^- + O_3 \rightarrow CNO^- + O_2$$

and $2CNO^- + 3O_3 \rightarrow$ products

Three moles of ozone per mole of thiocyanate has been suggested in the literature. This was not confirmed in this work.

It is hypothesized that the mechanism of the above reactions may involve ozone decomposition to products which increase the rate of the oxidation process.

(8) Enhancement of ozone mass transfer into a solution of barren bleed from Giant Yellowknife Mines Ltd. was found to be an order of magnitude higher than that for the enhancement using simple cyanide solutions of the same cyanide strength.

(9) Treatability studies on the barren bleed indicated an ozone use of 0.94 moles per mole of total cyanide and thiocyanate. Cyanide and thiocyanate were reduced to near the objective levels. Total cyanide was reduced to 1-2 mg/L. This residual was speculated to be iron cyanide complexes. Thiocyanate was reduced to below detectable levels.

(10) An economic assessment of an ozonation system for Giant Yellowknife Mines indicated capital cost estimates between 750,000 and 1,200,000 dollars with annual operating costs, including ammortization, near $300,000 (averaged over a 10 year period).

## 6.2 Recommendations

(1) Further study is required to determine the steps necessary to achieve total cyanide destruction. The 0.1 mg/L total cyanide objective may have been inappropriate due to the non-lethal nature of iron cyanide. Thus a split objective may be more appropriate segregating the iron cyanide complexes from the remainder of the "total cyanides". Nevertheless, iron cyanide should be reduced to less than 2 mg/L. Ozonation testing on iron cyanide complexes is required to fully evaluate ozone as a suitable treatment technique for the gold milling industry since many of the gold mills in Canada have higher iron cyanide present than Giant Yellowknife Mines Ltd.

(2) Considerable confusion exists in the literature and in the environmental field with regard to the meaning of the word "cyanide". Various analytical methods result in inclusion or exclusion of various cyanide complexes. Thus, comparison of treatment capability reported in the literature is dependent upon the analytical technique used. A critical review should be undertaken which would define categories of cyanide species, relating them to a specific analytical method.

(3) The mathmatical evaluation of the ozonation of cyanide has been based on two chemical models, namely,

$$A + B \rightarrow C \qquad \ldots\ldots (6.1)$$

$$C + A \rightarrow \text{products} \qquad \ldots\ldots (6.2)$$

and,

$$A + B \rightarrow \text{products} \quad \ldots\ldots (6.3)$$

The former model, mathmatically definable for the fast reaction regime, has not been mathmatically approximated in the literature for the transition from fast to instantaneous regimes. This transition was speculated to be the appropriate regime for the ozone cyanide reaction. Thus, it is recommended that the theoretical analysis of absorption accompanied by two irreversible reactions utilizing the absorbing component be investigated. Expansion of this theoretical analysis to incorporate ozone-free radical development should also be attempted. The model would then be categorized as,

$$A \rightarrow A' \quad \ldots\ldots (6.4)$$

$$A' + B \rightarrow C \quad \ldots\ldots (6.5)$$

$$C + A' \rightarrow \text{products} \quad \ldots\ldots (6.6)$$

(4) Further study is required to determine the relationship between ozone decomposition and reactivity of ozone with respect to cyanide depletion. The mechanism of cyanide ozonation and kinetics should be investigated so as to verify the results obtained in this work.

(5) The diffusivity of cyanide in water and sodium hydroxide solution should be experimentally measured. To a lesser degree a similar evaluation should be made for ozone.

## BIBLIOGRAPHY


(1) Alder, M.G., and G.R. Hill, J. Amer. Chem. Soc., 72, 1884 (1950).

(2) American Public Health Association (APHA) "Standard Methods for the Examination of Water and Wastewater", 13th ed., American Public Health Association, Washington (1971).

(3) American Public Health Association (APHA), "Standard Methods for the Examination of Water and Wastewater", 14th ed., American Public Health Association, Washington (1975).

(4) Astarita, G., "Mass Transfer with Chemical Reaction", Elsevier Publishing Co., Amsterdam (1967).

(5) Balyanskii, G.V., M.E. Selin, and V.B. Kolychev, Zhurnal Prikladnoi Khimii, 45, 2152 (1972).

(6) Barkley, D.J., and J.C. Ingles, "A Rapid Colorimetric Solvent-Extraction Procedure for the Determination of Cyanide in Gold-Mill Effluents and Receiving Waters", Dept. of Energy, Mines and Resources, Reseach Report R 221, Ottawa (1970).

(7) Burdick, G.E., and M. Lipchuetz, Trans. Amer. Fisheries Soc., 78, 192 (1948).

(8) Craigen, W.J.S., and F.J. Kelly, "Economic Evaluation of Cyanide Removal Process", Energy Mines and Resources Canada, Report 77-5, Ottawa (1977).

(9) Danckwerts, P.V., A.I.Ch.E. Journal, 1, 456 (1951).

(10) Danckwerts, P.V., and A.J. Gillham, Trans. Instn. Chem. Engs., 44, T42 (1966).

(11) Doudoroff, P., Sewage and Ind. Wastes, 28, 1020 (1956).

(12) Eiring, L.V., Tsvetnye Metally, 42, 73 (1969).

(13) Evans, F.L., "Ozone in Water and Wastewater Treatment", 18, Ann Arbor Science Publishers Inc., Ann Arbor (1972).

(14) Ford-Smith, M.H., "The Chemistry of Complex Cyanides: A Literature Review", Dept. of Scientific and Industrial Research, National Chemical Library, London (1964).

(15) Garrison, R.L., C.E. Mauk, and H.W. Prengle, "Cyanide Disposal by Ozone Oxidation", U.S. National Technical Information Service, AD-775 152, Washington (1974).

(16) Gilliland, E.R., R.F. Baddour, and P.L.T. Brian, A.I.Ch.E. Journal, 4, 223 (1958).

(17) Goldstein, M., Pollution Engineering, 36, 21 (1976).

(18) Hatta, S., Tech. Repts. Tohoku Imp. Univ., 8, 1 (1928).

(19) Hardisty, D.M., and H.M. Rosen, "Proceedings of the 32nd Industrial Waste Conference, May 10, 11 and 12, 1977, Purdue University, Lafayette, Indiana", Ann Arbor Science Publishers Inc., Ann Arbor (1978).

(20) Heist, J.A., Water, 70, 456 (1973).

(21) Herbert, D.W.M., and J.C. Merkens, J. Exp. Biol., 29, 632 (1952).

(22) Hewes, C.G., and R.R. Davison, A.I.Ch.E. Journal, 17, 141 (1971).

(23) Higbie, R., Trans. A.I.Ch.E., 31, 365 (1935).

(24) Hill, A.G., and H.T. Spenser, "Proceedings First International Symposium on Ozone for Water and Wastewater Treatment", 367, International Ozone Institute, Waterbury (1975).

(25) Hirschfelder, J.O., R.B. Bird, and E.L. Spotz, Trans. A.S.M.E. 71, 921 (1949).

(26) Holden, A.V., and K. Marsden, Water Pollution Abstracts, 10, 19 (1966).

(27) International Critical Tables, 6, 252 (1967).

(28) Ikehata, A., "Proceedings First International Symposium on Ozone for Water and Wastewater Treatment", 227, International Ozone Institute, Waterbury (1975).

(29) Kelada, N.P., C. Lue-Hing, and D.T. Lordi, "Cyanide Species and Thiocyanate Methodology in Water and Wastewater", 41, Metropolitan Sanitary District of Greater Chicago Report No. 77-20, Chicago (1977).

(30) Klein, M.J., R.I. Brabets, and C.K. Layton, "Proceedings First International Symposium on Ozone for Water and Wastewater Treatment", 1, International Ozone Institute, Waterbury (1975).

(31) Khandelwal, K.K., A.J. Barduhn, and C.S. Grove, Jr., Ozone Chemistry and Technology: Advances in Chemistry Series, 21, 78 (1959).

(32) Kinman, R.N., "Proceedings First International Symposium on Ozone for Water and Wastewater Treatment", 56, International Ozone Institute, Waterbury (1975).

(33) Leclair, B., Canada Centre for Inland Waters "Personal communication", (1977).

(34) Lee, M.K., G.G. See, and R.A. Wynveen, paper presented at Symposium on Advanced Ozone Technology, Nov. 16, 1977, Toronto (1977).

(35) Lewis, W.K., and W. Whitman, Ind. Eng. Chem., 16, 1215 (1924).

(36) Mathiew, G.I., "Ozonation for Destruction of Cyanide in Canadian Gold Mill, Effluents - A Preliminary Review", Energy, Mines and Resources Canada, Report 77-11, Ottawa (1977).

(37) McCarthy, J.J., W.F. Cowen, and E.S.K. Chain, "Proceedings of the 32nd Industrial Waste Conference, May 10, 11, and 12, 1977, Pardue University, Lafayette, Indiana", 294, Ann Arbor Science Publishers Inc., Ann Arbor (1978).

(38) McKee, J.E., and W.H. Wolf, "Water Quality Criteria", State Water Quality Control Board Publication No. 3-A, Los Angeles (1963).

(39) Melnyk, P.B., and A. Netzer, "Proceedings of the International Ozone Institutes Forum on Ozone Disinfection, Chicago, June 1976", Ozone Press Internationale, Jamesville (1977).

(40) Nebel, C., R.D. Gottschling, J.L. Homes, and P.C. Unangst, "Proceedings Second International Symposium on Ozone Technology", 374, Ozone Press Internationale, Jamesville (1976).

(41) Nernst, Z., physik. Chem., 2, 613 (1888).

(42) Nijsing, R.A.T.O., Ph.D. Thesis, University of Delft, Delft (1957).

(43) Nijsing, R.A.T.O., R.H. Hendriksz, and H. Kramers, Chem. Eng. Sci., 10, 88 (1959).

(44) Ohio River Valley Sanitation Commission, J.W.P.C.F., 32, 65 (1960).

(45) Perry, R.H., C.H. Chilton, and S.D. Kirkpatrick, "Perry's Chemcial Engineers' Handbook", 4th ed., McGraw-Hill Book Company, New York (1963).

(46) Prober, R., P.B. Melnyk, and L.A. Mansfield, "Proceedings of the 32nd Industrial Waste Conference May 10, 11, and 12, 1977, Pardue University, Lafayette, Indiana", 17, Ann Arbor Science Publishers Inc., Ann Arbor (1978)

(47) Richards, D.A., and M. Fleischman, "Proceedings Second International Symposium on Ozone Technology", 57, Ozone Press Internationale, Jamesville (1976).

(48) Ritcey, G.M., "Treatment of Gold Mill Effluents for Removal and Recovery or Destruction of Cyanide - A Summary of the Joint Project with Six Gold Mills", Energy, Mines and Resources Canada, Report 77-15, Ottawa (1977).

(49) Sada, E., H. Kumazawa, M.A. Butt, and D. Hayashi, Chem. Eng. Sci, 31, 839 (1976).

(50) Selm, R.P., Advances in Chemistry Series, 21, 66 (1959).

(51) Serfass, E.J., and R.F. Muraca, Plating, 43, 1027 (1956).

(52) Shambaugh, R.L., and P.B. Melnyk, "Proceedings of the International Ozone Institute - Forum on Ozone Disinfection", 24, Ozone Press Internationale, Chicago (1976).

(53) Shambaugh, R.L. and P.B. Melnyk, "Proceedings of the International Ozone Institutes Forum on Ozone Disinfection, Chicago, June 1976", Ozone Press Internationale, Jamesville (1977).

(54) Sharma, M.M., and P.V. Danckwerts, Brit. Chem. Eng., 15, 522 (1970).

(55) Shedlovsky, J., J. Amer. Chem. Soc., 54, 1405 (1932).

(56) Sherwood, T.K., and J.C. Wei, A.I.Ch.E. Journal, 1, 522 (1955).

(57) Sondak, N.E., and B.F. Dodge, Plating, 48, 173 (1961).

(58) Sondak, N.E., and B.F. Dodge, Plating, 48, 280 (1961).

(59) Stumm, W., Helvetia Chem. Acta., 37, 773 (1954).

(60) Tang, J., University of Alberta, "Personal Communication", 1978.

(61) Tyler, R.G., W. Maske, H.J. Westin, and W. Matthews, Sewage and Ind. Wastes, 23, 1150 (1951).

(62) Van Krevelen, D.W., and P.H. Hoftijzer, Rec. Trav. Chim., 67, 563 (1948).

(63) Vidwans, A.D., and M.M. Sharma, Chem. Eng. Sci, 22, 673 (1967).

(64) Vinograd, J.R., and J.W. McBain, J. Amer. Chem. Soc., 63, 2008 (1941).

(65) Walker, C.A., and W. Zabban, Plating, 40, 777 (1952).

(66) Wallace, R.R., and M.J. Hardin, "Chemical and Biological Characteristics of Seepages from Tailings Areas at Giant Yellowknife Mines, Ltd., into Great Slave Lake, Northwest Territories in 1974"., Environment Canada EPS-5-NW-74-1 (1974).

(67) Wilke, C.R., and P. Chang, A.I.Ch.E. Journal, 1, 264 (1955).

(68) Wiskel, B., and H. Erkku, Report on Results of Giant Yellowknife Mines Ltd. DPAT Study (unpublished), 1978.

(69) Wuhrmann, K., and H. Woker, Schweizer Zeitscher Hydrologie., 11, 210 (1948).

# APPENDIX A

## ANALYTICAL METHODS

## A.1 Details of Silver Nitrate Titration

A solution of exactly 3.27 g $AgNO_3$ was dissolved in 1 litre of distilled water. Standard solutions of cyanide were prepared to verify the standard silver nitrate solution.

The reaction which occurs is

$$2CN^- + Ag^+ \rightarrow Ag(CN)_2^-$$

Molecular weight of silver nitrate 169.9 g/gmole

Molality of silver nitrate solution 0.01925 M

Molecular weight of cyanide ion 26 g/gmole

1 mL of silver nitrate solution contains $1.92 \times 10^{-5}$ gmole

A solution of 1 mg/L $CN^-$ contains $3.846 \times 10^{-5}$ gmole

Since 1 mole of $Ag^+$ combines with 2 moles of $CN^-$

$\therefore$ 1 mL of silver nitrate solution = 1 mg of $CN^-$

Generally 100 mL of sample were titrated.

Let A = number of mL of standard $AgNO_3$ for the sample titration

B = number of mL of standard $AgNO_3$ for the blank titration

Then (A-B) equals the number of mL of standard $AgNO_3$ complexing the $CN^-$ present in the sample.

$$\text{mg/L } CN^- = \frac{(A-B)}{\text{volume of sample in mL}} \times 1000 \frac{\text{mL}}{\text{L}}$$

Thus for a 100 mL sample

$$\text{mg/L } CN^- = (A-B)\text{mL} \times 10$$

The limit of sensitivity of this method is approximately 0.1 mg/L $CN^-$ however the indistinct color change limited to reliability to 0.3 mg/L $CN^-$.

A.2 Carbon Dioxide Measurement

(a) Standardization of NaOH and HCl solutions

Solutions of HCl were made using concentrated HCl and distilled water. A desired normality around 0.01 N was verified by titrating with THAM. Thus obtaining the normality of HCl, this standard acid was then used to standardize the NaOH. The NaOH required frequent standardization since its strength changes due to absorption of $CO_2$ from the air. The HCl strength remains essentially constant.

The NaOH solution was maintained under a nitrogen environment in a sealed container so that the strength would remain relatively constant for long periods.

(b) Titration to determine $CO_2$ absorbed

For the determination of $CO_2$ in the water a known volume of water containing dissolved $CO_2$ was added to a known volume of pre-standardized sodium hydroxide solution. The NaOH reacted with the $CO_2$ to give $Na_2CO_3$ .

$$2NaOH + CO_2 \rightleftharpoons Na_2CO_3 + H_2O + NaOH \text{ (excess)} \quad \ldots (A.1)$$

Upon titration with the standard HCl the following chemical changes occur.

1) The excess NaOH is neutralized

$$NaOH + HCl \rightleftharpoons NaCl + H_2O \quad \ldots (A.2)$$

2) Carbon dioxide is liberated from sodium carbonate via two stages

i) $Na_2CO_3 + HCl \rightleftarrows NaHCO_3 + NaCl$ ... (A.3)

ii) $NaHCO_3 + HCl \rightleftarrows H_2CO_3 + NaCl$

$\rightleftarrows H_2O + CO_2\uparrow + NaCl$ ... (A.4)

The description of the calculation is best followed using the sample of a pH curve for the blank NaOH solution and that solution containing dissolved $CO_2$ (Figure A.1).

The blank NaOH standard solution when titrated with standardized HCl gives a titration curve typical to strong acid-strong base titrations with a rapid change in pH about the equivalence or inflexion point. In this case the conversion of NaOH to NaCl occurs directly.

The first equivalence point encountered when back titrating the sample containing $CO_2$ corresponds to the neutralization of the excess NaOH present in the sample as well as the conversion of $Na_2CO_3$ to $NaHCO_3$. This is chemically defined by reactions (A.2) and (A.3). The volume of HCl used is denoted on Figure A.1 as $v_1$ mL.

The second equivalence point represents the complete conversion of NaOH to NaCl through the $Na_2CO_3$ and is defined by reaction (A.1).

Thus the volume of HCl required to convert the sodium bicarbonate to sodium chloride is $(v_2-v_1)$ mL. The amount of carbon dioxide given off in this step is the same as that in the initial sample thus the number of moles of HCl used between the two equivalence points, namely $N_{HCl}\ (v_2-v_1)$, is the number of moles of $CO_2$ absorbed. $N_{HCl}$ is the normality of the hydrochloric acid.

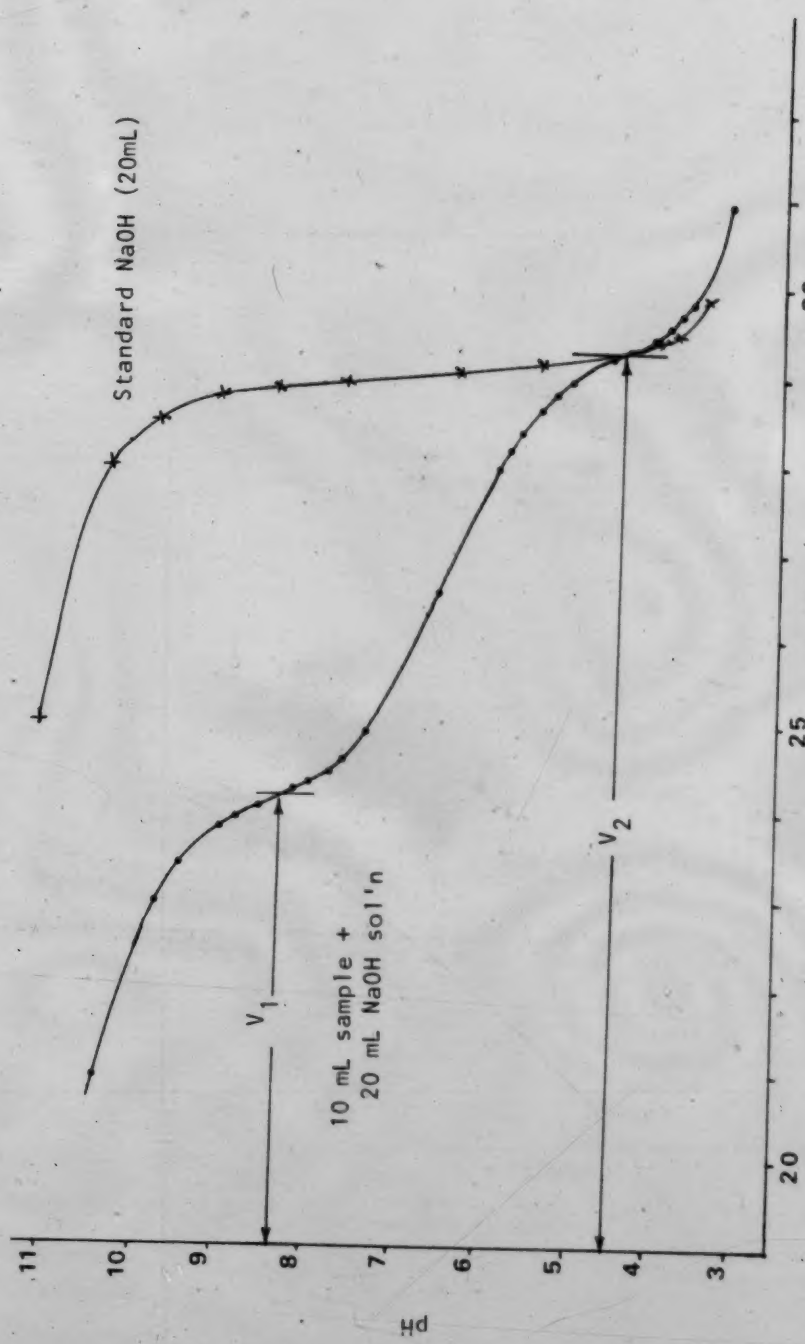


Figure A.1 Typical Potentiometric Titration Curve for Carbon Dioxide Back-Titration and NaOH Titration with HCl

Calculations

no. moles of $CO_2$ in initial sample = no. moles of $Na_2CO_3$

= no. moles of $Na_2HCO_3$

Since $N_{HCl}(v_2-v_1)$ = no. of moles of HCl to convert $NaHCO_3$ to $CO_2$

$\therefore$ $N_{HCl}(v_2-v_1)$ = no. of moles of $CO_2$

concentration of $CO_2$ in intial sample = $\frac{\text{no. of moles of } CO_2}{\text{volume of initial sample}}$

$\therefore$ concentration of $CO_2 = C_{CO_2} = \frac{N_{HCl}(v_2-v_1)}{v_{sample}}$

# APPENDIX B

## REACTOR CONDITIONS AND DETAILED RESULTS

TABLE B.1

REACTOR CONDITIONS AND RESULTS - $CO_2$ ABSORPTION INTO WATER

| Run | Liquid T | s | Q | $\bar{\theta}$ | $c_o$ | $c_o'$ | $k_L^o$ @ T $\times 10^3$ | $k_L^o$ @ 25°C $\times 10^3$ |
|---|---|---|---|---|---|---|---|---|
| | °C | rpm | mL/s | s | gmole/L | gmole/L | cm/s | cm/s |
| 1 | 23.6 | 79 | 1.29 | 403 | 0.0059 | 0.0331 | 3.6 | 3.6 |
| 2 | 23.6 | 79 | 1.29 | 403 | 0.0058 | 0.0322 | 3.5 | 3.6 |
| 3 | 23.6 | 93 | 1.19 | 437 | 0.0069 | 0.0324 | 4.1 | 4.1 |
| 4 | 23.9 | 93 | 1.27 | 409 | 0.0068 | 0.0321 | 4.4 | 4.4 |
| 5 | 23.1 | 106 | 1.26 | 412 | 0.0080 | 0.0334 | 5.0 | 5.2 |
| 6 | 23.2 | 108 | 1.29 | 403 | 0.0100 | 0.0333 | 7.0 | 7.2 |
| 7 | 23.8 | 102 | 1.29 | 403 | 0.0072 | 0.0326 | 4.8 | 4.9 |
| 8 | 23.8 | 113 | 1.29 | 403 | 0.0087 | 0.0323 | 6.0 | 6.1 |
| 9 | 20.8 | 110 | 0.43 | 1209 | 0.0192 | 0.0353 | 6.5 | 6.9 |
| 10 | 22.1 | 99 | 0.41 | 1268 | 0.0165 | 0.0342 | 4.9 | 5.0 |

TABLE B.2 BARREN BLEED RUNS
CONTACT CONDITIONS AND SOLUTION ANALYSES

| RUN | BATCH CONTACT | | | SIMPLE | TOTAL | CNS | CNO |
|---|---|---|---|---|---|---|---|
| | TIME OF OZONATION (min) | BUBBLING(B) | SPARGED(S) pH | CN mg/L | CN mg/L | mg/L | mg/L |
| Feed for 39, 40, 41, 42 | 0 | - | 11.0 | 260 | 370 | 110 | - |
| 39 | 5 | B | 9.0 | 64 | 220 | 87 | - |
| 40 | 10 | B | 8.0 | 13 | 88 | 60 | - |
| 41 | 20 | B | 7.0 | 1.8 | 9.2 | 3 | - |
| 42 | 40 | B | 7.7 | 1.5 | 3.3 | < 2 | - |
| Feed for 43, 44 45, 46 | 0 | - | 10.18 | 190 | 370 | 110 | - |
| 43 | 63 | B | 7.64 | < 0.5 | 3.3 | < 2 | - |
| 44 | 60 | B | 7.66 | < 0.5 | 3.9 | < 2 | - |
| 45 | 120 | B | 7.60 | < 0.5 | 1.7 | < 2 | - |
| 46 | 120 | B | 7.66 | < 0.5 | 3.0 | < 2 | - |
| Feed for 47 | 0 | - | 11.45 | 190 | 420 | 110 | - |
| Feed for 48 | 0 | - | - | 200 | 410 | 110 | - |
| 47 | 240 | B | 6.64 | < 0.5 | 1.5 | < 2 | - |
| 48 | 240 | B | - | < 0.5 | 1.7 | < 2 | - |
| 49 | 5.2 | S | 10.36 | 74 | 260 | 98 | 290 |
| Feed for 49 | 0 | - | 11.34 | 240 | 450 | 120 | 73 |
| | 0 | - | - | 240 | 440 | 120 | 64 |
| 50 | 120 | S | 7.88 | < 1.0 | 2.3 | < 0.05 | 53 |
| Feed for 50, 51, 52, 53 | 0 | - | 11.21 | 220 | 460 | 120 | 52 |
| | 0 | - | 11.25 | 250 | 460 | 120 | 36 |
| 51 | 120 | S | 7.89 | < 1.0 | 2.6 | < 0.05 | 93 |
| 52 | 13 | S | 9.14 | 11 | 66 | 64 | 570 |
| 53 | 60 | S | 8.28 | 1.0 | 1.6 | < 0.05 | 200 |
| 54 | 60 | S | 8.28 | < 1.0 | 0.24 | < 0.05 | 220 |
| Feed for 54 | 0 | - | 11.22 | 240 | 460 | 120 | 54 |

| RUN | $O_3$ UPTAKE gmole/s | LIQUID VOLUME | THEORETICAL $O_3$ UPTAKE ($\Delta$CN + 4$\Delta$CNS) gmole/s |
|---|---|---|---|
| 39 | $2.18 \times 10^{-5}$ | .92 | $2.45 \times 10^{-5}$ |
| 49 | $2.2 \times 10^{-5}$ | .90 | $2.83 \times 10^{-5}$ |
| 52 | $2.1 \times 10^{-5}$ | .92 | $2.44 \times 10^{-5}$ |

P = 1.2 atm in reactor

# APPENDIX C

# CALCULATION DETAILS

## C.1 Diffusivities of Ozone and Cyanide in Water

### Ozone-Water Diffusivity

The diffusivity of ozone in water was calculated using the Wilke and Chang correlation simliar to the calculations of *Hill and Spenser (1975)*

$$D_{AB} = (7.4(10^{-8})(\phi M_B)^{.5} T)/(\mu(v_A)^{.6}) \quad \ldots (C.1)$$

$D_{AB}$ = diffusivity of ozone in dilute solution in water ($cm^2/s$)

$\phi$ = 2.6 for water

$M_B$ = molecular weight of solvent = 18 g/gmole

$T$ = temperature (K) = 295K

$\mu$ = solution viscosity = 0.8937 centipoise

$v_A$ = solute molal volume at the boiling point ($cm^3$/gmole) = 35.45 $cm^3$/gmole

$D_{AB} = 1.985 \times 10^{-5}$ $cm^2/s$

Conversions of the physical mass transfer coefficients for the carbon dioxide water system to those for the ozone water system were accomplished by;

$$k^{o}_{L_{O_3-H_2O}} = k^{o}_{L_{CO_2-H_2O}} \left(\frac{D_{O_3-H_2O}}{D_{CO_2-H_2O}}\right)^{.5} \quad \ldots (C.2)$$

where $D_{O_3-H_2O}$ and $D_{CO_2-H_2O}$ were corrected for the same temperature using the Nernst-Einstein relation (equation 4.2).

### Cyanide-Water Diffusivity

In order to utilize the instantaneous reaction regime and the transition from fast to instantaneous reaction regime the value for cyanide-water and cyanate-water diffusivities were required.

If molecular diffusion in electrolyte solutions is assumed the Nernst equation (equation 4.21) is used where;

$$D_{AB} = \frac{RT}{F^2}\left(\frac{1/n_+ + 1/n_-}{1/\lambda_+^0 + 1/\lambda_-^0}\right) \qquad \ldots (C.3)$$

$D_{AB}$ = diffusivity of NaCN, NaCNS or NaCNO in dilute solution in water ($cm^2/s$)

R = gas constant (J/gmole K)

$\lambda_+^0$, $\lambda_-^0$, - zero concentration ionic conductance (mhos/equivalent)

$n_+$, $n_-$, valances of cation and anion, respectively

F = Faraday = 96500 C/g equivalent

Diffusion coefficients for ionic species may be approximated using;

$D_{AB} = RTu\pm/Fn\pm$ where $u\pm$ is the ionic mobility of the cation or anion

$u\pm = \lambda_\pm^0/F$

$$D_{AB} = RT\lambda_\pm^0/F^2 n\pm \qquad \ldots (C.4)$$

Difficulty arises in obtaining values for $\lambda_\pm^0$ for $CNO^-$ and $CN^-$. Only one reference from the International Critical Tables gives two values of electrolyte conductance ($\Lambda = \lambda_+ + \lambda_-$) for KCN. No value for $CNO^-$ could be found and adequate information exists for KCNS. Figure C.1 shows the behaviour of equivalent conductance against concentration, approaching $\Lambda^0$ as the concentration approaches zero. From the plot a value of $\Lambda_{KCNS}^0$ can be obtained and thus $\lambda_{CNS}^0$ can be calculated from

$$\lambda_{CNS}^0 = \Lambda_{KCNS}^0 - \lambda_K^0 \qquad (\lambda_K = 63.5 \text{ mhos/equivalent})$$

Since no information exists for $\Lambda_{KCN}^0$, the behaviour of KCN equivalent

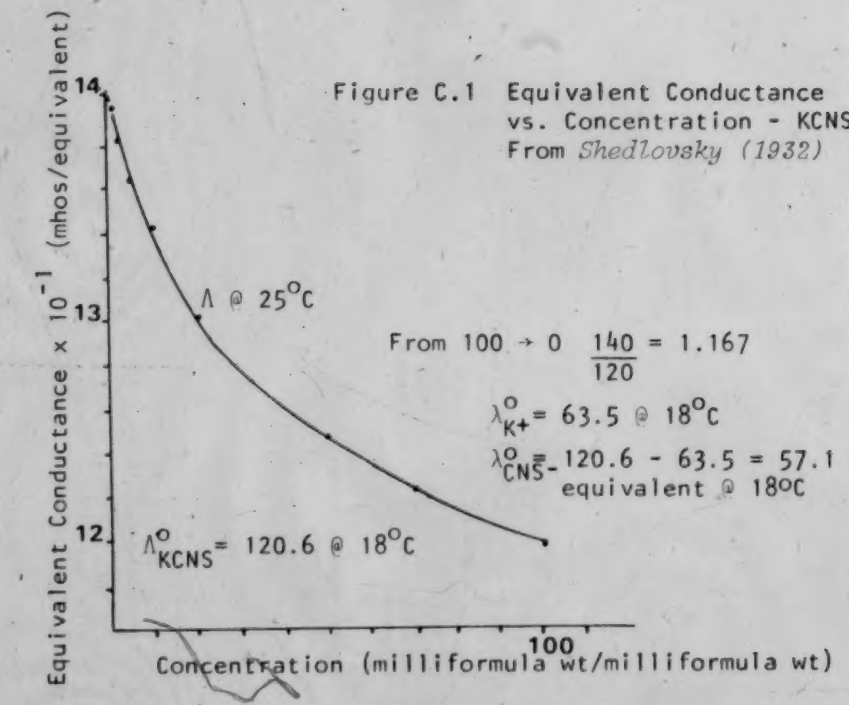


Figure C.1 Equivalent Conductance vs. Concentration - KCNS From *Shedlovsky (1932)*

From 100 → 0 $\frac{140}{120}$ = 1.167

$\lambda^{o}_{K^+}$ = 63.5 @ 18°C

$\lambda^{o}_{CNS^-}$ = 120.6 - 63.5 = 57.1 mhos/equivalent @ 18°C

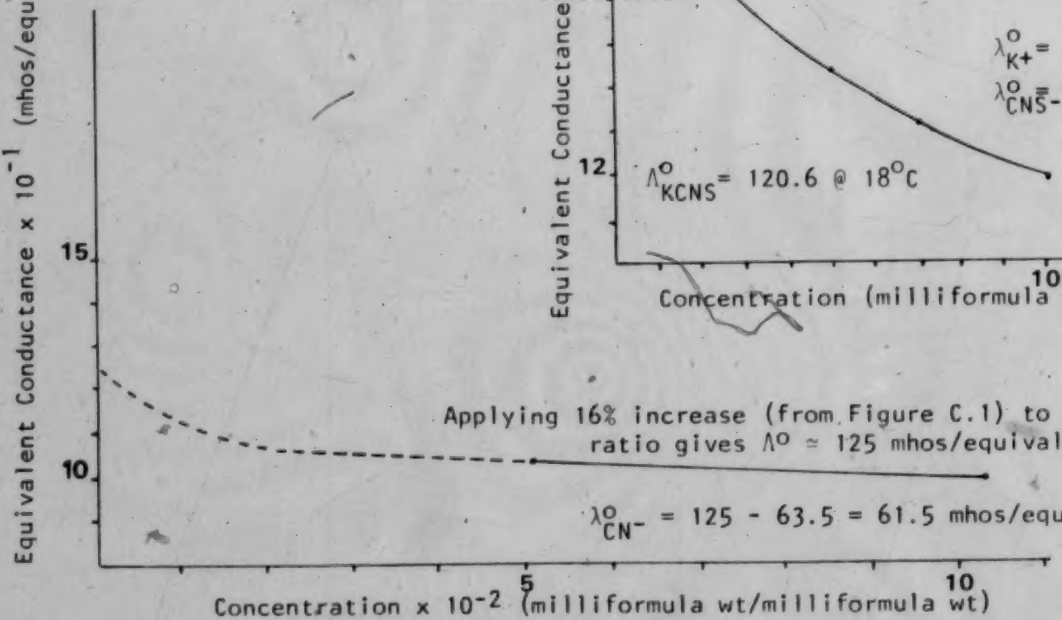


Applying 16% increase (from Figure C.1) to first 100 concentration ratio gives $\Lambda^{o} \simeq$ 125 mhos/equivalent @ 18°C

$\lambda^{o}_{CN^-}$ = 125 - 63.5 = 61.5 mhos/equivalent @ 18°C

Figure C.2 Equivalent Conductance vs Concentration - KCN

conductance in the region of the infinite dilution was assumed to follow that of KCNS and the two data points, shown on Figure C.2 were extrapolated on this basis. A value of $\Lambda^0_{KCN}$ of 125 mhos/equivalent was obtained from which $\lambda^0_{CN^-}$ was calcualted to be 61.5 mhos/equivalent ($\lambda^0_{CNS^-}$ = 57.1 mhos/equivalent).

As no values of conductance could be found for any salt of $CNO^-$, it was assumed this cyanide species behaved similarly yielding the same order of magnitude conductance value.

The above data applied to T = 18°C and from equations (C.3) and (C.4) the molecular diffusivity of NaCN and ionic diffusivity of $CN^-$ were found to be $1.3 \times 10^{-5}$ $cm^2/s$ and $1.6 \times 10^{-5}$ $cm^2/s$, respectively.

The value of the diffusivity of $CN^-$ in the reactor NaOH solution used in the experiments likely approached the higher values as indicated by *Sherwood and Wei (1955)*. The value of $D_{CN^-} = 1.6 \times 10^{-5}$ $cm^2/s$ at 18°C was used for this work.

The ionic diffusivity for $CNS^-$ was calculated to be $1.48 \times 10^{-5}$ $cm^2/s$ at 18°C.

Comparison

In order to compare $D_{CN^-}$, $D_{CNO^-}$ and $D_{CNS^-}$ with $D_{O_3}$ in water it was assumed all species diffusivities varied with temperature in the same manner. The diffusivity of ozone in water was found above to be $1.984 \times 10^{-5}$ $cm^2/s$ at 25°C. Correcting this to 18°C was done as follows;

$$\frac{D\mu}{T} = \text{constant}$$

$$D_{O_3} @ 18^oC = \frac{D_{O_3} @ 25^oC \ (\mu_{25^oC})}{\mu_{18^o}} \times \frac{T_{18}}{T_{25}}$$

$$= 1.984 \times 10^{-5} \times \left(\frac{.8937}{1.0559}\right)\left(\frac{291}{298}\right)\frac{cm^2}{sec} = 1.64 \times 10^{-5} \ cm^2/s$$

$$\frac{D_{CN^-}}{D_{O_3}} = \frac{1.6 \times 10^{-5}}{1.64 \times 10^{-5}} = 0.98 \simeq 1.0$$

$$\frac{D_{CNS^-}}{D_{O_3}} = \frac{1.48 \times 10^{-5}}{1.64 \times 10^{-5}} = 0.9$$

Assume $\frac{D_{CNO^-}}{D_{O_3}} = 1.0$

C.2 Mass Transfer Coefficient for Carbon Dioxide-Water System

Run 7. Results

The measured reactor conditions for this run was:

P = 3.3 cm $H_2O$ over atmospheric

Patm = 69.93 cm Hg

S = 102 rpm

T = 23.8°C

Q = 1.3 mL/s

Conversion pressure to atmospheres

$$P = \frac{69.93}{76} + \frac{3.3}{1033.2} = 0.923 \text{ atm}$$

The corresponding Henry's law coefficient was

$H = 1.586 \times 10^3$ atm/mole fraction.

A sample of 10 mL of water was taken from the sample chamber and added to 20 mL of NaOH. For this particular run the NaOH contained some $CO_2$ (not shown on Figure A.1). Both the mixed sample and blank NaOH were titrated using standardized HCl, of 0.016 M, an potentiometrically mapped.

The required volumes of HCl added were:

To the sample $v_1$ = 24.2 mL, $v_2$ = 29.2 mL

To a 30 mL NaOH $v_1$ = 42.7 mL, $v_2$ = 43.3 mL

Amount of $CO_2$ in sample of water =

$$= (29.2 - 24.2)\text{mL} \times .016 \frac{\text{gmole}}{\text{L}} - (43.3 - 42.7)\text{mL HCl} \times .016 \frac{\text{gmole}}{\text{L}} \times \frac{20 \text{ mL NaOH used in run}}{30 \text{ mL NaOH used for standardization}} = 0.0736 \text{ millimol}$$

Conc of $CO_2$ in sample

$$= \frac{0.0736 \text{ millimoles}}{10 \text{ mL}}$$

$$c_o = C_{CO_2} = 0.00736 \text{ gmole/L}$$

$$c_o' = \frac{.923 \text{ atm}}{1586 \frac{\text{atm}}{\text{mole fraction}}} \times \frac{\text{gmole } H_2O}{18 \text{ g } H_2O} \times 1000 \frac{\text{g } H_2O}{\text{L}} = .0323 \frac{\text{gmole}}{\text{L}}$$

Calculation of physical mass transfer coefficient, $k_L^o$, (assuming gas phase resistance is negligible) is defined by;

$$k_L^o a(c_o - c_o) = Q(c_o - c_{oi}) \qquad c_{oi} = 0$$

$$k_L^o = Qc_o/a(c_o' - c_o)$$

$$= 1.3 \frac{\text{mL}}{\text{sec}} \left(\frac{.00735 \text{ gmole/L}}{79 \text{ cm2} \times 1000 \text{ mL/L}}\right) \times \left(\frac{1}{0.0323 - .00735}\right)\text{gmole/L} \times 1000/\text{L}$$

$$= 4.8 \times 10^{-3} \text{ cm/s @ } 23.8^\circ\text{C}$$

Conversion to $k_L^o$ @ 25°C

$$D_{CO_2} \text{ @ } 25^\circ\text{C} = 1.96 \times 10^{-5} \text{ cm}^2/\text{s} \text{ (Perry et al. (1963))}$$

$$D_{CO_2} \text{ @ } 23.8^\circ\text{C} = \frac{D_{CO_2} \text{ @ } 25^\circ\text{C} \times \mu H_2O \text{ @ } 25^\circ\text{C}}{\mu H_2O \text{ @ } 23.8^\circ\text{C}} \times \frac{296.8 \text{ K}}{298 \text{ K}} =$$

$$= \frac{1.96 \times 10^{-5} \text{ cm}^2/\text{s}(.8937 \text{ centipoise})}{.9185 \text{ centipoise}} \times \frac{296.8 \text{ K}}{298 \text{ K}}$$

$$= 1.9 \times 10^{-5} \text{ cm}^2/\text{s}$$

$$k_L^{\circ} @ 25^{\circ}C = 4.8 \times 10^{-3} \text{ cm/s} \left(\frac{1.96 \times 10^{-5}}{1.90 \times 10^{-5}}\right)^{.5} = 4.9 \times 10^{-3} \text{ cm/s}$$

The results of the carbon dioxide absorption into water over a range of stirring speeds from 79 - 113 rpm are shown in Table B.1.

C.3 Calculation of Gas Phase Resistance from $SO_2$ Absorption Study

From gas chromatograph the concentration of $SO_2$ in carrier gas was found to be 2.2% (inlet) and 0.39% (outlet) while nitrogen concentration was found to be 97.63% inlet and 98.4% outlet. The remaining percentage was attributable to water vapor.

Flow from rotameter $N_2$ flow rate = 0.0283 sL/s

$SO_2$ inlet flow rate = 33.5 scc/min

Total flow rate = (0.0283 sL/s x 60 s/min)/0.9763 = 1.739 sL/min

Inlet $SO_2$ flow rate = 0.022 x 1.739 sL/min = 0.0383 sL/min = 38.3 s/min

= (0.0383 sL/min)/22.4 sL/gmole = $1.708 \times 10^{-3}$ gmole/min

Total outlet flow rate = (0.0283 sL/s x 60 s/min)/0.984 = 1.725 sL/min

This calculation assumes the nitrogen flow rate is constant.

Total $SO_2$ outlet flow rate = 0.0039 x 1.725 sL/min/22.4 sL/gmole

= $3.0 \times 10^{-4}$ gmole/min

Calculated response = $\frac{33.5 \text{ scc/min}}{38.3 \text{ scc/min}} = 0.875$

$SO_2$ transferred from gas to liquid,

$V_a = 1.708 \times 10^{-3}$ gmole/min x 0.875 - $0.3 \times 10^{-3}$ gmole/min x 0.875 = $1.232 \times 10^{-3}$ gmole/min

Bulk phase $SO_4$ gas concentration = outlet $SO_4$ concentration

$$= \frac{3.0 \times 10^{-4} \text{ gmole/min}}{1.726 \text{ sL/min}} \times 0.875 = 0.152 \text{ gmole/sL}$$

To calculate $k_G$ and $k_g$ the following reactor conditions were known;

$T = 20.5^{o}C$

Pressure in reactor = 1.269 atm

$P_{SO_2} = 1.269 \times 0.0039 = 4.95 \times 10^{-3}$ atm

S = 106 rpm

$k_G = 1.232 \times 10^{-3} \frac{\text{gmole}}{\text{min}} / (60 \text{ s/min} \times 79 \text{ cm}^2 \times 4.95 \times 10^{-3} \text{ atm})$

$= 5.25 \times 10^{-5}$ gmole/cm$^2$s atm

$k_g = k_G RT = 5.25 \times 10^{-5}$ gmole/cm$^2$s atm $\times$ 0.082 atm L/gmole K $\times$ 1000 cm$^3$/L $\times$ 293.5 K

$= 1.26$ cm/s

The relationship

$k_{g_{O_3}} = k_{g_{SO_2}} (D_{O_3\text{-air}}/D_{SO_2\text{-}N_2})^{.5}$ was used to convert $SO_2$ measurement to $O_3$.

To do so, calculation of $D_{O_3\text{-air}}$ and $D_{SO_2\text{-}N_2}$ were calculated using the Wilke-Lee modification of the Hirschfelder-Bird-Spotz method, namely,

$$D_{AB} = \frac{(0.00107 - 0.000246\sqrt{1/M_A + 1/M_B})T^{1.5}\sqrt{1/M_A + 1/M_B}}{Pt(r_{AB})^2(f(k'T/\varepsilon_{AB}))}$$

Data for $D_{SO_2\text{-}N_2}$

$T = 293.5$ K

$P_t = 1.26$ atm

$M_A = M_{SO_2} = 64$

$M_B = M_{N_2} = 28$

$r_{SO_2\text{-}N_2} = 3.95$ from *Perry et al. (1963)*

$\varepsilon_{SO_2\text{-}N_2}/k' = 151.8$

$\frac{k'T}{\varepsilon} = \frac{293.5}{151.8} = 1.93$

$f(k'T/\varepsilon) = 0.544$ from *Perry et al. (1963)* Table 14.45

$$D_{SO_2\text{-}N_2} = \frac{(0.00107 - 0.000246\sqrt{1/64 + 1/28})(293.5)^{1.5}\sqrt{1/64 + 1/28}}{1.26(3.95)^2(0.544)}$$

$= 0.109\ cm^2/s$

Data for $D_{O_3\text{-air}}$

$T = 293.5$

$P_t = 1.26$ atm

$M_A = M_{O_3} = 48$

$M_B = M_{air} = 29$

$r_{O_3\text{-air}} = 3.78$

$\varepsilon/k' = 133$ derived using $\varepsilon_{O_3}/k' = 1.15$ (Boiling Temperature)

$= 1.15(161\ K) = 185.1$

$\frac{k'T}{\varepsilon} = 2.2$

$f(k'T/\varepsilon) = 0.52$ from *Perry et al. (1963)* Table 14.45

$$D_{O_3\text{-air}} = \frac{(0.00107 - 0.000246\sqrt{1/48 + 1/29})293.5^{1.5}\sqrt{1/48 + 1/29}}{1.26(3.78)^2(0.52)}$$

$= 0.124\ cm^2/s$

$k_{g_{O_3}} = k_{g_{SO_2}}(D_{O_3\text{-air}}/D_{SO_2\text{-}N_2})^{.5}$

$= 1.26\ cm/s\ (0.124/0.109)^{.5} = 1.35\ cm/s$

TABLE C.1

RUN II DATA

Patm = 69.65 cm Hg
Pgauge = 25.0 cm Hg
$\Delta P$ = pressure differential between atmosphere and fume hood = 0.01 cm Hg
S = 106 rpm
Start Time 1410
a = 79 $cm^2$

| Sample Type | Replicate Value | Time | Temp. °C | Time to Measure 0.1 cu. ft. s | Sample Period s | Titrant Quantity mL $Na_2S_2O_3$ | mL $AgNO_3$ |
|---|---|---|---|---|---|---|---|
| Gas Inlet | 1 | 1455 | 23.05 | 75.4 | 82.6 | 36.69 | |
| | 2 | 1542 | 23.3 | 76.1 | 85.6 | 38.1 | |
| | 3 | 1620 | 23.3 | 76.1 | 85 | 37.48 | |
| Gas Outlet | 1 | 1508 | 23.05 | 75.9 | 84.4 | 36.0 | |
| | 2 | 1532 | 23.3 | 75.8 | 88.6 | 38.3 | |
| | 3 | 1610 | 23.3 | 75.9 | 85.8 | 36.85 | |
| | | | | Flow rate (mL/s) | | | |
| Liquid Inlet* | 1 | 1415 | | | | | 10.12 |
| | 2 | 1630 | | | | | 10.15 |
| Liquid Outlet* | 1 | 1450 | 23.3 | 0.83 | | | 8.54 |
| | 2 | 1530 | 23.3 | 0.83 | | | 7.75 |
| | 3 | 1550 | 23.5 | 0.83 | | | 7.87 |
| | 4 | 1612 | 23.5 | 0.83 | | | 7.8 |
| | 5 | 1623 | 23.5 | 0.83 | | | 7.83 |

*All liquid samples 100 mL
Titration of blank (deionized water) required 0.025 mL $AgNO_3$

## C.4 Calculation of $k_L$ and I based on Run II Data (Simple Cyanide System)

Ozone Uptake and $c_o'$

Flow rate calculation

Inlet sample replicate #1

$$Q = \frac{0.1 \text{ cu.ft}}{75.4 \text{ s}} \times 28.316 \frac{\text{L}}{\text{cu.ft.}} \times \frac{273}{296.06} \left(\frac{69.65 - 2.114}{76}\right) =$$

$$= 0.03078 \text{ sL/s}$$

The value 2.114 cm Hg is the vapor pressure of water at 296.06 K assuming saturation.

Amount $O_3$ absorbed in bubbler. (inlet sample replicate #1)

Titration represents the following chemical reactions

$$O_3 + 2KI + H_2O \rightleftarrows I_2 + 2KOH + O_2$$

$$2Na_2S_2O_3 + I_2 \rightarrow Na_2S_4O_6 + 2NaI$$

Therefore two moles of $Na_2S_2O_3$ are required for each mole of $O_3$.

$[Na_2S_2O_3] = 0.1$ M

$$\text{Moles } O_3 \text{ absorbed} = \frac{36.69 \text{ mL}}{1000 \text{ mL}} Na_2S_2O_3 \times 0.1 \text{ gmole/L } \frac{Na_2S_2O_3}{2} =$$

$$= 1.834 \times 10^{-3} \text{ gmole}$$

Rate of uptake $= 1.834 \times 10^{-3}$ gmole/82.6 s $= 0.02221 \times 10^{-3}$ gmole/s

Concentration of $O_3 = 0.0221 \times 10^{-3}/0.03078 = 0.7216 \times 10^{-3}$ gmole/sL

Similarly all replicates calcualted

| Inlet | Replicate | Flow Rate (sL/s) | $O_3$ Uptake x $10^3$ (gmole/s) | Gas Concentration x $10^3$ (gmole/L) |
|---|---|---|---|---|
| | 1 | 0.03078 | 0.02221 | 0.7216 |
| | 2 | 0.03044 | 0.02225 | 0.7309 |
| | 3 | 0.03044 | 0.02205 | 0.7245 |
| Outlet | Replicate | | | |
| | 1 | 0.03057 | 0.02133 | 0.6977 |
| | 2 | 0.03044 | 0.02161 | 0.7100 |
| | 3 | 0.03052 | 0.02132 | 0.6979 |

Average Flow Conditions

Inlet Flow = 0.03055 sL/s

Inlet Concentration = $0.7257 \times 10^{-3}$ gmole/L

Outlet Flow = 0.03051 sL/s

Outlet Concentration = $0.7019 \times 10^{-3}$ gmole/L

Ozone Absorbed in Reactor

$$\overline{Va} = 0.7257 \times 10^{-3}(.03055) - 0.7019 \times 10^{-3}(0.03051)$$

$$= 7.55 \times 10^{-7} \text{ gmole/s}$$

% $O_3$ in Outlet Gas (Dry Basis)

$$= 0.7019 \times 10^{-3} \text{ gmole/sL} \times 22.4 \text{ sL/gmole} \times 100\% = 1.572\%$$

Partial Pressure-Ozone

$$P = \left(\frac{69.64 + 25 - 0.01 - 2.145}{76}\right)0.0157 = 0.0191 \text{ atm}$$

where 2.145 is vapor pressure of $H_2O$ at $T_{gas}$.

Henry's Law constant calculation (data from Table 14.29 *Perry et al. (1963)*)

$H = 3760 \text{ @ } 20^{\circ}C$

$H = 4570 \text{ @ } 25^{\circ}C$

$\therefore \text{ @ } T_{gas} = 23.5 \qquad H = 4327 \text{ atm/mole fraction}$

$$c_o' = \frac{0.091 \text{ atm}}{4327 \text{ atm/mole fraction}} \times \frac{48}{18} \frac{\text{gm } O_3}{\text{gmole } O_3} \frac{\text{gmole } H_2O}{\text{gm } H_2O} \times 1000 \frac{\text{mg } O_3}{\text{gm } O_3}$$

$$\times \ 1000 \frac{\text{gm } H_2O}{L} = 11.8 \text{ mg/L}$$

Cyanide Depletion

As per Appendix A.2

$[CN^-]$ mg/L = (A-B) x 1000/volume of sample (mL)

where A = mL of standard $AgNO_3$ titrant for cyanide sample

B = mL of standard $AgNO_3$ titrant for blank

For Liquid Outlet Replicate #1

$[CN] = (6.54 - 0.025) \times 1000/100 = 85.15$ mg/L

Similarly other liquid samples

Inlet $[CN^-] = (100.95 + 101.25)/2 = 101.1$ mg/L

$= 3.889 \times 10^{-3}$ gmole/L

Outlet $[CN^-] = 85.15, 77.25, 78.45, 77.75, 78.05$ mg/L

Average of last four values

$= 77.88$ mg/L $= 2.996 \times 10^{-3}$ gmole/L $= b_o$

Cyanide depletion

$$\Delta CN^- = \frac{0.83 \text{ mL/s}(101.1 - 77.88)\text{mg/L}}{26000 \text{ gm/gmole} \times 1000 \text{ mL/L}} = 7.4 \times 10^{-7} \text{ gmole/s}$$

Calculation of q, $k_L$ and I

$$q^{-1} = \frac{\Delta O_3}{\Delta CN} = \frac{7.55 \times 10^{-7} \text{ gmole/s}}{7.4 \times 10^{-7} \text{ gmole/s}} = 1.02$$

From Table 5 average value of $q^{-1} = 1.2$

$$K_L = \frac{1.2\ (7.4 \times 10^{-7}\ \text{gmole/s})}{79\ \text{cm}^2 \times 11.8\ \text{mg/L}} \times 48000\ \frac{\text{mg } O_3}{\text{gmole}} \times 1000\ \text{cm}^3/\text{L}$$

$$= 4.572 \times 10^{-2}\ \text{cm/s}$$

Rearranging equation 3.16

$$1/k_L = 1/K_L - RT/Hk_g$$

$k_g$ (av) = 1.53 cm/s

R = 82.1 atm $cm^3$/gmole K

T = 23.5°C = 296.5 K

H = 77890 atm $cm^3$/gmole $O_3$

$1/k_L = 1/4.572 \times 10^{-2}$ cm/s - (82.1 x 296.5)/(77890 x 1.53) s/cm

= 2.167 x 10 s/cm

$k_L = 4.61 \times 10^{-2}$ cm/s

% change = $1/k_L / 1/K_L$ = 99.17%

Thus gas phase resistance is negligible and $k_L = K_L$

$k_L^{\circ}$ @ 25°C = $5.8 \times 10^{-3}$ cm/s for s = 106 (Table 1)

Correcting for temperature

$$k_L^{\circ} \text{ @ } 23.5^{\circ}C = 5.8 \times 10^{-3} \left(\frac{1.907 \times 10^{-5}}{1.984 \times 10^{-5}}\right)^{.5}$$

$$= 5.69 \times 10^{-3}\ \text{cm/s}$$

where $D_{O_3}$ @ 23.5°C = $1.907 \times 10^{-5}$ $cm^2$/s

$D_{O_3}$ @ 25°C = $1.984 \times 10^{-5}$ cm/s

Enhancement Factor

$$I = 45.72 \times 10^{-3}/5.69 \times 10^{-3} = 8.0$$

## C.5 Calculation of Kinetic Constants

### Transition Regime

Rearranging equation 2.71

$$I^2 \left(\tanh\sqrt{\frac{t_D}{t_r}\left(\frac{I_\infty - I}{I_\infty - 1}\right)}\right)^2 = \frac{t_D}{t_r}\left(\frac{I_\infty - I}{I_\infty - 1}\right)$$

or $I^2(\tanh A) = B$

where $I_\infty = 1 + \frac{D_2}{D_1}\frac{b_o}{qc_o'}$

Now if $A > 3$ then $\tanh(A) \simeq 1.0$. This was the case for all runs.

Therefore

$$I^2 = B = \frac{t_D}{t_r}\left(\frac{I_\infty - I}{I_\infty - 1}\right)$$

And since $t_r = 1/k$ then

$$k = \frac{I^2}{t_D b_o}\left(\frac{I_\infty - 1}{I_\infty - I}\right)$$

For run II

$I = 8.0$ $\qquad D_2/D_1 = 1.0$ $\qquad q = 1/1.2 = .83$

$$I_\infty = 1 + \frac{1.0(77.88/26000 \text{ gmole/L})}{0.83 \times 11.8/4800 \text{ gmole/L}} = 15.6$$

$$t_D = D/k_L{}^{o2} = 1.907 \times 10^{-5} \text{ cm}^2/\text{s}/(5.69 \times 10^{-3} \text{ cm/s})^2$$

$$= 0.59 \text{ s}$$

$$\therefore k = \frac{(8.0)^2(15.6 - 1.0)}{0.59(77.88/26000)(15.6 - 8.0)} = 6.96 \times 10^4 \text{ L/gmole s}$$

Check if $A > 3$

$$A = \left(0.59 \times 6.96 \times 10^4 \left(\frac{15.6 - 8.0}{15.6 - 1.0}\right)\right)^{.5} = 146$$

Fast Reaction Regime

Using the methodology outlined in section 3.5.4.2.2 with run 11 data the following is found;

1) Assume k = 27600 L/gmole s

2) Calculate $k_2$ = 27600/5.1 = 5410 L/gmole s

3) Use equation 3.38 to solve for $b_{No}$

$$b_{No} = \left(\frac{1}{5.1 \times 2.996 \times 10^{-3} \text{ gmole/L}} + \frac{1}{(3.889 - 2.996)10^{-3} \text{ gmole/L}}\right)^{-1}$$

$$= 8.437 \times 10^{-4} \text{ gmole/L} = 35.4 \text{ mg/L}$$

4) Calculate $K_L$ using equation 3.40

$$K_L = \left(1 + \frac{1.5}{5.1} \times \frac{8.437 \times 10^{-4} \text{ gmole/L}}{2.996 \times 10^{-3} \text{ gmole/L}}\right)$$

$$\left(\frac{0.83 \text{ ml/s } (3.889 \times 10^{-3} - 2.996 \times 10^{-3}) \text{gmole/L}}{79 \text{ cm}^2 \times 11.8/48000 \text{ gmole/L}} \times \frac{1000 \text{ cm3/L}}{1000 \text{ mL/L}}\right)$$

$$= 1.083(38.2 \times 10^{-3}) = 41.3 \times 10^{-3} \text{ cm/s}$$

$$k_L = K_L = 41.3 \times 10^{-3} \text{ cm/s}$$

$$I = 41.3 \times 10^{-3}/5.69 \times 10^{-3} = 7.3$$

5) Calculate $k_1$

$$k_1 = k_L^2/D = (41.3 \times 10^{-3})^2/1.907 \times 10^{-5} \text{ s}^{-1} = 89.4 \text{ s}^{-1}$$

$$k_1 = kb_o + 1.5\, k_2 b_N$$

$$= 27600 \times 2.996 \times 10^{-3} \text{ s}^{-1} + 1.5 \times 5410 \times 8.437 \times 10^{-4}$$

$$= 89.45 \text{s}^{-1}$$

Verification of ratio of rate

The average measured ozone use was 1.2 gmole ozone for a mole of cyanide destroyed. Using equation 3.39 a verification of the assumed ratio of reaction rates ($k/k_2$) can be attempted

$$1/q = 1.2 = 1 + 1.5k_2 b_{No}/k_{bo} \quad \ldots (3.39)$$

By rearranging

$$k/k_2 = 7.5\ b_{No}/b_o$$

Solution by trial and error, where

1) Assume $k/k_2$
2) Solve for $b_{No}$ from equation 3.38
3) Check value of $k/k_2$ by solving equation 3.39

For run 11

1) $k/k_2 = 1.94$
2) $$b_{No} = \left(\frac{1}{1.94 \times 2.996 \times 10^{-3}\ \text{gmole/L}} + \frac{1}{3.889 \times 10^{-3} - 2.996 \times 10^{-3}\ \text{gmole/L}}\right)^{-1}$$
$$= 7.74 \times 10^{-4}\ \text{gmole/L}$$
3) $k/k_2 = 7.5\ (7.74 \times 10^{-4}/2.996 \times 10^{-3}) = 1.94$

Similarlyfor other randomly selected runs

| Run | $k/k_2$ | Run | $k/k_2$ |
|---|---|---|---|
| 1 | 1.87 | 16 | 1.89 |
| 4 | 4.17 | 18 | 2.7 |
| 9 | 2.22 | 24 | 2.0 |
| 13 | 3.33 | 26 | 2.56 |
| 15 | 1.58 | 28 | 5.65 |
| 17 | 8.40 | | |

Now if a value of $k/k_2 = 2.0$ were used instead of 5.1, the rate constants for run II are

Assume $k = 25000$ L/gmole s

$k_2 = 12500$ L/gmole s

$b_{No} = 7.74 \times 10^{-4}$ gmole/L

$k_L = 41.3 \times 10^{-3}$ cm/s

$k_1 = 89.4 s^{-1}$

Check $k_1 = 25000 \times 2.996 \times 10^{-3} + 1.5 \times 12500 \times 7.74 \times 10^{-4}$ $s^{-1}$

$= 89.4 s^{-1}$

Instantaneous Reaction Regime

Rearranging equation 2.72 and assuming measured $I = I_\infty$

$$D_2 = D_1(I - 1)/qc_o'/b_o$$

For run II

$$D_2 = 1.907 \times 10^{-5} \text{ cm/s } (8.0 - 1.0)\ 0.833 \times \frac{11.8}{48000} \text{ gmole/L} \times \frac{26000}{77.88} \text{ gmole/L}$$

$$= 0.91 \times 10^{-5} \text{ cm/s}$$

On average runs 1-27 $D_2 = 1.37 \times 10^{-5}$ cm/s

C.6 Calculations for Barren Bleed Runs

Theoretical Ozone Uptake

Based on ozone stoichiometric coefficients of 1, 1.5 and 3 for the cyanide, cyanate and thiocyante reactions the theoretical ozone uptake in one litre of solution

Moles of $O_3$ required for thiocyanate reaction = $3\Delta[CNS]$

Moles of cyanide generated from thiocyanate reaction = $\Delta[CNS]$

Moles of $O_3$ required for cyanide reaction = $[CN]_i + \Delta[CNS] - [CN]_b$

Moles of cyanate generated = $[CN]_i + \Delta[CNS] - [CN]_b$

Moles of cyanate reacted = $[CNO]_i + ([CN]_i + \Delta[CNS] - [CN]_b) - [CNO]_b$

Moles of ozone required for cyanate reaction = 1.5 x moles cyanate reacted

Theoretical $O_3$ Uptake = Q($O_3$ required for cyanide + thiocyanate + cyanate reactions)

$$\bar{V}_T a = Q(2.5\Delta[CN] + 5.5\Delta[CNS] + 1.5\Delta[CNO])$$

Theoretical $O_3$ Required for cyanide and thiocyanate reaction

$$\bar{V}'_T a = Q\ (\Delta[CN] + 4\Delta[CNS])$$

Data from run 34 (see Table 8)

$CN_{Ti}$ = (350 + 370)/2 = 360 mg/L

$CN_{Tb}$ = (150 + 160)/2 = 155 mg/L

$CNO_i$ = 110 mg/L

$CNO_b$ = (420 + 450)/2 = 435 mg/L

$CNS_i$ = 110 mg/L

$CNS_b$ = ( 68 + 67)/2 = 67.5 mg/L

Q = 1.08 mL/s

Measured $O_3$ uptake = $\bar{V}a = 1.12 \times 10^{-5}$ gmole/s

$C_o'$ = 6.72 mg/L

Calculated Uptake

$$\bar{V}_T a = \frac{1.08\ mL/s}{1000\ mL/L}\left(2.5\left(\frac{360-155}{26000}\right) + 5.5\left(\frac{110-67.5}{58000}\right) + 1.5\left(\frac{110-435}{42000}\right)\right) gmole/L$$

$$= 1.31 \times 10^{-5}\ gmole/s$$

$$\bar{V}_T' a = \frac{1.08 \text{ mL/s}}{1000 \text{ mL/L}} \left(\frac{360-155}{26000} + 4\left(\frac{110-67.5}{58000}\right)\right) \text{ gmole/L}$$

$$= 1.17 \times 10^{-5} \text{ gmole/s}$$

$$\bar{V}/\bar{V}_T = 0.85$$

$$\bar{V}/\bar{V}_T' = 0.96$$

Calculation of $k_L$ and I

$$K_L = \bar{V}H/ap$$

$$= \frac{1.12 \times 10^{-5} \text{ gmole/s}}{79 \text{ cm}^2 \times 6.72 \text{ mg/L}} \times 48000 \text{ mg/gmole} \times 10^3 \text{ cm}^3\text{/L}$$

$$= 1.01 \text{ cm/s}$$

$$1/k_L = 1/K_L - RT/Hk_g$$

$R = 82.1$ atm $\text{cm}^3$/gmole

$T = 22.4^{\circ}\text{C} = 295.4^{\circ}\text{k}$

$k_g = 1.53$ cm/s

$H = 74678$ atm $\text{cm}^3$/gmole $O_3$ (from *Perry et al. (1963)* Table 14.29)

$1/k_L = 1/1.01$ s/cm $- (82.1 \times 295.4)/(1.53 \times 74678)$ s/cm

$= 0.832$ s/cm

$k_L = 1.20$ cm/s

$k_L^{\circ} = 5.6 \times 10^{-3}$ cm/s from Table 9

$I = 1.20/5.6 \times 10^{-3} = 214$